Vol 3 No 9
1957

# SOVIET ATOMIC ENERGY

АТОМНАЯ ЭНЕРГИЯ
(ATOMNAYA ÉNERGIYA)

TRANSLATED FROM RUSSIAN

CONSULTANTS BUREAU, NEW YORK

# INVESTIGATIONS OF γ-RAYS EMITTED IN THERMAL-NEUTRON CAPTURE IN VANADIUM, MANGANESE, COBALT AND ALUMINUM

L. V. Groshev, A. M. Demidov, V. N. Lutsenko and V. I. Pelekhov

Using a magnetic spectrometer to analyze the Compton electrons, measurements have been made of the energies and intensities of γ-rays emitted by the nuclei formed in thermal-neutron capture in vanadium, maganese, cobalt and aluminum. The γ-ray spectrum was studied in the range from 0.25 to 11.5 Mev in vanadium and 0.25 to 8 Mev in manganese, cobalt and aluminum. γ-transition schemes have been drawn up for $V^{52}$, $Mn^{56}$, $Co^{60}$ and $Al^{28}$. The γ-rays accompanying radioactive decay of $Mn^{54}$ have also been studied.

The present work is an extension of the study of γ-rays emitted by nuclei in thermal-neutron capture which has been carried out at the RFT*Reactor, Academy of Sciences, U.S.S.R. The experimental conditions, methods of measurement and spectrometer have been described earlier [1]. Below we report the results of an investigation of the γ-rays from vanadium, manganese, cobalt and aluminum.

## Vanadium

The sample contained 850 grams of vanadium oxide $V_2O_5$. The γ-ray spectrum was studied in the region from 0.25-11.5 Mev. The raw spectrum of γ-rays from $V_2O_5$ is shown in Fig. 1 where along the abscissa axis is plotted Hρ in gauss-cm (below) and the γ-ray energy in Mev (above). Along the ordinate axis is plotted the number of coincidences obtained in ten minutes, after subtraction of the background (the number of coincidences from the sample when surrounded by a layer of boron-carbide) and introduction of corrections for non-Compton electrons from pairs formed by γ-rays in the radiator. The measurements were carried out with a radiator 100 μ in thickness. In the lower left in Fig. 1 is shown the portion of the spectrum corresponding to energies below 1.1 Mev, which was measured with a thinner radiator (25 μ).

In Fig. 2 is shown the corrected γ-ray spectrum for vanadium. The γ-ray energy in Mev is plotted along the abscissa axis; the values of $\nu(E)H\rho$ are plotted along the ordinate axis, where $\nu(E)$ is the number of γ-photons per neutron capture per unit energy interval (1 Mev). The use of the quantity $\nu(E)H\rho$ is convenient because of the fact that in this case, over a wide energy interval (1.8–10 Mev), the height of the peak is approximately proportional to the intensity of the corresponding γ-ray because the quantity $\delta/H\rho$ (where δ is the half-width of the peak) remains constant. At energies below 1.8 Mev electron scattering in the radiator disturbs the proportionality indicated above.

In Table 1 we present the energies and intensities of the γ-rays from vanadium obtained in the present work and by other authors. The lines shown in Table 1 (excluding the line from $Cr^{52}$ with an energy of 1.434 Mev, found in the β-decay of $V^{52}$) represent about 67% of the total energy radiated by the sample. The remaining energy goes into γ-rays in the unresolved part of the spectrum.

The line intensities were determined both by normalizing the total energy radiated by the vanadium nucleus with respect to the neutron binding energy and by comparison with the γ-line at 1.434 Mev [1]. It was found that the intensity values obtained by both methods were in agreement if the intensity of the γ-line at 1.434 Mev was taken as equal to one γ-photon per capture [2].

RFT* = "reactor for physical and technical research." -- Editor's note.]

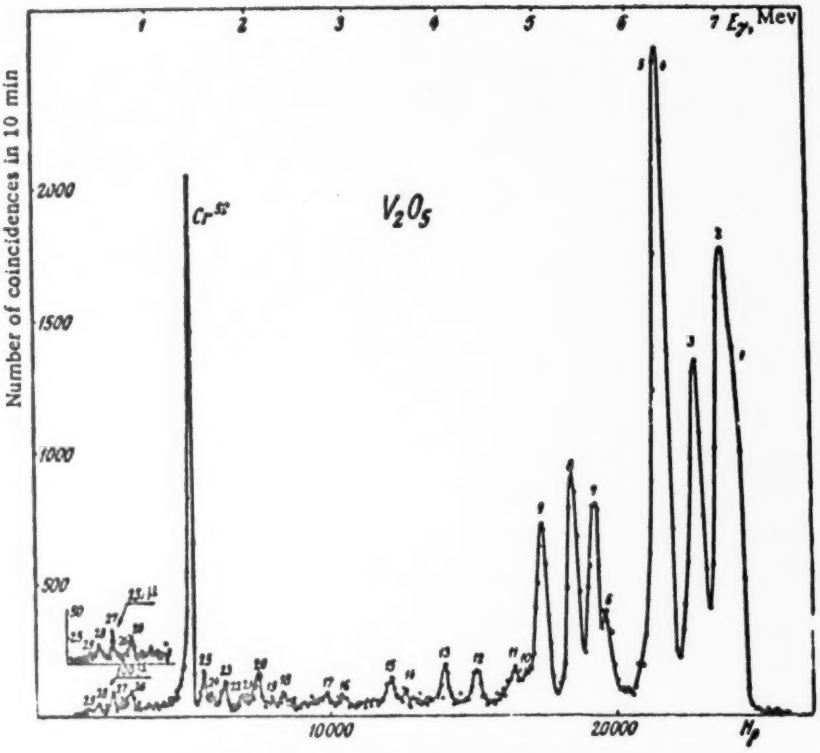


Fig. 1. Raw γ-ray spectrum in $V_2O_5$.

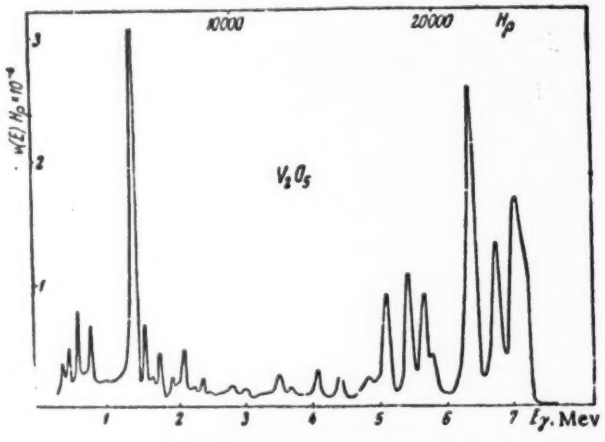


Fig. 2. Corrected γ-ray spectrum in $V_2O_5$.

Vanadium has two stable isotopes: $V^{51}$ (99.8 %) and $V^{50}$ (0.2%). Although the cross section for thermal-neutraon capture in $V^{50}$ is not known its contribution to the total capture cross section ($\sigma = 4.7 \pm 0.2$ barns) must be small since the activation cross section in $V^{51}$ is $4.5 \pm 0.9$ barns [7]. In determining the γ-ray intensity by the first method we have assumed that all the γ-rays are emitted by the $V^{52}$ nucleus.*

* The fact that the intensities obtained by the two methods indicated above were in agreement supports this assumption.

TABLE 1

Energies and Intensities of γ-rays from Vanadium

| Line No. | Results of the present work | | Results of Bartholomew and Kinsey | | Results of Reier and Shamos [5] | Results of Braid [6] | | Results of Hamermesh and Hummel |
|---|---|---|---|---|---|---|---|---|
| | $E_\gamma$ Mev | $I^*$) | $E_\gamma$ Mev | $I^*$) | $E_\gamma$ Mev | $E_\gamma$ Mev | $I^*$) | $E_\gamma$ Mev |
| 1 | 7.30±0.015 | 5.7 | 7.305±0.007 | 11 | | | | 7.4 |
| 2 | 7.16±0.015 | 10 | 7.154±0.008 | 18.5 | | | | |
| 3 | 6.86±0.01 | 8 | 6.868±0.008 | 14 | | | | 6.8 |
| | | | 6.62±0.02 | 0.7 | | | | |
| 4 | 6.51±0.01 | 12 | 6.508±0.006 | 25 | | | | |
| 5 | 6.46±0.02 | 7 | | | | | | |
| 6 | 5.87±0.02 | 2 | 5.879±0.015 | 3 | | | | |
| 7 | 5.73±0.02 | 5.6 | 5.744±0.08 | 9 | | | | 5.7 |
| 8 | 5.51±0.01 | 7.2 | 5.511±0.008 | 10 | | | | |
| 9 | 5.19±0.01 | 6.5 | 5.21±0.01 | 6 | | | | 5.3 |
| 10 | 4.99±0.02 | ~0.8 | 4.98±0.02 | 2 | | | | |
| 11 | 4.85±0.02 | ~1 | 4.85±0.02 | 2 | | | | |
| 12 | 4.45±0.015 | 1.3 | 4.45±0.02 | 3 | | | | |
| 13 | 4.14±0.015 | 1.7 | 4.15±0.03 | 4 | | | | |
| 14 | 3.69±0.03 | ~0.4 | 3.73±0.03 | 3 | | | | |
| 15 | 3.54±0.02 | 1.3 | 3.59±0.02 | 3 | | | | |
| | | | 3.36±0.02 | 2 | | | | |
| 16 | 3.05±0.02 | ~0.4 | | | | | | |
| 17 | 2.85±0.02 | ~0.6 | | | | | | |
| 18 | 2.44±0.02 | 1 | | | | | | |
| 19 | 2.30±0.02 | ~0.5 | | | | | | |
| 20 | 2.13±0.01 | 3.4 | | | | 2.25 | 5 | |
| 21 | 2.02±0.02 | 1.1 | | | | | | |
| 22 | 1.93±0.015 | 1.6 | | | | | | |
| 23 | 1.77±0.01 | 3.8 | | | | | | |
| 24 | 1.65±0.01 | 1.3 | | | | | | |
| 25 | 1.55±0.01 | 5.8 | | | | | | |
| | 1.434±0.005 | 100 | | | | 1.46±0.03 | 87 | |
| 26 | 0.84±0.01 | 6 | | | 0.82 | 0.84±0.03 | 8 | |
| 26' | 0.79±0.015 | 3 | | | | | | |
| 27 | 0.652±0.005 | 9.0 | | | 0.64±0.02 | 0.63±0.03 | 6 | |
| 28 | 0.42±0.01 | 7 | | | 0.43±0.02 | 0.42±0.03 | 5 | |

* Intensity in photons per hundred neutron captures.

** The intensity value in vanadium obtained by Bartholomew and Kinsey [3] are too high. In more recent work they have shown [4] that these values must be reduced by a factor of 1.6. The corrected values agree with the present results.

In Ref. [3] γ-lines with energies greater than the binding energy in $V^{52}$: $E_1 = 7.67 \pm 0.02$ Mev, $E_2 = 7.83 \pm 0.02$ Mev and $E_3 = 7.98 \pm 0.02$ Mev (the intensities are correspondingly 0.25, 1.3, and 0.5 quanta per 100 capture events in a natural isotopic mixture). These lines were assigned to the $V^{51}$ nucleus (the neutron binding energy $B_n = 11.15 \pm 0.2$ Mev [8]). The γ-ray spectrum for vanadium was examined with special care in the region from 7.3 to 11.5 Mev. In this region there were no lines with intensity greater than 0.05 quanta per 100 capture events in a natural isotopic mixture. The peaks at energies of 7.3 and 6.51 Mev were also studied with higher resolving power (a peak half-width of 1.3% instead of 2%) thus making it possible to resolve the components.

In Fig. 3 is shown the γ-transition scheme in the $V^{52}$ nucleus. The scheme has been drawn up using the data on energy levels found in studies of the $V^{51}$ (d, p) $V^{52}$ reaction [9]. On the left are shown the energy levels; on the right are shown the orbital momenta $l_n$ carried into the nucleus in the (d, p) reaction as well as the total moment I and the parity p. The numbers next to the arrows which indicate the γ-transitions denote the intensity (number of γ-photons per 100 capture events). The numbers used to designate the lines are written below (see Table I and Fig. 1).

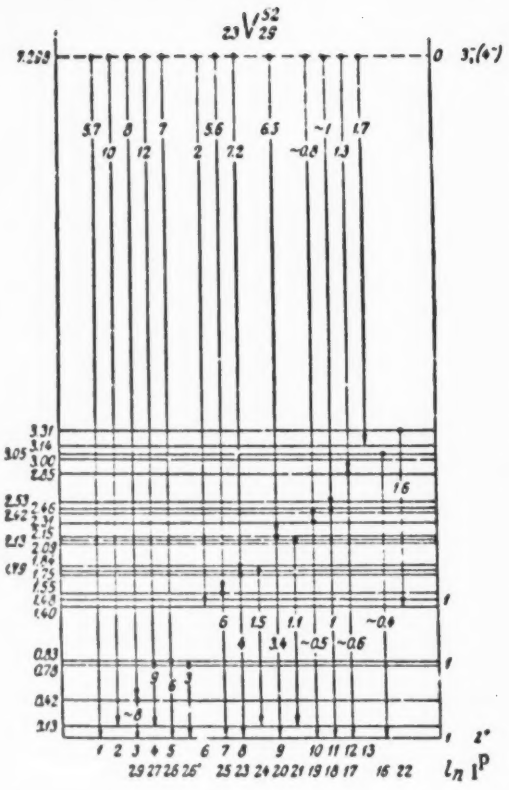


Fig. 3. γ-transition scheme in $V^{52}$.

The majority of γ-lines are found to be in good agreement with this level scheme.

The total moment of the ground state of $V^{52}$ is $2^+$ [2]. The total moment of the configuration formed after capture of a thermal neutron by the $V^{51}$ nucleus,• however, may be $3^-$ or $4^-$. Since the parity of the initial state of the $V^{52}$ nucleus is opposite to the parity of the ground state, whereas the transition No. 1 between these states has a sizeable intensity (approximately 6 γ-photons per 100 capture events), this transition must be E1. Hence the original state must be $3^-$.

King and Parkinson [10] have found that the ground state of $V^{52}$ and the levels at 0.79 and 1.6 Mev have $l_n = 1$. Consequently, transitions from the initial state to these levels must exhibit a change of parity. If it is assumed that the intensities of these transitions is of the same order of magnitude as the No. 1 transition it is most probable that they are also E1-transitions.

## Manganese

The sample contained 470 grams of manganese dioxide. In Figs. 4 and 5 are shown the raw and corrected $MnO_2$ spectra. Higher resolution was used to separate the group of peaks near 7 Mev (peak half-width of 1.3%). In Fig. 6 is shown the resolution of this group into components.

The line intensities were determined by normalization with respect to the neutron binding energy. The energies and intensities of the γ-rays from manganese are shown in Table II. It is apparent from Table II that the results of all authors are in agreement, within the limits of experimental error. The gamma-rays resolved in the present work are responsible for 66% of the energy radiated by the sample (excluding the γ-rays associated with the β-decay of $Mn^{56}$ which have energies of 0.85, 1.81 and 2.12 Mev [2], [11]).

The γ-ray spectrum associated with the radioactive decay of $Mn^{56}$ was examined with special interest. In this part of the work the sample was removed from the thermal column of the reactor and placed at a distance of approximately 2 meters from the spectrometer. The spectrum is shown in Fig. 7. Along the ordinate axis is plotted the number of coincidences, taking into account the $Mn^{56}$ decay during the course of the measurement. A fourth line, in addition to those indicated above, was found. Its energy and intensity (in percent for 1 decay event) are shown in Table III.

The intensity of the γ-lines associated with the $Mn^{56}$ decay were determined by comparison with the J line•• the intensity of which was determined by a measurement of the γ-ray spectrum in neutron capture. In this spectrum the lines marked 22, 23, and 25 apparently correspond to the B, V, and G lines in the γ-ray spectrum associated with the $Mn^{56}$-decay.

Decay schemes for $Mn^{56} \xrightarrow{\beta^-} Fe^{56}$ [2], [11], (and also for $C^{56} \xrightarrow[K\text{-capture}]{\beta_1^+} Fe^{56}$) are shown in Fig. 8.••• The G and A γ-lines discovered in the present work fit in well with the level scheme for the $Fe^{56}$ nucleus and correspond to transitions from the 3.37 Mev level to the first excited state and the ground state. This situation indicates the existence of an additional β-decay branch in $Mn^{56}$ (denoted in Fig. 8 by the dotted line). It is note-

• In what follows we will call this the initial state.

••[Lettering scheme given in text and diagrams is transliterated from the Russian and is consistent within this paper – Translator's note.]

••• We also include the levels for the $Fe^{56}$ nucleus found in studies of the $Fe^{56}$ (p,p') $Fe^{56}$ reaction [12].

worthy that while for the 2.67 and 2.97 Mev levels the transition to the first excited state is 50-100 times stronger than the transition to the ground state, in the 3.37 Mev level the intensities of the corresponding transitions are approximately the same. This difference may be explained by assuming that the moment in the 3.37 Mev level is equal to 1.

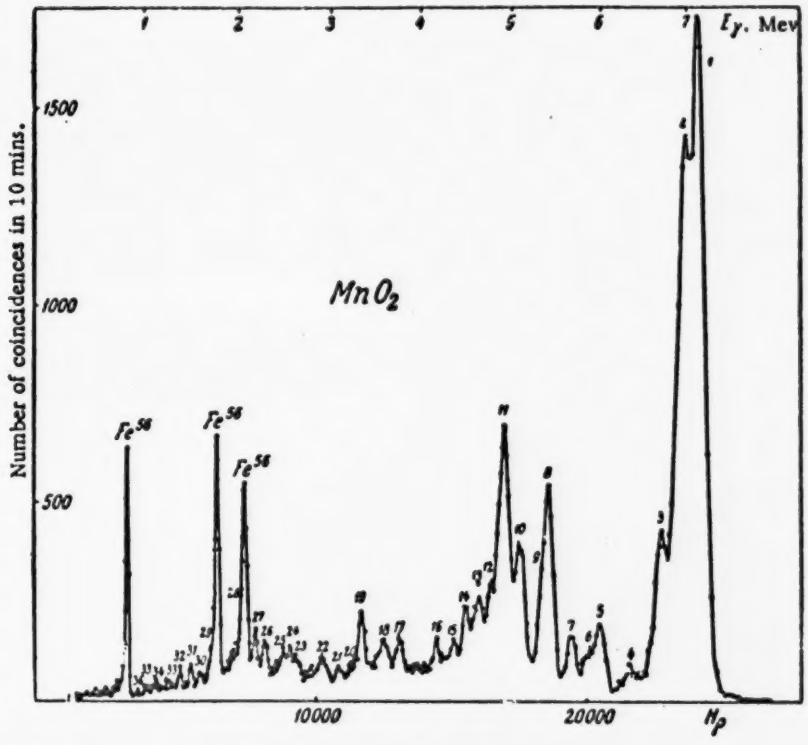


Fig. 4. Raw γ-ray spectrum in $MnO_2$.

Although the levels in the $Mn^{56}$ nucleus have been investigated several times using the (d, p) reaction [13], the results of different work are in poor agreement and have not been used by us. In setting up the γ-transition scheme shown in Fig. 9 it has been assumed that most of the γ-rays with energies greater than half the binding energy correspond to transitions from the initial state to the corresponding level of the nucleus.

The ground state of $Mn^{56}$ is $2^+$ [14]. The initial state of $Mn^{56}$ may be $2^-$ or $3^-$. In Ref. [15], in which the capture of polarized neutrons, polarized by $Mn^{56}$, was studied, it was established that the capture cross section is larger in the case in which the spin of the neutron is antiparallel to the moment of the target nucleus. Hence, it is more probable that the initial state of $Mn^{56}$ is $2^-$. The No. 1 transition is of type E1. It is reasonable to assume that the other transitions from the original state, with intensities of the same order of magnitude, are also E1 transitions. This situation limits the choice for the corresponding excited levels to $1^+$, $2^+$ and $3^+$.

## Cobalt

The sample contained 335 grams of cobalt oxide $Co_2O_3$. The γ-ray spectrum was investigated in the region 0.25-8 Mev.

The raw γ-ray spectrum for cobalt is shown in Fig. 10. In the same figure is shown the portion of the spectrum below 1 Mev, taken with a radiator thickness of 25 μ. The corrected γ-ray spectrum for cobalt is shown in Fig. 11. In Table IV are shown the energies and intensities found in the present work and the data obtained by other authors, all of which are in good agreement. The γ-ray intensities were found by normalizing

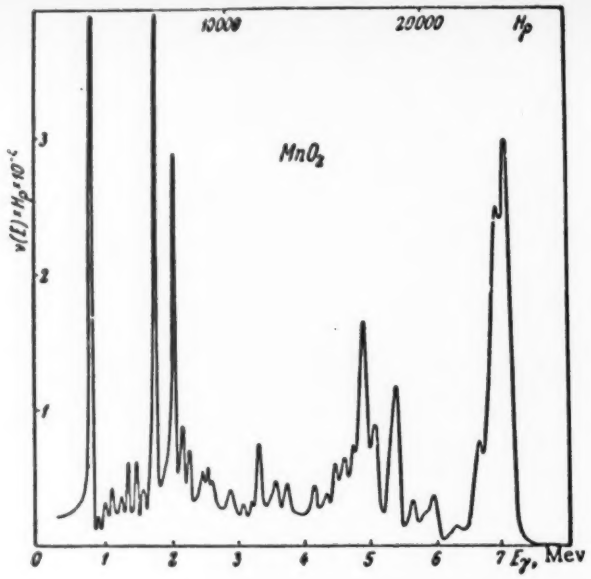


Fig. 5. Corrected γ-ray spectrum in $MnO_2$.

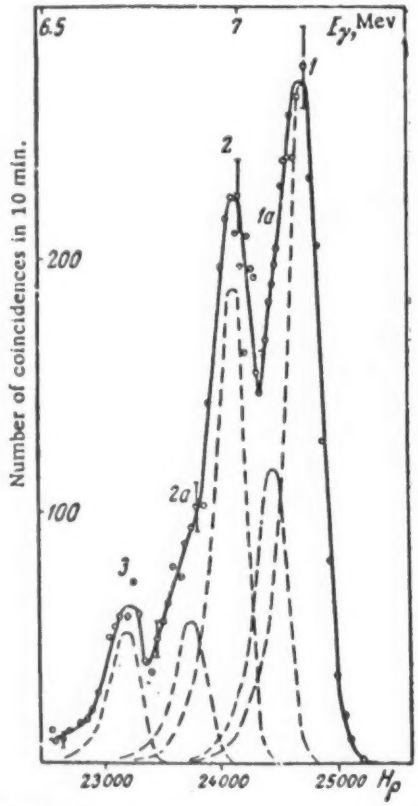


Fig. 6. Portion of the raw γ-spectrum for $MnO_2$ in the region from 6.5 to 7 Mev. The half-width of the peak is 1.3 precent.

the radiated energy with respect to the neutron binding energy. The line numbered 38 coincides with the energy of positron annihilation line; however, it is possible that this line is partly due to a transition in $Co^{60}$. The gamma-rays, on which the data is given in Table IV, are responsible for 67% of the energy radiated by the $Co^{60}$ nucleus.

In Fig. 12 is shown the γ-transition scheme in $Co^{60}$. To set up this scheme we have used data on the energy levels found from (d, p) reactions [16]. The authors of Ref. [16] found a discrepancy between the binding energy of the last neutron $B_n = 7.509 \pm 0.003$ Mev obtained from the $Co^{59}$ (d, p) $Co^{60}$ reaction and the energy $E\gamma = 7.486 \pm 0.006$ Mev found by Bartholomew and Kinsey [3] for the γ-line designated 1 (γ-ray with greatest energy). Hence there is some question as to whether this line corresponds to the transition to the ground state of $Co^{60}$ as assumed by Bartholomew and Kinsey, or the transition to an isomeric state with an energy of 0.059 Mev. Recently published data on the mass of $Co^{59}$ [17] makes it possible to calculate the binding energy of the last neutron in $Co^{60}$. The value which is obtained $B_n = 7.498 \pm 0.007$ tends to support the suggestion of Bartholomew and Kinsey.

The binding energy of the last neutron can also be found from the sum of the γ-line energies appearing in the cascade (Table V).

Table V gives some idea as to the accuracy with which the γ-transitions found in the present work fit in with the level scheme.

TABLE 2

Energies and Intensities of γ-rays in Manganese

| Line No. | Results of the present work | | Results of Bartholomew and Kinsey | | Results of Reier and Shamos | Results of Hammermesh and Hummel |
|---|---|---|---|---|---|---|
| | $E_\gamma$ Mev | $I$*) | $E_\gamma$ Mev | $I$*) | $E_\gamma$ Mev | $E_\gamma$ Mev |
| 1 | 7.26±0.01 | 12.3 | 7.261±0.006 | 12 | | 7.2 |
| 1a | 7.15±0.03 | 5.5 | 7.15±0.02 | 4 | | |
| 2 | 7.04±0.015 | 9.1 | 7.048±0.008 | 6.5 | | |
| 2a | 6.96±0.03 | 2.7 | | | | |
| 3 | 6.79±0.02 | 2.5 | 6.779±0.008 | 2.5 | | |
| 4 | 6.41±0.02 | 0.3 | 6.43±0.01 | 0.5 | | |
| 5 | 6.10±0.015 | 2.1 | 6.11±0.01 | 1 | | |
| 6 | 5.92±0.02 | 0.8 | 5.91±0.02 | 0.5 | | |
| 7 | 5.76±0.015 | 1.7 | 5.77±0.01 | 1 | | |
| | — | — | 5.63±0.02 | 0.3 | | |
| 8 | 5.52±0.015 | 6 | 5.528±0.01 | 4 | | |
| 9 | (5.41±0.03)**) | 1.5 | — | — | | |
| 10 | 5.20±0.015 | 4.5 | 5.21±0.01 | 3 | | |
| 11 | 5.03±0.015 | 9.3 | 5.04±0.02 | 6 | | 5.0 |
| 12 | 4.85±0.03 | ~2.8 | 4.81±0.01 | 2 | | |
| 13 | 4.72±0.025 | ~3.2 | 4.72±0.02 | 2 | | |
| 14 | 4.56±0.025 | ~2.4 | 4.55±0.01 | 2 | | |
| 15 | 4.42±0.02 | ~1.1 | — | — | | |
| 16 | 4.21±0.02 | 1.3 | 4.24±0.01 | 2 | | |
| | | | 4.10±0.03 | 1 | | |
| 17 | 3.83±0.02 | 1.5 | 3.82±0.02 | 1 | | |
| 18 | 3.64±0.02 | 1.6 | | | | |
| 19 | 3.42±0.015 | 3.1 | | | | |
| 20 | (3.25±0.02) | ≥0.5 | | | | |
| 21 | 3.12±0.02 | ≥0.5 | | | | |
| 22 | 2.96±0.02 | ≥1.1 | | | | |
| 23 | 2.66±0.02 | ≥1.2 | | | | |
| 24 | 2.60±0.02 | ≥1.6 | | | | |
| 25 | 2.52±0.02 | ≥1.6 | | | | |
| 26 | 2.34±0.01 | 2.8 | | | | |
| 27 | 2.22±0.01 | 3.8 | | | | |
| | 2.12±0.01 | 18 | | | 2.05 | |
| 28 | 2.05±0.02 | 2.2 | | | | |
| | 1.81±0.01 | 27 | | | 1.77 | |
| 29 | 1.73±0.015 | 2.2 | | | | |
| 30 | (1.62±0.015) | ~1.2 | | | | |
| 31 | 1.53±0.01 | 3.4 | | | | |
| 32 | 1.405±0.01 | 3.2 | | | | |
| 33 | (1.32±0.015) | ~1.1 | | | | |
| 34 | 1.15±0.01 | ~1.7 | | | | |
| 35 | 1.05±0.01 | ~1.6 | | | | |
| 36 | 0.97±0.01 | 1.2 | | | | |
| | 0.852±0.005 | 99 | | | 0.82 | |
| 37 | | | | | 0.308±0.015 | |
| 38 | | | | | 0.266±0.015 | |
| 39 | | | | | 0.206±0.01 | 0.190 |
| 40 | | | | | 0.098±0.005 | 0.090 |

*) Intensities in quanta per hundred neutron captures.

**) The energies of γ-lines whose existence was not established reliably are shown in brackets.

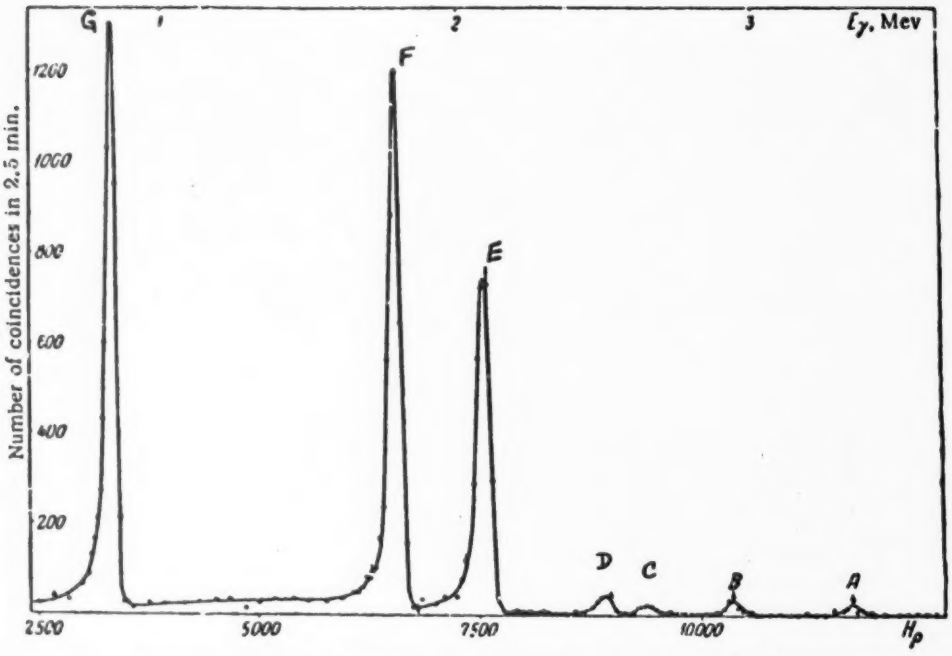


Fig. 7. Raw γ-ray spectrum accompanying decay of $Mn^{56}$.

TABLE 3

Energies and Intensities of γ-rays Accompanying β-decay in $Mn^{56}$

| Results of the present work | | | Results of other authors [11] | |
|---|---|---|---|---|
| Line No. | $E_\gamma$ Mev | Intensity percent per decay | $E_\gamma$ Mev | Intensity percent per decay |
| G | 0.855±0.005 | 99 | 0.845±0.015 | 100 |
| F | 1.814±0.008 | 23 | 1.8 ±0.04 | 30 |
| E | 2.117±0.008 | 15 | 2.13±0.04 | 20 |
| D | 2.518±0.010 | 0.6 | | |
| C | 2.672±0.010 | 0.26 | 2.7±0.2 | ~0.1 |
| B | 2.97±0.015 | 0.3 | 3.0±0.1 | ~0.2 |
| A | 3.37±0.015 | 0.3 | | |

The ratio of the sums of the intensities for γ-transitions in the ground state and isomeric state with an energy of 0.059 Mev are in agreement with the ratio of the corresponding activation cross sections 1.4 ± 0.6 [18].

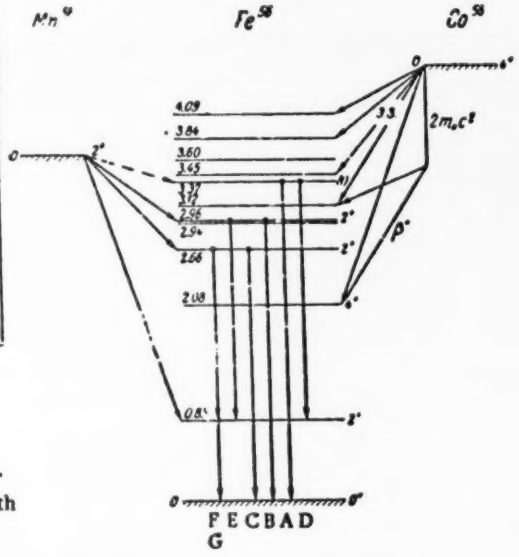


Fig. 8. β-decay scheme for $Mn^{56}$ and $Co^{56}$.

TABLE 4

Energies and Intensities of γ-rays in Cobalt

| Results of the present work | | | Results of Kinsey and Bartholomew [4] | | Results of Estulin et al. [23] | | Results of Reardon et al. [25] | | Results of Reier and Shamos [5] | Results of Hamermesh and Hummel [24] |
|---|---|---|---|---|---|---|---|---|---|---|
| line No. | $E_\gamma$ Mev | $I^*$) | $E_\gamma$ Mev | $I^*$) | $E_\gamma$ Mev | $I^*$) | $E_\gamma$ Mev | relative intensities | $E_\gamma$ Mev | $E_\gamma$ Mev |
| 1 | 7.49 ±0.01 | 2.7 | 7.486±0.006 | 3 | | | | | | 7.0 |
| 2 | 7.20 ±0.01 | 4.4 | 7.201±0.006 | 4 | | | | | | |
| | — | — | 7.041±0.01 | 1.3 | | | | | | |
| 3 | 6.98 ±0.025 | ~3 | 6.974±0.01 | 2.5 | | | | | | |
| 4 | 6.87 ±0.01 | 8.8 | 6.867±0.006 | 7 | | | | | | |
| 5 | 6.68 ±0.01 | 8.9 | 6.690±0.006 | 6 | | | | | | |
| 6 | 6.48 ±0.01 | 6.5 | 6.474±0.006 | 5 | | | | | | |
| 7 | 6.25 ±0.03 | 1 | 6.250±0.009 | 0.7 | | | | | | |
| | — | — | 6.110±0.015 | 0.5 | | | | | | |
| 8 | 5.97 ±0.02 | 9.8 | 5.966±0.006 | 5.6 | | | | | | |
| | — | — | 5.726±0.01 | 1.7 | | | | | | 5.8 |
| 9 | 5.67 ±0.03 | 12.6 | 5.646±0.006 | 6.3 | | | | | | |
| 10 | 5.33 ±0.03 | ⩾0.6 | 5.351±0.01 | 0.7 | | | | | | |
| 11 | 5.19 ±0.02 | 2.9 | 5.179±0.01 | 2 | | | | | | |
| 12 | 4.90 ±0.02 | 3.1 | 4.903±0.008 | 2.5 | | | | | | |
| 13 | 4.60 ±0.03 | ⩾1.2 | 4.59 ±0.02 | 0.6 | | | | | | |
| 14 | 4.35 ±0.03 | ⩾0.8 | 4.37 ±0.02 | 1 | | | | | | |
| 15 | 4.16 ±0.03 | ⩾0.8 | 4.18 ±0.02 | 0.8 | | | | | | |
| 16 | 4.00 ±0.03 | ⩾0.9 | 4.03 ±0.02 | 1 | | | | | | |
| 17 | 3.92 ±0.03 | ⩾1.8 | | | | | | | | |
| 18 | 3.72 ±0.03 | ⩾1.5 | 3.69 ±0.02 | 0.7 | | | | | | |
| 19 | 3.60 ±0.03 | ⩾0.8 | | | | | 3.58 | 19 | | |
| 20 | (3.35 ±0.03) | ⩾0.4 | 3.36 ±0.02 | 1 | | | | | | |
| 21 | (3.21 ±0.03) | ⩾0.7 | | | | | | | | |
| 22 | (2.88 ±0.02) | ⩾0.3 | | | | | | | | |
| 23 | (2.59 ±0.02) | ⩾0.6 | | | | | | | | |
| 24 | 2.30 ±0.02 | ⩾0.9 | | | | | | | | |
| 25 | 2.20 ±0.02 | ⩾0.9 | | | | | | | | |
| 26 | 2.03 ±0.02 | ⩾0.9 | | | | | 2.00 | 20 | | |
| 27 | 1.84 ±0.01 | 4.8 | | | | | | | 1.82±0.04 | |
| 28 | 1.78 ±0.01 | 2.4 | | | | | | | | |
| 29 | 1.69 ±0.01 | 1 | | | | | | | | |
| 30 | (1.60 ±0.01) | ⩾0.5 | | | | | | | | |
| 31 | 1.520±0.005 | 5 | | | | | | | 1.48±0.04 | 1.5 |
| 32 | 1.25 ±0.03 | ~1.2 | | | | | 1.30 | 19 | | 1.1 |
| 33 | 0.96 ±0.01 | 3.6 | | | | | | | | |
| 34 | 0.91 ±0.01 | 2.6 | | | | | | | | |
| 35 | 0.80 ±0.01 | 5.8 | | | | | | | 0.82±0.02 | |
| 36 | 0.735±0.005 | 5 | | | | | | | 0.65±0.02 | |
| 37 | 0.562±0.005 | 13.5 | | | | | | | | |
| 38 | 0.511±0.005 | ~11 | | | | | 0.52 | 100 | | |
| 39 | 0.454±0.005 | 8 | | | | | | | | |
| 40 | 0.290±0.01 | >10 | | | 0.276±0.004 | 22 | | | 0.289±0.01 | |
| 41 | | | | | 0.226±0.004 | 22 | | | 0.237±0.005 | 0.220 |

*) Intensity in quanta per hundred neutron captures.

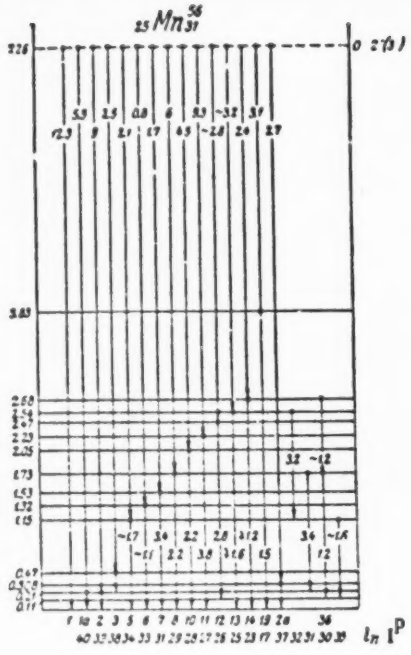


Fig. 9. γ-transition scheme in $Mn^{56}$.

TABLE 5

Sum of Energies of γ-lines in a Cascade

| Designation of the line appear-appear in the cascade | Sum of line energies, Mev |
|---|---|
| 2; 40 | 7.49 ±0.02 |
| 3; 39; 0.059 Mev | 7.493±0.03 |
| 4; 37; 0.059 Mev | 7.487±0.015 |
| 5; 35 | 7.47 ±0.02 |
| 6; 33; 0.059 Mev | 7.499±0.02 |
| 7; 32 | 7.50 ±0.06 |
| 8; 31 | 7.49 ±0.025 |
| 9; 27 | 7.51 ±0.04 |
| 11; 24 | 7.49 ±0.04 |
| 12; 23 | 7.49 ±0.04 |
| 13; 22 | 7.48 ±0.05 |
| Mean value | 7.491±0.01 |

According to some data, the resonance at 134 ev, lying closest to the original state of cobalt, which is apparently determined by thermal neutron capture, has $4^-$ [19]; other data indicate $3^-$ [20]. The existence of a comparatively strong transition between the initial state and the ground state, having $5^+$ [21] would tend to support the first value.

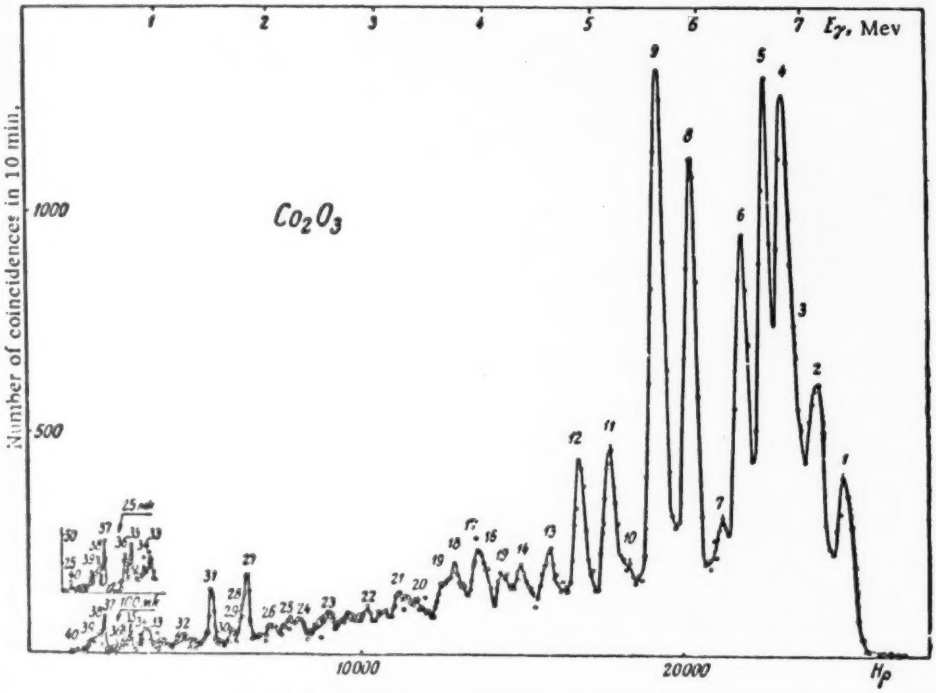


Fig. 10. Raw γ-ray spectrum in $Co_2O_3$.

TABLE 6

Energies and Intensities of γ-rays in Aluminum

| Results of the present work | | | Results of Kinsey et al.[22] | | Results of Braid[6] | |
|---|---|---|---|---|---|---|
| line number | $E_\gamma$ Mev | $I^*$) | $E_\gamma$ Mev | $I^*$) | $E_\gamma$ Mev | $I^*$) |
| 1 | 7.73±0.015 | 24 | 7.724±0.006 | 35 | | |
| | -- | — | 7.34±0.04 | 0.7 | | |
| | -- | — | 6.98±0.04 | 0.7 | | |
| 2 | 6.76±0.02 | 1.7 | 6.77±0.02 | 1.4 | | |
| | — | — | 6.61±0.03 | 0.4 | | |
| | — | — | 6.50±0.03 | 0.4 | | |
| 3 | 6.35±0.02 | 2.3 | 6.33±0.02 | 2 | | |
| | — | — | 6.22±0.03 | 0.7 | | |
| 4 | 6.13±0.02 | 3 | 6.13±0.02 | 2 | | |
| | — | — | 6.01±0.05 | 0.7 | | |
| 5 | (5.88±0.03) | 0.8 | 5.89±0.04 | 1.0 | | |
| | -- | — | 5.78±0.03 | 1.4 | | |
| | — | — | 5.60±0.02 | 3 | | |
| 6 | 5.45±0.25 | 1.6 | 5.41±0.03 | 3 | | |
| | — | — | 5.32±0.03 | 1 | | |
| | — | — | 5.21±0.02 | 3 | | |
| 7 | 5.14±0.015 | 3.9 | — | — | | |
| 8 | 4.91±0.02 | 2.4 | 4.94±0.05 | 1.4 | | |
| 9 | 4.73±0.015 | 8 | 4.79±0.02 | 9 | | |
| 10 | 4.66±0.02 | 5 | 4.66±0.05 | 7 | | |
| 11 | 4.42±0.02 | 1 | 4.45±0.02 | 3 | | |
| 12 | 4.26±0.015 | 6.1 | 4.29±0.02 | 8 | | |
| 13 | 4.13±0.02 | 6 | 4.16±0.02 | 6 | | |
| | — | — | 4.06±0.04 | 3 | | |
| 14 | 3.88±0.02 | 6 | 3.88±0.02 | 8 | | |
| 15 | (3.80±0.03) | 1.3 | — | — | | |
| 16 | 3.60±0.015 | 4.5 | 3.62±0.02 | 6 | | |
| 17 | 3.47±0.015 | 5.2 | 3.46±0.02 | 4 | | |
| 18 | (3.32±0.03) | 0.6 | 3.29±0.02 | 5 | | |
| 19 | 3.04±0.01 | 5.1 | 3.02±0.05 | 15 | | |
| 20 | 2.96±0.015 | 8 | — | — | ~3.1 | |
| 21 | 2.82±0.02 | ~2 | 2.84±0.03 | 13 | ~2.8 | 42 |
| 22 | 2.61±0.01 | 5 | | | ~2.5 | |
| 23 | 2.28±0.01 | 5.1 | | | 2.26±0.03 | 14 |
| 24 | 2.12±0.02 | 3 | | | | |
| | 1.78±0.01 | 100 | | | 0.97±0.03 | 10 |

• Intensity in quanta per hundred neutron captures.

## Aluminum

The sample which was investigated contained 99.99% aluminum. The aluminum γ-ray spectrum was investigated in the energy region 0.3-8 Mev. In Figs. 13 and 14 are shown respectively the raw and corrected spectra. The dotted lines indicate the portion of the spectrum in which the γ-lines at 7.38 Mev are subtracted out; these were assigned to the nucleus $Pb^{208}$ (lead cap).

In Table 6 we show the energy and intensities of γ-rays in aluminum obtained in the present work and by other authors.• The intensity was determined by normalizing the radiated energy with respect to the neutron

• In the work by Kinsey and Bartholomew [22] the γ-spectrum in $Al^{28}$ was measured with a half-width of 65 kev; thus these authors were able to distinguish more lines at energies above 5 Mev than was possible in the present work.

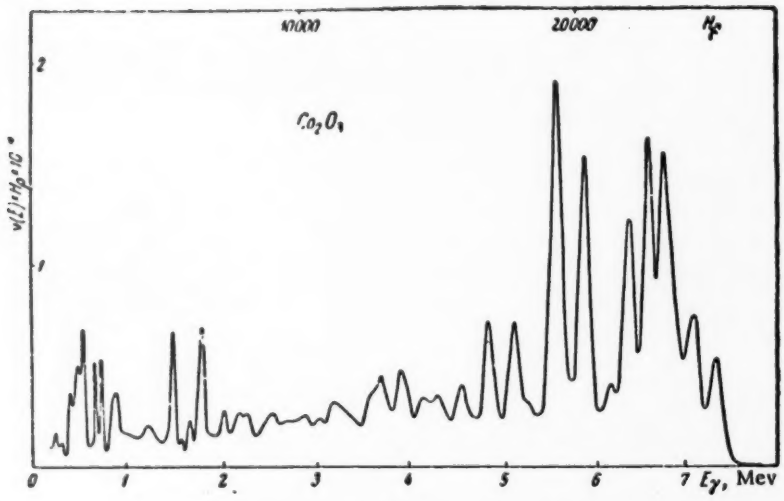


Fig. 11. Corrected γ-ray spectrum in $Co_2O_3$.

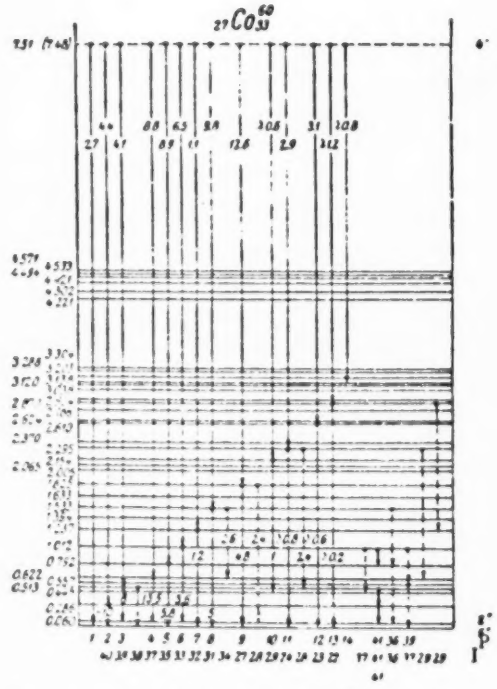


Fig. 12. γ-transition scheme in $Co^{60}$.

binding energy and by comparison with the γ-line ($E_\gamma$ = = 1.78 (Mev) in $Si^{28}$ found in the decay of $Al^{28}$. The intensity values found by both methods were in agreement.

The gamma rays resolved in the aluminum spectrum (with the exception of the line at 1.78 Mev characteristic of $Al^{28}$ decay) were responsible for 69% of the energy radiated by $Al^{28}$.

In Fig. 15 we show the γ-transition scheme for the $Al^{28}$ nucleus. The data on the energy levels were taken from Ref. [26].

On the right in Fig. 15 are shown the values of the orbital momentum carried into the nucleus by the neutron in the (d, p) reaction [27] as well as the total momenta at parity forseveral levels obtained in a study of the β-decay reaction $Mg^{28} \xrightarrow{\beta^-} Al^{28} \xrightarrow{\beta^-} Si^{28}$ [28]. In spite of the large number of levels, the assignment of γ-transitions to a definite cascade is established uniquely in the majority of cases. In some cases the γ-transition sequence in the cascade is not unique. In these cases the various possibilities are shown in the diagram with the less probable transition shown by dotted lines. To determine the more probable transition use was made of the fact that of two γ-transitions in a cascade going through a highly excited level, the first γ-transition should be more intense than the subsequent transition. However, the ambiguity remains in lines 9 and 20, in which both transitions are of the same intensity.

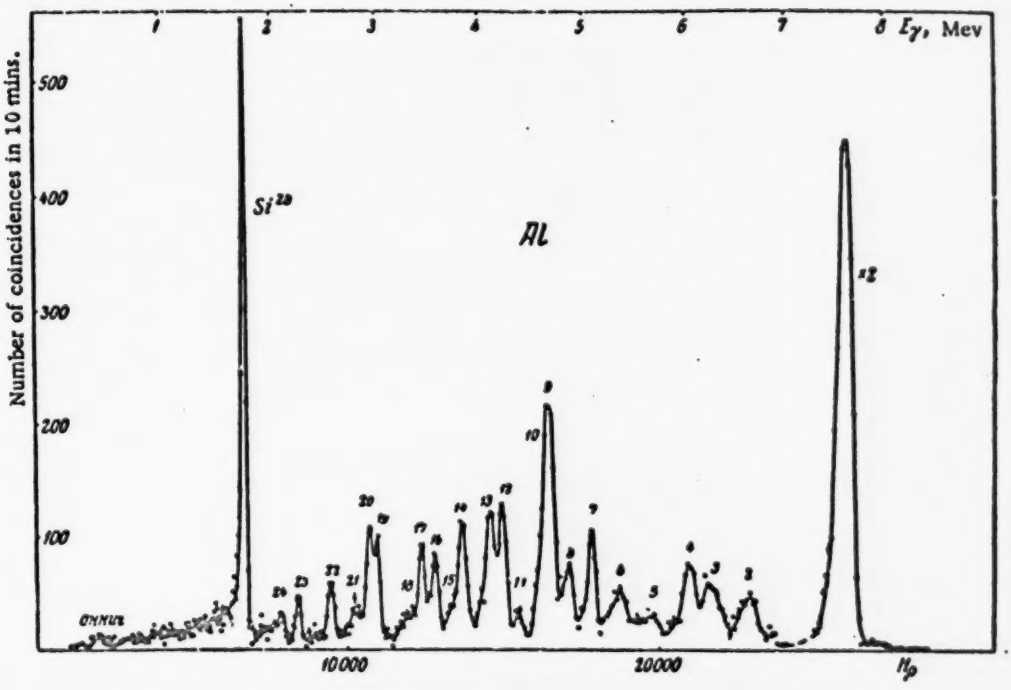


Fig. 13. Raw γ-ray spectrum in Al.

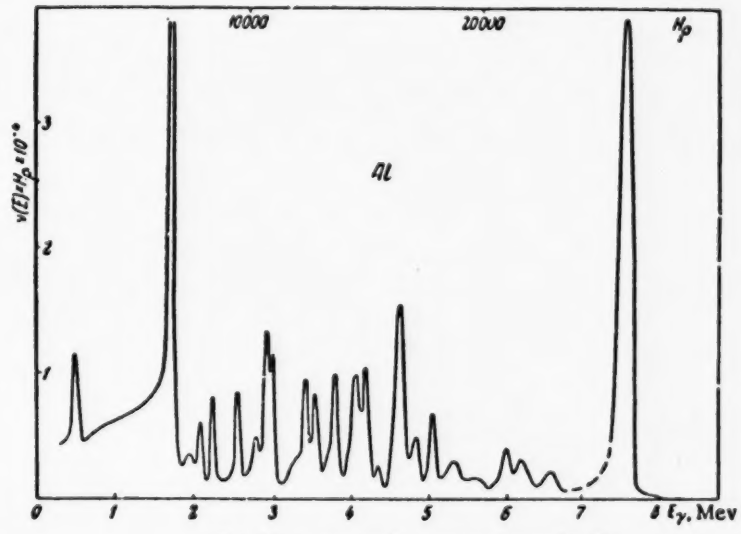


Fig. 14. Corrected γ-ray spectrum in Al.

The multipole-order of the γ-transitions from the original state can be determined from the same considerations as used in the $V^{52}$ case. Transitions going to a level with odd $I_n$ are E1 transitions while transitions to a level with even $I_n$ are M1 (with a possible admixture of E2).

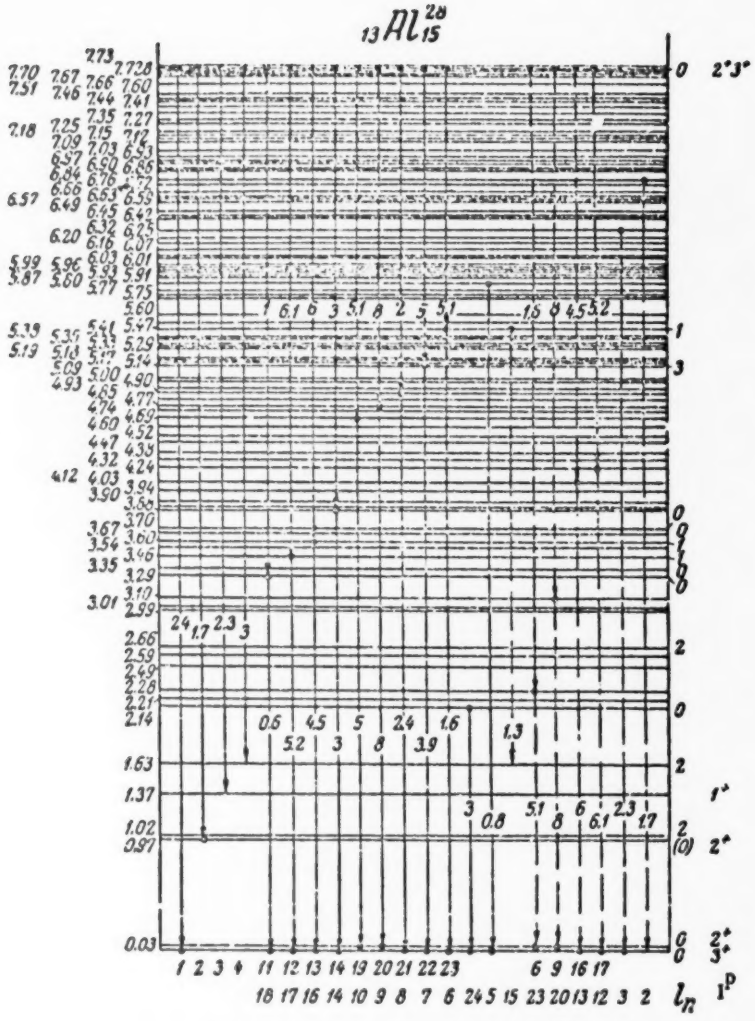


Fig. 15. γ-transition scheme in $Al^{28}$.

In Fig. 16 is shown a comparison of proton yields in (d, p) reactions (at $\theta = 90°$ with a deuteron energy of 1.8 Mev) for different levels in the $Al^{28}$ nucleus [25] and the relative intensities of the γ-transitions from the initial state to the corresponding level. The excitation energy of the nucleus is plotted horizontaliy. The relative γ-transitions,intensities, and proton yields are shown by vertical lines; for the γ-transitions the line lengths are proportional to the number of γ-photons in one neutron capture, divided by $E^3_{\gamma i}$, where $E_{\gamma i}$ is the energy of the corresponding γ-transition. Division of the intensity by $E^3_{\gamma i}$ compensates for the energy dependence of the transition if the transition from the initial state is a dipole transition.

It is apparent from Fig. 16 that the most intense γ-transitions are to levels which, for the conditions indicated above, have the largest cross section for the (d, p) reaction. In this same figure are shown similar diagrams for the next even-odd nucleus $_{14}Si^{29}_{15}$, having the same neutron configuration as $_{13}Al^{28}_{15}$. The same relationship is observed in this case.

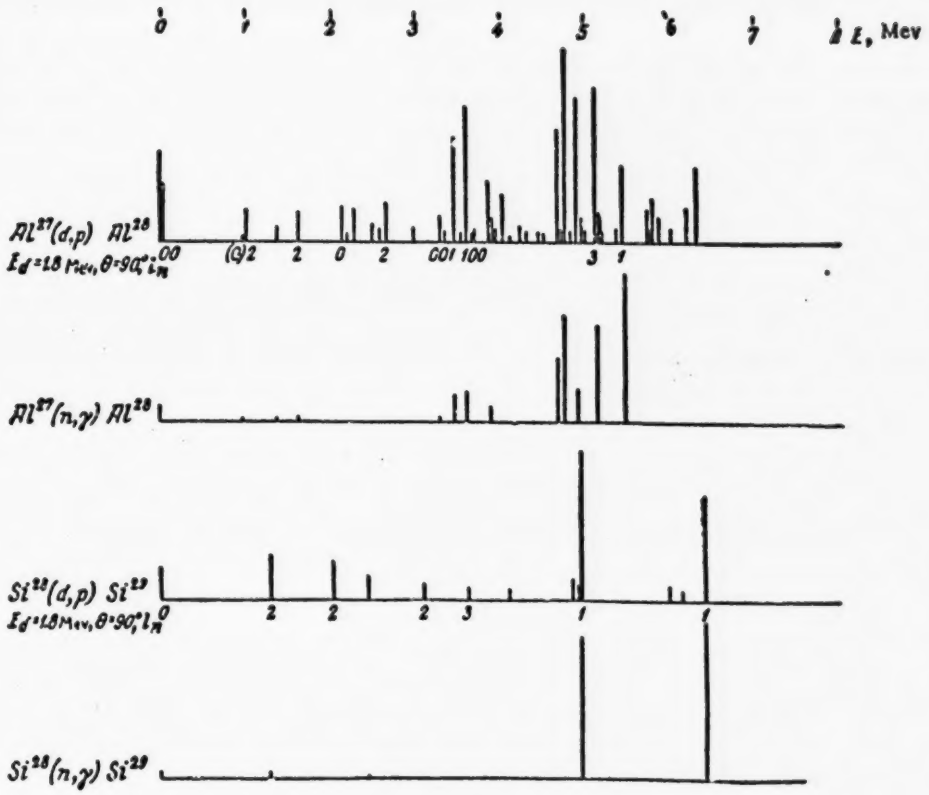


Fig. 16. Comparison of proton yields in (d, p) reactions for different levels in $Al^{25}$ [25] and $Si^{29}$ [30] nuclei, and relative probabilities of the γ-transitions from the initial state to the corresponding levels in the reaction (n, γ).

TABLE 7

Comparison of Experimental and Theoretical Radiative Widths

| Radiating nucleus | Total radiative width $\Gamma_\gamma$, ev | Mean distance between level | Transition energy $E_\gamma$, Mev | Intensity, quanta per neutron capture | Type of transition | $\frac{\Gamma_i\ exp}{2\ D\Gamma_i\ theo}$ |
|---|---|---|---|---|---|---|
| $V^{52}$ | 1.0 [4] | 0.002 [32] | 7.3 | 0.057 | *E1* | 0.024 |
| | | | 6.5 | 0.12 | *E1* | 0.07 |
| | | | 5.73 | 0.056 | *E1* | 0.05 |
| $Mn^{56}$ | 0.5 [31] | 0.002 [31] | 7.26 | 0.123 | *E1* | 0.024 |
| $Co^{60}$ | 0.5 [31] | 0.01 [31] | 7.49 | 0.027 | *E1* | 0.001 |
| $Al^{28}$ | 5 [4] | 0.05 [32] | 7.72 | 0.24 | *M1* | 1.2 |
| | | | 6.76 | 0.017 | *M1* | 0.14 |
| | | | 6.35 | 0.023 | *M1* | 0.2 |
| | | | 6.13 | 0.03 | *M1* | 0.3 |
| | | | 4.42 | 0.01 | *M1* | 0.3 |
| | | | 4.26 | 0.06 | *E1* | 0.04 |
| | | | 4.13 | 0.06 | *E1* | 0.04 |
| | | | 2.28 | 0.05 | *E1* | 0.2 |
| | | | 2.61 | 0.05 | *E1* | 0.14 |

The total radiated widths and level densities at excitation energies equal to the neutron binding energy, are known for $V^{52}$, $Mn^{56}$, $Co^{60}$ and $Al^{28}$. Using the intensities in numbers of $\gamma$-photons per neutron capture obtained in the present work, it is possible to find the partial radiative widths for the $\gamma$-transitions from the initial state, the multipole order of which is known; these can then be compared with the values calculated from the formula given by Weisskopf as in Refs. [1], [4], and [33]. The comparison shown in Table VII indicates that the mean ratio $\Gamma_i^{exp}/2D\Gamma_i^{theor}$ 0.06 for E1-transitions and 0.4 for M1-transition. These results are in agreement with those obtained by Kinsey and Bartholomew [4] obtained with medium and heavy nuclei and with the results in light nuclei given a review by Wilkinson [33].

## LITERATURE CITED


[1] L. V. Groshev, B. P. Adyasevich and A. M. Demidov, Physics Research. (Report presented by the Soviet Delegation to the International Conference on the Peaceful Use of Atomic Energy, Geneva 1955) Izd. Akad. Nauk SSSR 1955, p. 252.

[2] B. S. Dzhelepov and L. K. Peker, Decay Schemes for Radioactive Isotopes, Izd. AN SSSR, 1957.

[3] G. A. Bartholomew and B. B. Kinsey, Phys. Rev. 89, 386 (1953).

[4] B. B. Kinsey and G. A. Bartholomew, Phys. Rev. 93, 1260 (1954).

[5] M. Reier and M. H. Shamos, Phys. Rev. 100, 1302 (1955).

[6] T. H. Braid, Phys. Rev. 102, 1109 (1956).

[7] Atlas of Neutron Cross Sections of the Elements, Izd. AN SSSR. 1955.

[8] R. Sher, J. Halpern and A. K. Mann, Phys. Rev. 84, 387 (1951).

[9] J. E. Swager and L. A. Cox, Phys. Rev. 92, 102 (1953).

[10] J. S. King and W. S. Parkinson, Phys. Rev. 89, 1080; 90, 381A (1953).

[11] L. G. Elliot and M. Detsch, Phys. Rev. 64, 321 (1943); G. R. Bishop, P. Wilson and H. Halban, Phys. Rev. 77, 416 (1950); A. Sakai, J. L. Dick, W. S. Anderson and J. D. Kurbatov, Phys. Rev. 95, 101 (1954).

[12] W. W. Buechner and A. Sperduto, Bull. Am. Phys. Soc. 1, No. 1, 39 (1956).

[13] A. B. Martin, Phys. Rev. 72, 378 (1947); W. D. Whitehead and N. P. Heydenburg. Phys. Rev. 79, 99 (1950); A. Abranov, DAN 73, 92 (1950).

[14] F. R. Metzger and W. B. Todd, Phys. Rev. 92, 904 (1953).

[15] S. Bernstein, L. D. Roberts, C. P. Stanford, L. W. T. Dabbs and T. E. Stephenson, Phys. Rev. 94, 1243 (1954).

[16] G. M. Fogelsong and D. G. Foxwell, Phys. Rev. 96, 1601 (1954).

[17] K. S. Quisenberry, T. T. Scolman and A. O. Nier, Phys. Rev. 104, 461 (1956).

[18] M. Deutsch and G. Scharf-Goldhaber, Phys. Rev. 83, 1059 (1951).

[19] E. R. Rae, The proceedings of the 1954 Glasgow conference on nuclear and meson physics. Pergamon Press, London, N.Y., 71, 1955.

[20] F. G. Seidl, D. J. Hughes, H. Palevsky, J. S. Levin, W. J. Kato and N. G. Sjöstrand, Phys. Rev. 95, 476 (1954).

[21] W. Dobrowolski, R. V. Jones and G. D. Jeffers, Phys. Rev. 101, 1001 (1956).

[22] B. B. Kinsey, G. A. Bartholomew and W. H. Walker, Phys. Rev. 83, 519 (1951).

[23] L. V. Estulin, L. F. Kalinkin and A. S. Melioransky, J. Exptl. Theoret. Phys. 31, 886 (1956).

[24] B. Hamermesh and V. Hummel, Phys. Rev. 88, 916 (1952).

[25] W. A. Reardon, R. W. Krone and R. Stump, Phys. Rev. 91, 334; 91, 442A (1953).

[26] W. W. Buechner, M. Mazari and A. Sperduto, Phys. Rev. 101, 188 (1956).

[27] H. A. Enge, W. W. Buechner, A. Sperduto and M. Mazari, Bull. Am. Phys. Soc. 1, No. 4, 212 (1956).

[28] R. K. Sheline, N. R. Johnson, P. R. Bell, R. C. Davis and F. K. McGowan, Phys. Rev. 94, 1642 (1954).

[29] H. A. Enge, W. W. Buechner and A. Sperduto, Phys. Rev. 88, 963 (1952).

[30] D. M. Van Patter and W. W. Buechner, Phys. Rev. 87, 51 (1952).

[31] J. S. Levin and D. J. Hughes, Phys. Rev. 101, 1328 (1956).

[32] T. D. Newton, Can. J. Phys. 34, 804 (1956).

[33] D. H. Wilkinson, Phil. Mag. 1, 127 (1956).

Received March 23, 1957

BLANK
PAGE

# THE (p, n) REACTION IN LITHIUM AND THE GROUND STATE OF $Be^6$

G. F. Bogdanov, N. A. Vlasov, S. P. Kalinin, B. V. Rybakov and V. A. Sidorov.

Using a time-of-flight method the neutron spectra in the $Li^6$ + + p and $Li^7$ + p reactions have been investigated at a proton energy of 9 Mev. Neutron groups have been found in the (p, n) reaction corresponding to the ground state in $Be^6$ and the three lowest states of $Be^7$ as well as a continuous neutron spectrum at lower energy, due to more complicated reactions. The observation of the neutron group for the $Li^6(p, n)Be^6$ reaction is the first experimental indication of the existence of the $Be^6$ nucleus. The energy of the $Li^6(p, n)Be^6$ reaction is 5.2 Mev, the width of the ground state in $Be^6$ is $T < 0.3$ Mev. The differential cross sections for neutron formation have been measured at 0, 15, 30, 60 and 120°.

The experimental determination of the energy levels in the $Be^6$ nucleus is of interest because $Be^6$ is the third member of the isobaric triplet $He^6-Li^6-Be^6$; in the first two members of this triplet the energies are known for several similar states with isotopic spin T = 1. A comparison of the energies of similar levels in all three nuclei is important in connection with the verification of the charge invariance of nuclear forces and a determination of the Coulomb energy of these nuclei.

At the present time, with a single exception, there are no published experimental data on the existence of $Be^6$; this exception is an erroneous report given by Tyren and Tove [1] concerning the observation, in the product obtained by bombarding lithium and beryllium by protons, of a radioactive effect with a half life of 0.4 seconds, this being assigned to $Li^4$ or $Be^6$. An estimate of the energy of the ground state of $Be^6$, carried out on the basis of the known states of the neighboring nuclei [2], shows that the $Be^6$ nucleus is unstable against decay into an $\alpha$-particle and two protons; consequently its lifetime is very small. In this respect the $Be^6$ nucleus is similar to light nuclei such as $He^5$, $Li^5$ and $Be^8$. However, in spite of the short lifetimes these nuclei have a spectrum of discrete energy levels. It would be expected that $Be^6$ would also have a complete series of energy states.

In the present work we have investigated the spectrum associated with the neutrons formed when lithium isotopes are bombarded with 9.6-Mev protons. It was the purpose of this work to measure the energy of the ground state of the $Be^6$ nucleus, formed as a result of the $Li^6(p, n)Be^6$ reaction.

## METHOD OF MEASUREMENT

The work was carried out at the 1-1/2 meter cyclotron of the Institute for Atomic Energy, Academy of Sciences, U.S.S.R. [3], using a time-of-flight method with a single-channel fast neutron spectrometer. The 9.6-Mev protons were obtained by acceleration of molecular hydrogen ions. The proton energy was determined from range measurements in aluminum. An estimate of the monochromaticity of the beam carried out on the basis of the shape of the absorption curve in aluminum (due to straggling) indicated an energy spread of approximately ± 0.1 Mev.

In investigating the (p, n) reaction in lithium we used targets of natural lithium and lithium enriched in the $Li^6$ isotope, thus making it possible to distinguish between the effect of $Li^6$ and $Li^7$. In the experiment on

on the identification of the neutron group corresponding to the ground state of $Be^6$ and the measurement of the neutron angular distributions, targets 400 μ thick were used. In measuring the energy of the ground state of $Be^8$ and in estimating its width a target 90 μ in thickness was used.

The neutrons were detected by scintillation counter with a stilbene crystal (diameter 3 cm, height 2 cm) with a distance of one meter between the target and counter and with a tolane crystal (diameter 10 cm, height 4 cm •) at a distance of 7,3 meters. The general layout of the apparatus and the operation of the neutron spectrometer have been described in detail earlier [4]. The neutron source is pulsed because of the inherent modulation of the cyclotron beam. The photomultiplier pulses are fed to one arm of a coincidence circuit; control pulses, synchronized with the accelerating voltage of the cyclotron, are fed to the other arm. The distribution of neutron pulses in time is determined by measuring the coincidence counting rate as a function of delay of the control pulse. Zero time on the scale is established from the position of the γ-ray peak.

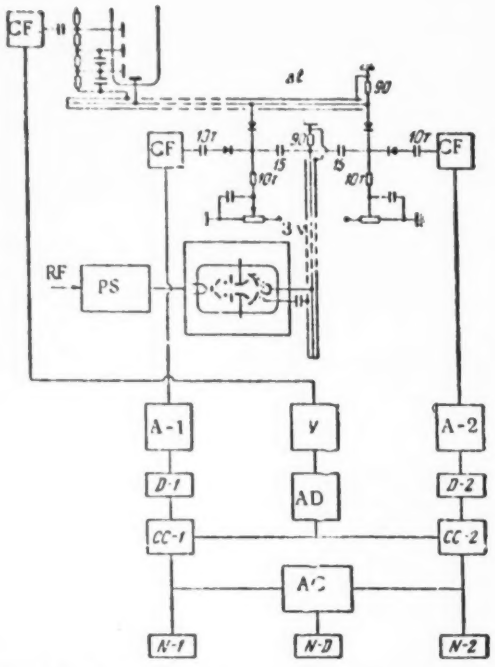

Fig. 1. Diagram of the time analyzer.

The simple coincidence circuit used earlier was found to have a number of shortcomings. In particular, its resolving time, determined by the pulse lengths, is a strong function of the amplitude of the photomultiplier pulses; this situation led to distortion of the neutron spectra when measurements were carried out over a wide range of neutron energy.

In the present work, instead of the simple coincidence circuit, use is made of a time analyzer with a differential channel, the width of which is virtually independent of the amplitude of the photomultiplier pulses.

The circuit of the time analyzer is shown in Fig. 1. It comprises two identical channels, each of which consists of a fast coincidence circuit, similar to that described earlier [4], a cathode follower (CF) and an amplifier (A-1 and A-2) with a discriminator (D-1 and D-2) at the output. One input of the coincidence circuit is common. The control pulses are fed to this input. The pulses from the photomultiplier anode are applied to the second inputs of the coincidence circuit. There is a delay $\Delta t$ between these inputs. The two fast coincidence channels and the anti-coincidence circuit between them (AC) comprise the differential channel of the analyzer (output N-D). The anti-coincidence circuit has a resolving time of approximately one microsecond and can distinguish those cases in which there is a pulse in the first channel and none in the second. The width of the differential channel is virtually equal to the time delay $\Delta t$ and does not depend on the duration of the pulses fed to the circuit. The width of each of the fast coincidence channels (outputs N-1 and N-2) is determined by the pulse duration, among other things, and can be made considerably larger than $\Delta t$.

It should be pointed out that the width of the differential channel is independent of the amplitude of the photomultiplier pulses; t position, however, can shift with a change in amplitude by an amount of the order of the rise time of the pulses from the photomultiplier (in the present case 2-3 millimicroseconds) when a wide amplitude range is used, as is required .. enhance the neutron detection efficiency, this shift leads to a certain impairment of the resolving power of the spectrometer.

The specifications of the time analyzer have been considerably improved through the use of an electron-beam tube with a plane deflected beam•• for forming the control pulses. In addition, the spectrometer contains

• The authors are indebted to their colleague at the Institute for Crystallography, Academy of Sciences, USSR, G. S. Velikov, L. M. Belyaev and G. F. Dobrzhansky for preparing high quality tolane crystals.

•• The authors are indebted to their colleagues at the Institute for Electronic and Electron Physics, Academy of Sciences USSR, E. V. Bykhovsky and A. M. Karchenko for furnishing us with a model of their newly-developed electron-beam tube.

an amplitude discriminator which makes it possible to vary the energy threshhold of the counter over wide limits and thus to make absolute measurements of neutron fluxes.

Pulses from one of the last dynodes of the photomultiplier are fed to the amplitude discriminator AD through a cathode follower and the amplifier A. The coincidence circuits CC1- and CC-2, which have a resolving time of approximately 1 microsecond select those pulses from the fast coincidence channels which fall within the desired amplitude limits.

To study the time distribution of pulses from the neutron counter the control-pulse delay is introduced by means of the phase-shifter PS, which shifts the sinusoidal radio-frequency voltage from the cyclotron RF before it is applied to the electron-beam tube.

In Fig. 2 are shown characteristic curves for the delayed coincidences in all three channels in detection of $\gamma$-rays from the target. The delay time $\Delta t$ is 5 millimicroseconds. The delayed-coincidence curve has approximately the same width at half height (curve D). The wide channels (curves 1 and 2) exhibit a flat top, corresponding to 100% efficiency in the fast-coincidence circuits. Thus it is possible to realize absolute measurements of intensities for narrow energy neutron groups; it is also possible to determine the effective width of the differential channel, the value of which is required for absolute measurements of continuous neutron spectra.

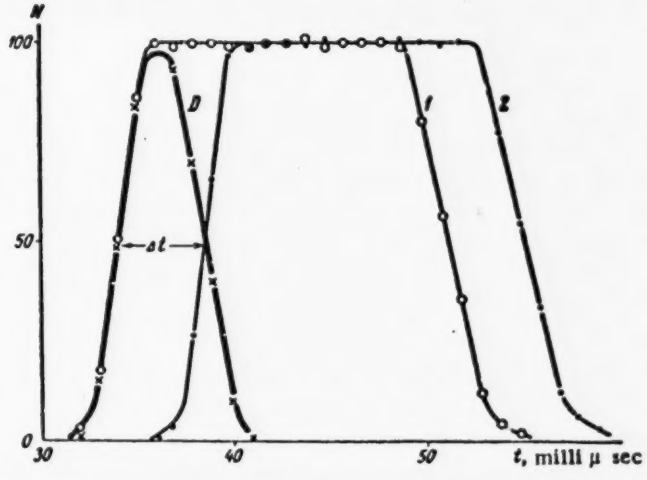


Fig. 2. Delayed coincidence curves in the differential (D) and the "wide" (1 and 2) channels of the time analyzer in detection of $\gamma$-rays from the target.

The energy of the recoil proton, corresponding to threshold, must be known for determining the efficiency of the scintillation counter. The calibration of the amplitude discriminator, which determines the counter threshold, was carried out by measuring the amplitude spectrum of the photomultiplier pulses corresponding to monoenergetic neutrons as selected by the time analyzer in time-of-flight measurements. Measurements at different neutron energies showed that the shape of the amplitude spectrum is in good agreement with the shape of the recoil-proton energy distribution, taking into account the nonlinear dependence of the light yield of the crystal on proton energy [5].

## RESULTS OF THE MEASUREMENTS

In Figs. 3 and 4 are shown the direct experimental time-of-flight neutron spectra for two targets with different $Li^6$ content. Fig. 3 pertains to lithium enriched by the $Li^6$ isotope (90.4% $Li^6$ + 9.6% $Li^7$); Fig. 4. pertains to natural lithium (7.5% $Li^6$ + 92.5% $Li^7$). The lithium was applied on a lead substrate. The measurements were carried out in turn with the target and with a "flag" (the lead carrier without the lithium); then the effects

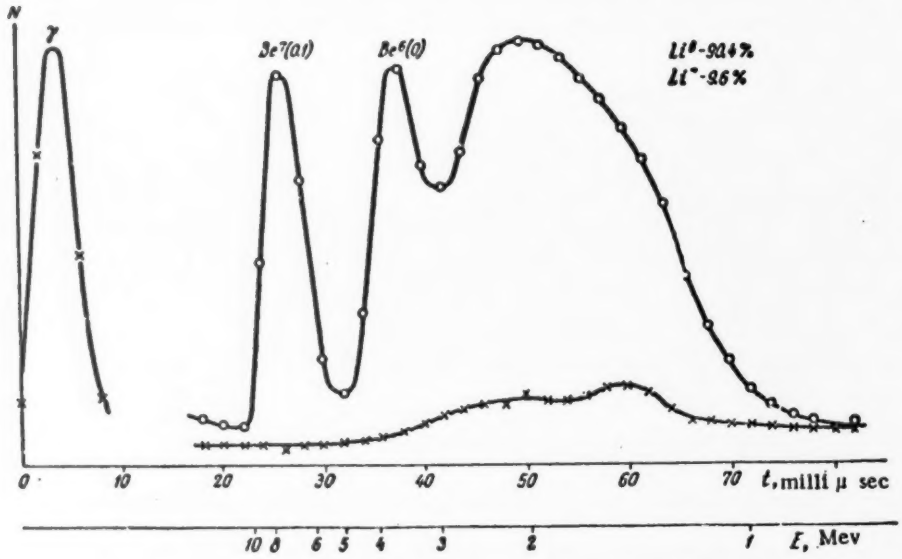


Fig. 3. Neutron distribution by time-of-flight using a lithium target enriched in the $Li^6$ isotope. The distance from the target to the counter is 1 meter. The lower curve is for the measurement with the "flag."

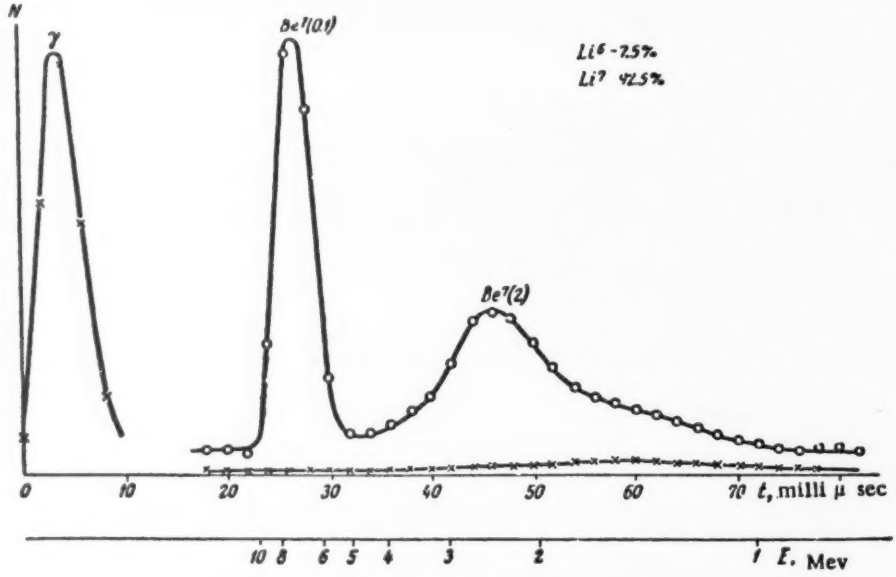


Fig. 4. Neutron distribution by time-of-flight for the target with natural lithium. The distance from the target to the counter is 1 meter. The lower curve is for the measurement with the "flag."

due to the lead carried could be subtracted out. The neutron counter was placed at a distance of 1 meter from the target at an angle of 0° with respect to the proton beam. The energy threshold of the counter was 0.9 Mev.

In Fig. 5 are shown the neutron spectra for the $Li^6 + p$ and $Li^7 + p$ reactions obtained on the basis of these measurements. In Figs. 3 and 5 the shape of the neutron group at 3.7 Mev corresponding to the $Li^6(p, n)Be^6$ reaction with the production of $Be^6$ in the ground state is fairly conspicuous. In addition there is observed a continuous spectrum of low-energy neutrons, associated with the multi-particle reactions $Li^6(p, pn)Li^5$ and $Li^6(p, 2pn)He^4$. The presence of this continuous spectrum makes it difficult to observe the neutron groups corresponding to possible excited states of $Be^6$.

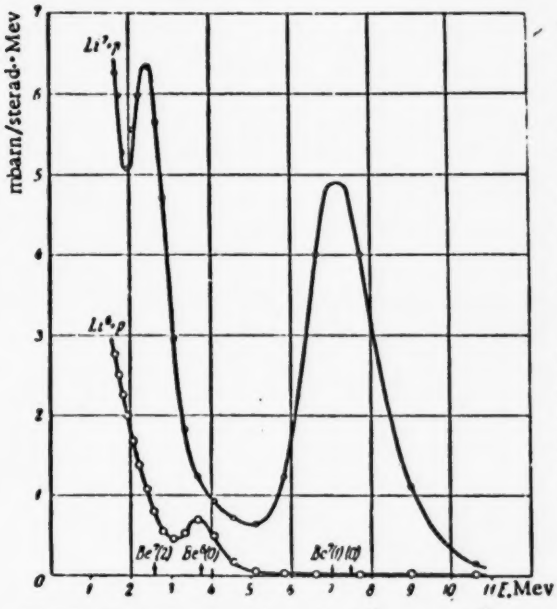


Fig. 5. Neutron spectra from the $Li^6 + p$ and $Li^7 + p$ reactions corrected for counter efficiency and conversion of the energy scale. The width of all peaks is that of the apparatus.

Two neutron groups are observed in the $Li^7 + p$ spectrum. One of these consists of two unresolved lines corresponding to the ground state and the first excited state (0.43 Mev) of $Be^7$. The other group corresponds to the second excited state (4.65 Mev) of $Be^7$. It is observed against the background of the continuous spectrum which is apparently a result of the $Li^7 (p, \alpha n) He^3$ reaction. In Fig. 6 is shown the first group, also taken at 0°, but with a considerably improved energy resolution and with a target-counter distance of 7.3 meters. In this case the doublet structure is clearly seen and the intensity ratio between the first line and the second is about 2 (within an accuracy of 10%).

Measurements of the neutron spectra from both targets were carried out at 0, 15, 30, 60 and 120°. In Fig. 6 are shown the angular distributions in the center-of-mass system for the neutron groups from the $Li^6 (p, n) Be^6$ reaction (ground state) and the doublet neutron group associated with the reaction $Li^7 (p, n)Be^7$. In the first case the smooth curves represent the expression

$$\sigma(\theta) = 0.19 + 0.23 \cos\theta + 0.70 \cos^2\theta \text{ (mbarn/sterad)}$$

and in the second case

$$\sigma(\theta) = 6.8 + 2.4 \cos^2\theta \text{ (mbarn/sterad)},$$

Integrating these expressions over $\theta$, we obtain the total cross section for the $Li^6 (p,n)Be^6$ reaction (ground state), which is $5 \pm 1$ mbarn, and the total production cross section for the doublet neutron group in the $Li^7(p,n)Be^7$ reaction, which is $100 \pm 20$ mbarn.

The last quantity is in good agreement with the measurements of Kalinin et al., [6], in which the cross section for $Be^6$ production in the bombardment of $Li^7$ by 9-Mev protons was $120 \pm 20$ mbarns.

To determine the energy and the width of the ground state of $Be^6$ the neutron group from the $Li^6 (p,n)Be^6$ reaction (ground state) was observed at 0° at a target-counter distance of 7.3 meters (Fig. 6). The thickness of the target was 90 $\mu$, corresponding to 200 kev for 9.6-Mev protons. To obtain the best spectrometer resolving power the amplitude discriminator was used to select a narrow range of pulse heights from the photomultiplier. The neutron time-of-flight, determined from the position of the maximum intensity of the neutron group, was found to be 260 millimicroseconds, corresponding to a neutron energy of 4.1 Mev.

The energy of the $Li^6 (p,n)Be^6$ reaction (ground state) found from these data is

$$Q = -5.2 \pm 0.2 \text{ Mev},$$

and the mass defect in $Be^6$ is $20.3 \pm 0.2$ Mev.

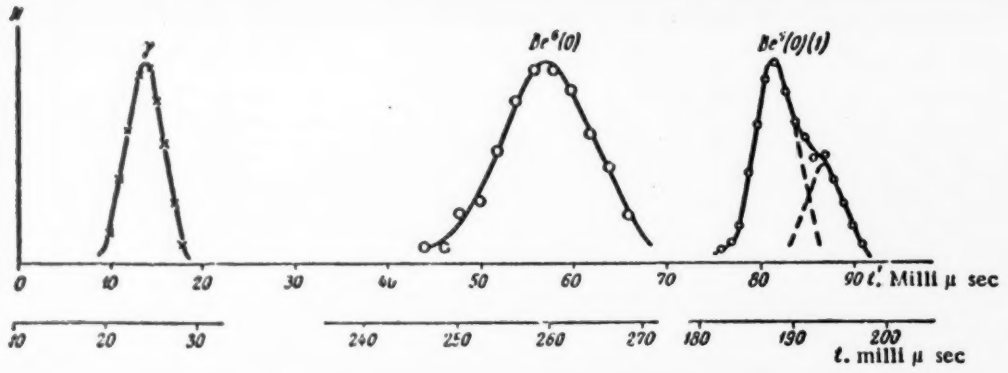


Fig. 6. Time-of-flight distributions for neutron groups from the $Li^6(p,n)Be^6$ (0) reaction and the doublet neutron group from the reaction $Li^7(p,n)Be^7$ (0,1), obtained with a target-counter distance of 7,3 meters. The delay t' of the control pulse is plotted along the abscissa axis using a scale with arbitrary zero. Above is plotted the true time-of-flight for each group. The group corresponding to t is observed in the third cycle of $Be^6$(0) from the cyclotron, starting from the γ peak. A period is 96 millimicroseconds ; the group corresponding to $Be^7$ (0,1) is measured in the second cycle.

The uncertainty in the determination of the reaction energy arises from errors in measuring the neutron time-of-flight and the uncertainty in the initial energy of the protons.

The energy width of the ground state of $Be^6$ can be estimated from the observed width of the neutron line (cf. Fig. 6) which exceeds considerably the width of the γ-peak, equal to the resolving power of the time analyzer. However, within the limits of accuracy of the measurements this effect can be explained by the lack of monochromaticity of the proton beam and the effect of target thickness. Thus the estimate can only give an upper limit to the width of the ground state $Be^6$

$$\Gamma < 0{,}3 \text{ Mev.}$$

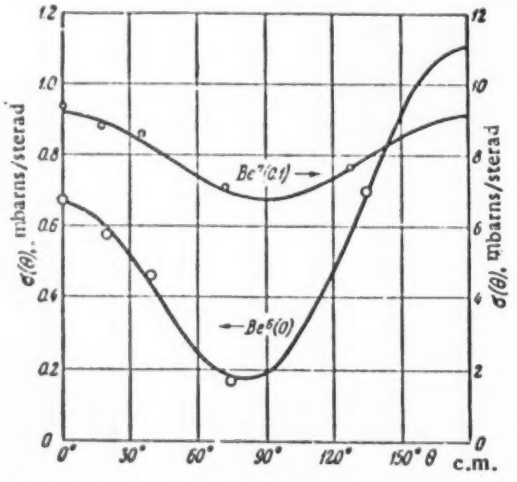


Fig. 7. Angular distributions for neutron groups corresponding to the $Li^6(p,n)Be^6$ reaction with the production of $Be^6$ in the ground state (left-hand scale) and the doublet group corresponding to the $Li^6(p,n)Be^6$ reaction with the production of $Be^7$ in the ground state and in the first excited state (right-hand scale).

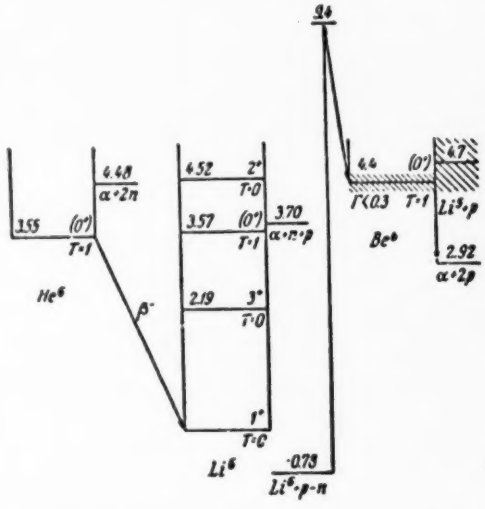


Fig. 8. Energy scheme for the lowest levels in $He^6$, $Li^6$ and $Be^6$.

## DISCUSSION OF THE RESULTS

As was to be expected, the $Be^6$ nucleus was found to be unstable against decay into an $\alpha$-particle and two protons. The energy of the ground state of $Be^6$ is 1.5 Mev higher than the energy of the $He^4 + 2p$ system (Fig. 8). The lifetime of $Be^6$ is $\tau \sim \frac{\hbar}{\Gamma} > 2 \cdot 10^{-21}$ sec.

Because of the overlapping of the $Be^6$ ground state and the wide level in $Li^5$ ($\Gamma \sim 1$ Mev) a cascade decay of $Be^6$ in accordance with the following scheme is possible:

$$Be^6 \rightarrow Li^5 + p \longrightarrow He^4 + 2p.$$

An estimate of the energy of the ground state of $Be^6$, carried out on the basis of the known energy of similar levels in $He^6$ (ground) and $Li^6$ (3.57 Mev) under the assumption that all three isobars have the same charge distribution, yields a value which is 0.4 Mev lower than the observed value. This situation points to the existence of certain correlation effects in the distribution of the two outer protons in $Be^6$.

An analysis of the effect of spatial correlation of the proton pair on Coulomb energy in light nuclei has been carried out by Carlson and Talmi [7]. Using the results of this work we can estimate the ratio of the differences in Coulomb energy in $Be^6 - Li^{6*}$ and $Li^{6*}$ under the assumption that in all three nuclei the two nucleons are in a $p_{3/2}$ state in the spherical oscillator potential well. This ratio turns out to be 1.556, whereas for a uniform charge distribution the ratio is 1.500.

The experimental value of the ratio ($2.0 \pm 0.3$) indicates considerable disagreement with the predicted value. To explain the discrepancy we must assume either a considerably tighter spatial correlation between the outer protons in $Be^6$ than was obtained by Carlson and Talmi or we must assume there is no similarity in the states in $He^6 - Li^{6*} - Be^6$, a situation which would violate charge invariance of nuclear forces.

The difference between the energy of $Be^6$ in the ground state and $Li^{6*}$ in a similar state, within the limits of accuracy in the measurements, agrees with the difference in energy in the ground states of $Be^7$ and $Li^7$; this result indicates that the charge distribution is similar in $Be^6$ and $Be^7$.

The angular distribution of neutrons from the $Li^6$ (p,n)$Be^6$ reaction has a rather pronounced minimum at 90°, indicating a large P-wave contribution in the reaction cross section. This does not contradict the assumption that the ground state of $Be^6$ probably has spin 0 and positive parity.

We should point out that the cross section for the $Li^6$ (p,n)$Be^6$ reaction (ground state) is very small, being 20 times smaller than the cross section for the $Li^7$ (p,n)$Be^7$ reaction with the production of $Be^7$ in the two lowest states.

The authors wish to thank their colleagues at the Cyclotron Laboratory, who made the present work possible; we are also indebted to A. I. Baz who participated in a discussion of the results.

## LITERATURE CITED

[1] H. Tyren and P. A. Tove, Phys. Rev. 96, 773 (1954).

[2] F. Ajzenberg and T. Lauritsen, Rev. Mod. Phys. 27, 77 (1955).

[3] L. M. Nemenov, S. P. Kalinin, L. F. Kondrashov, E. S. Mironov, A. A. Naumov, V. S. Panasyuk, N. D. Fedorov, N. N. Kaldin and A. A. Chubakov, J. Atomic Energy 2, 36 (1957).

[4] G. F. Bogdanov, A. A. Kurashov, B. V. Rybakov and V. A. Sidorov, J. Atomic Energy 1, 66 (1956).

[5] C. I. Taylor, W. K. Jentschke, M. E. Remley, F. S. Eby and P. G. Kruger, Phys. Rev. 84, 1134 (1951).

[6] S. P. Kalinin, A. A. Ogloblin and Yu. M. Petrov, J. Atomic Energy 2, 171 (1957).

[7] B. C. Carlson and I. Talmi, Phys. Rev. 96, 437 (1954).

Received April 1, 1957

BLANK
PAGE

# SPECTRA OF NEUTRONS INELASTICALLY SCATTERED ON $U^{238}$

N. I. Fetisov

The spectra of neutrons, inelastically scattered on $U^{238}$, have been measured with a Wilson cloud chamber. The neutron source was a heavy-ice target, bombarded by accelerated deuterons. The mean initial neutron energies were 2.5 and 3.5 Mev. The scatterer was a spherical layer of impoverished uranium 18 mm thick. The target was centered in the scatterer. The energy distribution for the inelastically scattered neutrons was measured in the energy range from 100 to 1,300 kev and is in agreement with the statistical theory. The most probable energy for the scattered neutrons is about 275 kev for neutrons with an initial energy of 2.5 Mev and about 375 kev for neutrons with an initial energy of 3.5 Mev.

At the present time there have been published only meagre experimental data on the spectra of inelastically scattered neutrons, particularly in inelastic scattering of neutrons by elements which are fissionable by fast neutrons.

In the present paper we report briefly on the result of spectrum measurements for neutrons with initial energies of 2.5 and 3.5 Mev, inelastically scattered on $U^{238}$.

## APPARATUS AND METHOD OF MEASUREMENT

The neutron source was a target of heavy ice upon which a beam of deuterons, accelerated in an ion accelerator, was incident. Great care was taken to reduce the mass of the target support in order to reduce neutron scattering effects in this support.

The scatterer was a spherical layer of impoverished uranium 18 mm in thickness, with an external diameter of 80 mm; it consisted of two hemispheres, fabricated from the solid metal. The extraneous-element content was negligibly small.

A Wilson chamber 200 mm in diameter and 60 mm high was used as the neutron detector. The wall thickness of the glass cylinder was 2 mm, the upper glass was 5 mm. The working volume of the chamber was expanded every 70 seconds by moving a light piston. A pulsed krypton-xenon tube was used as a light source in photographing the tracks of ionizing particles. Two objective lenses were used to obtain stereoptic pictures.

Measurements of the neutron spectrum in the region 100-500 kev were carried out with a chamber filled with hydrogen at a pressure of 250 mm Hg. The measurements in the region from 300 to 1,300 kev were carried out with a chamber filled with methane and nitrogen at a pressure of 360 mm Hg. The partial pressure of the nitrogen was 30 mm Hg. In the first case a small amount of water was introduced into the chamber and in the second case a small amount of a mixture of 50% ethyl alcohol and 50% water.

The range-energy relation for the recoil protons was computed from the known values of the stopping power of the gases. In the hydrogen-filled chamber this relation was verified using 200-kev neutrons obtained from the T (p,n) $He^3$ reaction. The stopping power of the gas mixture in the chamber filled with methane and

nitrogen was determined from the range of the 584-kev protons resulting from the $N^{14}(n,p)C^{14}$ reaction, which is induced by thermal neutrons. The background of scattered neutrons in the target holder, the walls of the chamber, and the surrounding objects was taken into account through supplementary measurements in which the uranium scatterer was removed. The background amounted to 10% of the effect being examined. In scanning the photographs, only those recoil-protons tracks were used which had a deflection angle $\theta < 15°$ with respect to the neutron trajectory and which lay completely inside the chamber. The tracks of recoil nuclei such as nitrogen, oxygen and carbon were of small length and were not considered. The $(n,\alpha)$ and (n,p) processes in nitrogen were less than 1% as compared with the neutron scattering on hydrogen.

The neutron energy was determined by measuring the angle $\theta$ and the tracks of the recoil protons. In forming the neutron spectrum from the experimental data consideration was given to the fact that the neutron scattering cross section in hydrogen is energy dependent and that a track of given length may not lie completely in the chamber.

## EXPERIMENTS WITH 2.5-MEV NEUTRONS

The experimental arrangement of the apparatus is shown in Fig. 1. The energy of the deuterons incident on the target was 100 kev, the mean energy of the scattered neutrons was 2.5 Mev. The accelerator was pulsed. Pulses of deuteron current were obtained by applying voltage pulses (2.5 kev) to the electrode closest to the ion source (cutoff electrode). The length of the ion pulse was about 5 $\mu$ sec. The ion current on the target during the pulse was 2.5 ma.

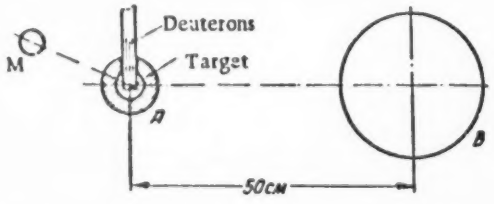


Fig. 1. Experimental arrangement used with 2.5-Mev neutrons.
a) scatterer; 2) Wilson chamber; M) monitor.

The intensity of the neutron flux was measured with an ionization chamber filled with boron trifluoride. The average number of neutrons in the pulse was $3 \cdot 10^6$. The accelerator pulses were synchronized with the operating cycle of the Wilson chamber in such a way that neutrons entered only after expansion was complete.

About 1,200 recoil proton tracks were investigated in the pictures which were chosen.

The scattered-neutron spectrum (Fig. 2) was drawn on the basis of these data and the data obtained with the scatterer withdrawn. The errors indicated in the Figure are statistical errors. The spectrum also includes neutrons produced in $U^{238}$ fission induced by fast neutrons. The contribution of neutrons due to $U^{235}$ fission was inconsequential.

To estimate the contribution due to fission neutrons the experimental curve was extended into the energy region above 1 Mev using the formula

$$N(E) = AEe^{-E/0.3} + BE^{1/2}e^{-0.775E},$$

where A and B are coefficients.

Using the inelastic scattering cross section $\sigma_{in} = 2.5$ barns, the fission cross section $\sigma_f = 0.5$ barns, and the secondary neutron ratio $\nu = 2.8$, it was found that $B/A = 0.06$ and the fission-neutron component was 20%. The same result is obtained from an estimate in which use is made of the values of $\sigma_f$ and $\nu$ given above and the data for emission of neutrons with a given energy in inelastic processes in the energy region below threshold for $U^{238}$ fission.

In making the estimate it was assumed that the fission neutron spectrum for $U^{238}$ has the same form as that of $U^{235}$ fission induced by thermal neutrons. The spectrum obtained after subtraction of the fission-neutron component is shown in Fig. 3. In the present experiment an estimate showed that about 10% of the inelastically scattered neutrons experience more than one inelastic collision. Thus, the neutron spectrum shown in Fig. 3 is somewhat modified as compared with a "pure" spectrum of inelastically scattered neutrons.

## EXPERIMENTS WITH 3.5-MEV NEUTRONS

The experimental arrangement is shown in Fig. 4. The deuteron beam, accelerated to an energy of 1 Mev, was incident on the target after passing through a magnetic analyzer and an aperture 10 mm in diameter.

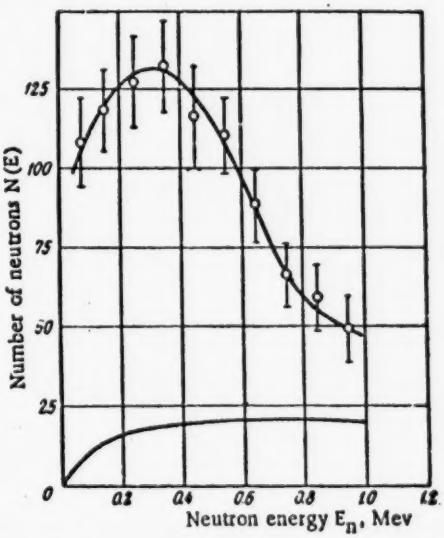


Fig. 2. Spectrum of inelastically scattered 2.5-Mev neutrons, including fission neutrons. The lower curve is the computed fission-neutron spectrum.

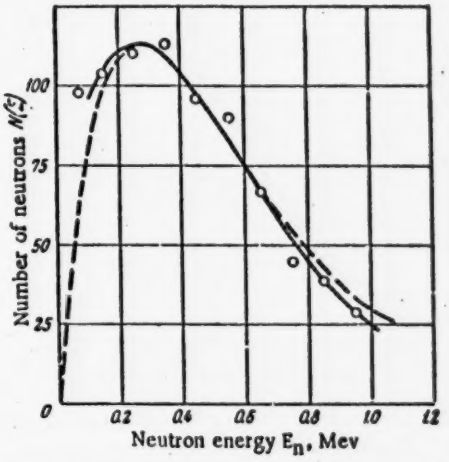


Fig. 3. Spectrum of inelastically scattered 2.5-Mev neutrons after subtraction of the fission neutrons. The dotted curve is obtained on the basis of the statistical theory, using a most probable energy of 275 kev.

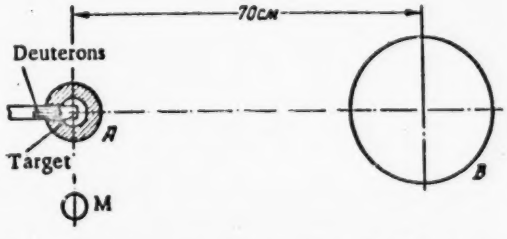


Fig. 4. Experimental arrangement used with 4-Mev-neutrons.
a) Scatterer; b) Wilson chamber; M) monitor.

The neutron flux was measured with a $U^{238}$-layer fission chamber. The method of measuring the spectrum was similar to that used in the preceding section except that the accelerator was not pulsed.

In all 850 tracks were used. The neutron spectrum, including fission neutrons, is shown in Fig. 5.

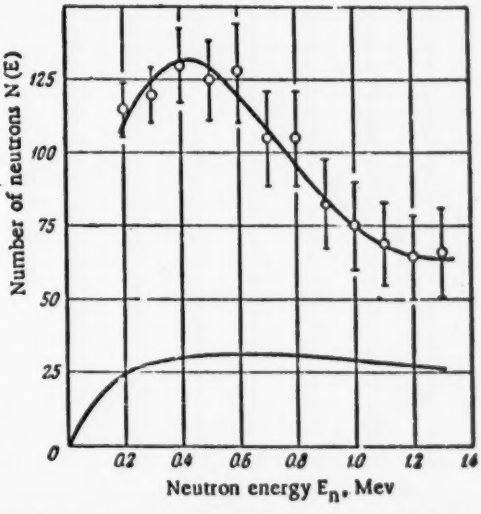


Fig. 5. Spectrum in inelastically scattered 3.5-Mev neutrons including fission neutrons. The lower curve is the computed spectrum for fission neutrons.

As in the preceding case an estimate was made of the fission-neutron contribution, which in this case was 24%. The spectrum of inelastically scattered neutrons, obtained after subtracting off the fission neutrons is shown in Fig. 6. In this case the energy of the scattered

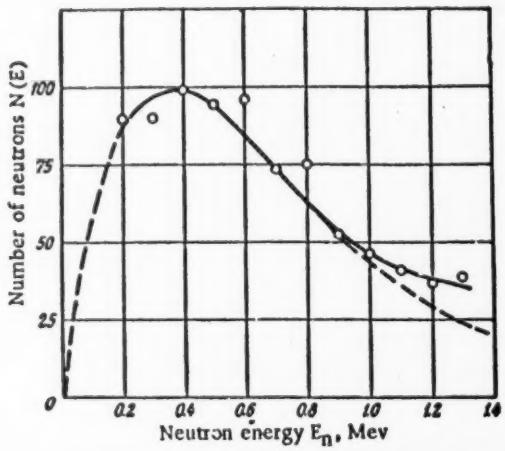


Fig. 6. Spectrum of inelastically scattered 3.5-Mev neutrons after subtraction of fission neutrons. The dotted curve is obtained on the basis of the statistical theory using the most probable energy of 375 Mev.

neutrons varies from 1.78 to 4.14 Mev. However, because of the pronounced anisotropy in the distribution of neutrons scattered by the target in the present geometry the main contribution (up to 70%) to the neutron spectrum is that due to neutrons inelastically scattered in the forward hemisphere. This result corresponds to a mean energy of 3.5 Mev for the primary neutron.

## SUMMARY

The energy distribution of neutrons inelastically scattered in $U^{238}$ indicates that a neutron can lose a large amount of energy in one inelastic collision. The experimental results which have been obtained are in agreement with the statistical theory, which predicts this large energy loss.

The dotted curves in Fig. 3 and 6 represent a distribution of inelastically scattered neutrons, on the basis of the statistical theory, with most probable energies of 2.75 and 3.75 kev respectively. The results of the present work are in good agreement with those of Cranberg and Levin,* who studied inelastic scattering of 2.45-Mev neutrons in $U^{238}$ using a time-of-flight method.

G. V. Kotelnikov participated in the present work. The author is indebted to B. P. Shemetenko and E. P. Ukraintsev for operation of the accelerator. The author also wishes to thank I. I. Bondarenko for participating in a discussion of the results, O. D. Kazachkovsky for valuable advice and A. I. Leipunsky for continued interest in this work.

Received April 25, 1957

* L. Cranberg, J. Levin, Phys. Rev. 103, 343 (1956).

# SEPARATION OF GERMANIUM AND MAGNESIUM ISOTOPES IN A SMALL ELECTROMAGNETIC SEPARATOR

V. M. Gusev, D. V. Chkuaseli and M. I. Guseva

A method is described for the electromagnetic separation of germanium and magnesium isotopes in a small electromagnetic separator with a focusing angle of 180°. The construction of an ion source and an ion collector (isotope receiver) is considered. The ion source, which maintains a discharge in the vapor of the element to be separated, operates satisfactorily in a temperature range up to 1500 °C. The construction of the receiver permits the simultaneous collection of all the isotopes of the element to be separated. The relation of the size of the ion current, focused on the receiver, to the method of discharge in the source was investigated. During the separation of germanium isotopes the ionic current at the receiver reached 15-20 ma; during magnesium separation it was 35-40 ma. Every hour ~ 40 mg of enriched germanium isotopes (or ~ 25 mg of enriched magnesium isotopes) was collected in the receiver's containers. The coefficient of material recovery was 2-6%. Mass-spectrometric analyses were carried out on metal samples for the enriched germanium isotopes and the compound $MgI_2$ for the magnesium isotopes. The enrichment coefficient for germanium and magnesium lay within the limits 17-175 depending on natural diffusion and mass of the isotopes.

## INTRODUCTION

The electromagnetic method is widely used for the separation of stable isotopes. The main advantages of this method over all others is its general applicability, high enrichment coefficient for one stage and the possibility of separating multi-isotope elements with the simultaneous enrichment of all the isotopes of the given element. At present the isotopes of almost all elements can be separated in large electromagnetic separators. Electromagnetic separators are also being used to a greater extent for the separation of radioactive isotopes as well. The main disadvantage of the electromagnetic method in comparison with "statistical" separation methods (gas diffusion, thermal diffusion, centrifuging, exchange reactions etc.) is its greater expense – greater specific outlay of energy.

Stable isotopes are being increasingly used in scientific investigations. In particular, enriched germanium and magnesium isotopes have been used for determination of the effective thermal neutron capture cross sections. Magnesium isotopes have been used for investigations of the nuclear energy levels [1].

The germanium and magnesium isotopes were separated in a small electromagnetic separator with a focusing angle of 180°. The apparatus was analogous in principle to Dempster's mass-spectrometer. The chamber of the apparatus with the ion source and isotope receiver is shown schematically in Fig. 1. A discharge was maintained in the ion source in the vapor of the element to be separated. The ions formed in the discharge were extracted through a narrow slit by the electric field of an ion-optical system and entered a transverse magnetic field in which they moved in circular orbits with a radius of

(1)

where m is the ionic mass; e is ionic charge; H is the strength of the magnetic field; U is the accelerating voltage.

The ion beams, corresponding to the different isotopes, were focused after turning through 180°. Collectors (receiver containers) were placed in the focus positions and the separated isotopes were collected in them. The distance between the foci of two isotopes with masses $m_1$ and $m_2$ (dispersion ) was determined by the formula

$$\Delta x = R\frac{|m_1 - m_2|}{m}, \qquad (2)$$

where m is the average mass of the two isotopes.

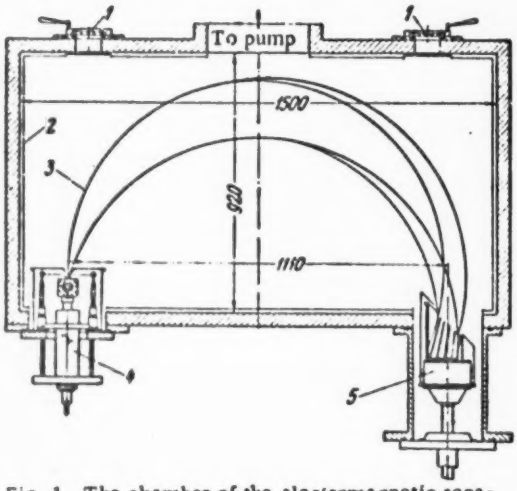


Fig. 1. The chamber of the electromagnetic separator with source and receiver.
1) Inspection window; 2) cooled jacket; 3) ion beam; 4) source; 5) receiver.

In the apparatus described, R equals 555 mm and the distance between adjacent isotope foci, differing by one mass unit, is ~ 7.5 mm for germanium and ~ 20 mm for magnesium. Therefore, a good enrichment of germanium isotopes may be obtained with less than 7.5 mm as the width of the line on the receiver.

The plane parallel, non-aberrational magnetic field of the separator allows focusing of an ion beam diverging at an angle of ± 12°.

The interior measurements of the apparatus' vacuum chamber are 920 x 1500 x 350 mm. The upper and lower covers of the chamber are at the same time the shoes of the electromagnet poles. The weight of the electromagnet is 30 t. There is a jacket inside the chamber, cooled with water, which keeps the vacuum chamber from over heating, as well as from being contaminated by condensation on the walls from the vapor of the elements being separated. The chamber is exhausted with an oil diffusion pump with a pumping speed of 4000 liters/sec.

## The Ion Source

In separating germanium and magnesium isotopes we used an ion source whose construction was based on the source developed by us with a group of colleagues under the direction of M. Ardeene in 1950.

The head of the source for germanium is shown in Fig. 2. It consists of crucible 7 and cathode 1 blocks and a main heater 6, which contains vapor regulating 5 and gas discharge 3 chambers. Germanium metal 10 is loaded into a cylindrical graphite crucible 9 with 25 g capacity, which is sufficient for ~ 30 hours of continuous source operation. The crucible is screwed into the graphite bottom of the main heater which consits of an elongated rectangular box of thin sheet tungsten, heated by passing a direct current (~ 1000 a) through it. The crucible is heated by a special cylindrical crucible furnace 8, made from molybdenum sheet and heated by a direct current. The range of operating temperatures of the source goes up to 1500 °C.

From the crucible, the vapor enters the vapor regulating chamber of the heater, which ensures a transverse supply of vapor, which is uniform over its whole height, to the gas discharge chamber, where it is ionized by an electron beam 4, emitted by the indirectly heated tungsten cathode 2, placed above the opening in the cover of the gas discharge chamber. The curve of the discharge lead corresponds to that of the magnetic lines of force in the discharge region (radius of curvature is ~ 700 mm). The front wall of the heater is similarly

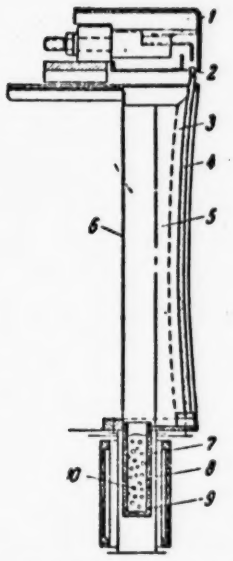


Fig. 2. Head of the ' . source for germanium. 1) Cathode block; 2) tungsten cathode; 3) gas discharge chamber; 4) discharge lead; 5) vapor regulating chamber; 6) main heater; 7) crucible block; 8) crucible furnace; 9) crucible; 10) germanium.

curved. The ions are extracted from the outlet slit (140 x 2 mm) in the front wall of the heater and accelerated by the electric field of the ion-optical system (Fig. 3), consisting of two bicylindrical electrodes – the main and the intermediate. The main electrode is earthed. The source head is under a high positive potential (20-25 kv) relative to earth. The potential of the intermediate electrode is a few kilovolts less that of the main electrode. The intermediate electrode creates a potential barrier checking the flow to the source head of electrons that compensate for the positive space charge of the beam.

For the separation of magnesium isotopes only. The crucible block was changed in the ion source described.

To obtain products with high isotopic purity, the stability of the discharge in the ion source, that of the electric field in the ion-optical system and that of the magnetic field in the separation space are of prime importance. Special systems are used for stabilizing the discharge current and the heater temperature on which the vapor pressure in the gas discharge chamber depends. Electronic stabilization systems ensure high stability of the accelerating voltage and the current of the electromagnet. The electrical supply system for the ion source, which is under a high potential, is regulated from a panel through a separating transformer.

Special investigations were carried out to determine the conditions for the ion source most suitable for isotope separation and in the course of these investigations optimal values were established for the vapor pressure in the gas discharge chamber, the discharge current, and voltage, the accelerating voltage and the vacuum in the separation chamber. The basic criteria for this were the magnitude of the ion current at the receiver and the degree of focusing of the beam, which was controlled by the size of the modulation coefficient of the ion beam current

$$M = \frac{\Delta I^+}{I^+}, \qquad (3)$$

where $I^+$ is the ion beam current; $\Delta I^+$ is the variable component of the beam current ($\Delta I^+$ was measured with an oscillograph or valve voltmeter).

The oscillations in the beam depended mainly on the conditions in the discharge. These investigations as well as those of other authors [2], showed that in a source with a discharge burning in pure metal vapors, there is a narrow range of values for the current, voltage and pressure in the discharge at which the oscillation level in the beam is minimal ($M \leq 1$-$2\%$) and the isotope lines are well focused (the isotope lines are understood to be the images of the outlet slit of the ion source formed on a receiving plate at the focus of the ion beam of a given isotope). Usually a compromise between the size of the ion current at the receiver and the degree of focusing of the isotope lines was necessary, as at high currents the focusing of the lines deteriorated.

Germanium and magnesium differ greatly from each other in their physico-chemical properties as well as in the number of stable isotopes that they possess. The relations of the ion current at the receiver $I^+$ and the modulation coefficient M to the power of the crucible furnace $W_c$, discharge current $I_d$ and discharge voltage $V_d$ were plotted to determine the optimal conditions for the discharge. The corresponding graphs for germanium are shown in Figs. 4,5 and 6. As can be seen in Fig. 4, with increasing $W_c$, which corresponds to rising vapor pressure in the gas discharge chamber, the magnitude of the current at the receiver increases and the intensity

of the oscillations in the beam passes through a minimum (M ~ 1%), whose position determines the optimal temperature for the crucible. During the separation process the temperature of the crucible furnace is maintained at a level of ~ 1300° for germanium and ~ 450° for magnesium (which corresponds to a vapor pressure at the metal surface of ~ $1 \cdot 10^{-2}$ mm Hg). In both cases the temperature of the main heater is maintained somewhat higher so as to prevent condensation of metal vapors on the walls of the heater. The ion current at the receiver first increases rapidly and then more slowly with an increase in the discharge current (see Fig. 5). The modulation coefficient exceeds the permissible value (M ~ 2%) at $I_d \geq 0.6$ a. Therefore, the operating value for the discharge current was taken as $I_d = 0.5$ a. The curves in Fig. 6 show that $I^+$ and M depend little on the discharge voltage $V_d$ over wide ranges. For magnesium the relations of $I^+$ and M to $W_c$, $I_d$ and $V_d$ have an analogous character. The data characterizing the optimal conditions of the source for the separation of germanium and magnesium isotopes are summarized in Table 1. Besides that, the table gives the magnitudes: $W_H$, the power used by the main heater, $\gamma$, the amount of isotopes deposited in the receiver containers in 1 hour (determined by measuring the current on the receiver), g, the hourly consumption of metal in the ion source and K, the coefficient of material recovery, calculated as the ratio $\frac{\gamma}{g}$. The separation took place at an operating vacuum in the chamber of $3-5 \cdot 10^{-5}$ mm Hg. An improvement or deterioration of the vacuum resulted in some diffusion of the lines, firstly, due to insufficient compensation of the positive space charge of the beam and secondly, due to an increase in ion scattering on the molecules of residual gas.

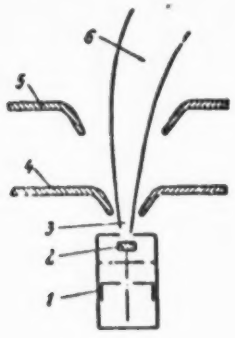


Fig. 3. Ion-optical system of the source.
1) Main heater; 2) discharge lead 3) slit for ion extraction; 4) intermediate electrode; 5) main electrode; 6) ion beam.

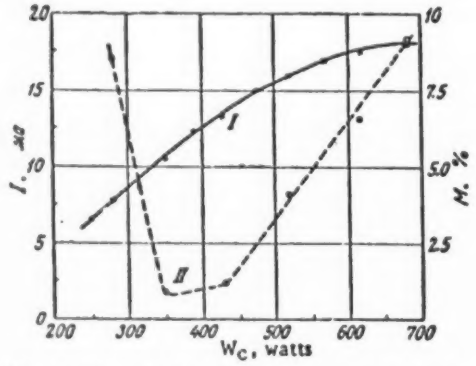


Fig. 4. The relation of the ion current at the receiver $I^+$ (I) and modulation coefficient M (II) to the power of the crucible furnace $W_c$ at constant discharge current and voltage: $I_d = 0.5$ a; $V_d = 250$ v.

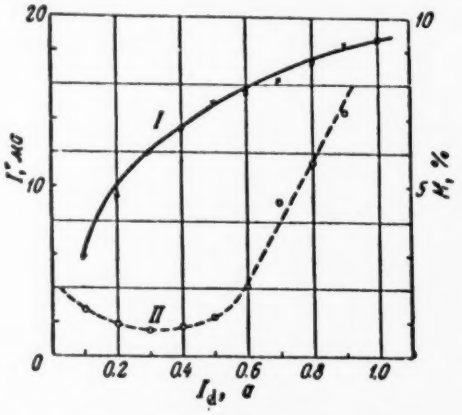


Fig. 5. The relation of the ion current at the receiver $I^+$ (I) and the modulation coefficient M (II) to the discharge current $I_d$ at constant discharge voltage $V_d$ = = 250 v and a crucible furnace power $W_c = 400$ watts.

## Isotope Receiver

The construction of the isotope receiver and the selection of materials for making it are determined by the amount of isotopes being separated, dispersion of the apparatus and the physicochemical properties of the element being separated. Germanium has five stable isotopes whose natural occurrence is: $Ge^{70}$ – 20.55%,

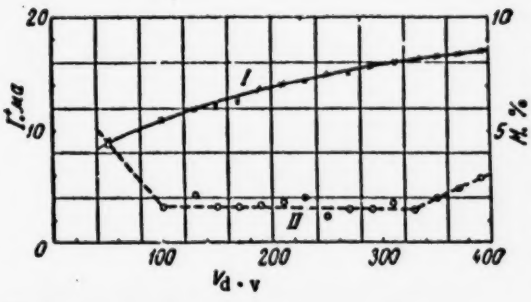


Fig. 6. The relation of the ion current at the receiver $I^+$ (I) and modulation coefficient M (II) to the discharge voltage $V_d$ at constant discharge current $I_d$ = 0,5 a and when a crucible furnace power $W_c$ = 400 watts.

$Ge^{72}$–27.37%, $Ge^{73}$–7.61%, $Ge^{74}$–36.70%, $Ge^{76}$–7.67%. Magnesium has three stable isotopes: $Mg^{24}$–78.60%, $Mg^{25}$–10.11%, $Mg^{26}$–11.29% [1]. For the simultaneous collection of all germanium isotopes, it is necessary to place five receiver containers in a small volume which mainly determines the construction of the receiver (Fig. 7). The ion beams are received by the copper dividing "knives" of the receiver. Part of the ions become embedded in them and others are reflected and deposited on the container linings. The embedded particles, together with the material of which the "knives" are made, are atomized by the following ions so that the main mass of the isotopes received is deposited on the unirradiated container linings of the receiver, which are also made of copper. The containers are placed in an over-all copper box whose perimeter is lined with a water cooler. Due to lack of space the containers were not electrically insulated from each other. The lines were set at the receiver by correlating currents at small collectors – "eyes" – insulated from each other and placed in the upper part of the receiver at the foci of the ion beams. The correlation of the currents at the "eyes" was kept equal to the ratio of the percentages of the isotopes in the natural mixture. Such a setting system was quite effective and gave positive results. A thin collector (1 mm width) was placed among the "eyes" for controlling the beam focusing with an oscillograph. For this purpose, with the receiver locked, the accelerating voltage was modulated (modulation frequency of 50 cps), the current on the collector was oscillographed and, by the appearance of the oscillogram, the operator could control the degree of resolution of the lines. An oscillogram of the germanium spectrum is shown in Fig. 8.

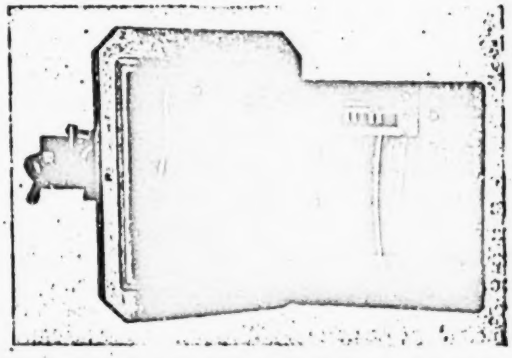

Fig. 7. Receiver for germanium isotopes. Small collectors ("eyes") can be seen in the upper section of the receiver for controlling the position of the isotope lines on the receiver.

The construction of a receiver for germanium was especially interesting from the point of view of building a universal separating receiver, suitable for the separation of the isotopes of a whole series of elements. It provides for the rearrangement of the separate containers as is necessary in changing from element to element.

In separating magnesium, due to the greater dispersion it was possible to insulate the containers electrically from each other and to evaluate directly the accuracy of the position of the lines on the receiver by the correlation of the currents falling onto the containers. Due to the high volatility of magnesium each container had to be water cooled.

After completing the separation cycle, the isotopes accumulated in the containers were removed from the receiver. The container linings were chemically treated with nitric acid (1 : 2), when a thin layer of germanium (or magnesium) mixed with copper was washed off. After removing the copper from the solution, the germanium and magnesium (in the form of $GeO_2$ and MgO) were precipitated and freed from impurities chemically. The chemical purity of the separated products was checked by spectrographic analysis. According to this analysis very small traces of copper, molybdenum, iron, tin and calcium were in the enriched samples. On the average, 50 to 80% of the expected (according to measurements of the receiver current) amount of isotopes was extracted from the containers, i.e., the value of the coefficient of collection and extraction of germanium and magnesium isotopes lies within the limits of 0,5 to 0,8. Greater losses were sustained in the separation of magnesium isotopes.

TABLE 1

| Element | $W_C$ watts | $W_H$ watts | $I_d$ a | $V_d$ v | $U$ kv | $I$ ma | $g$ g/hr | $\gamma$ mg/hr | $K$ % |
|---|---|---|---|---|---|---|---|---|---|
| Germanium | 300—500 | 4000 | 0.5 | 250 | 25 | 15—20 | 0.6—0.7 | 40 | 6.5 |
| Magnesium | 25—30 | 1600 | 0.5 | 250 | 16—17 | 35—40 | 1.0—1.2 | 25 | 2 |

TABLE 2

| Isotope | Natural occurence, % | Content in an enriched sample, % | Enrichment occurence, % | Weight of sample, mg | Content in sample enriched in the Oak Ridge Laboratory (USA), % |
|---|---|---|---|---|---|
| $Ge^{70}$ | 20,55 | 91,00 | 38 | 360 | 88,1 |
| $Ge^{72}$ | 27,37 | 92,70 | 34 | 400 | 89,2 |
| $Ge^{73}$ | 7,61 | 60,29 | 17 | 170 | 68,9 |
| $Ge^{74}$ | 36,74 | 97,00 | 55 | 1000 | 95,2 |
| $Ge^{76}$ | 7,67 | 92,41 | 175 | 100 | 79,3 |
| $Mg^{24}$ | 78,60 | 99,3 | 38 | 2130 | 99,5 |
| $Mg^{25}$ | 10,11 | 94,0 | 141 | 400 | 92,2 |
| $Mg^{26}$ | 11,29 | 93,0 | 102 | 650 | 98,1 |

Fig. 8. Oscillogram of a germanium isotope spectrum.


SUMMARY

Mass-spectrometric analysis of the enriched isotopes was carried out on a mass-spectrometer of the MC-3 type. Metal samples [3] were used for analyzing germanium and $MgI_2$ (using $MgI^+$ ions) for analyzing magnesium. The results obtained are summarized in Table 2, where the enrichment coefficient $\underline{n}$ stands for the ratio

$$\frac{N_1}{100-N_1} \Big/ \frac{N_0}{100-N_0}, \qquad (4)$$

where $N_0$ is the content (in %) of the isotope in the natural mixture; $N_1$ is the isotope content of the sample investigated.

The results of enrichment of these isotopes in large separators of the Oakridge Laboratory (USA) are given in the last column of the table for comparison [4].

The data given, as well as the results of the enrichment of other stable isotopes on the apparatus described show that it can effectively separate the isotopes of light and medium elements (with mass up to 100) in quantities

of tens and hundreds of milligrams in a relatively short period of time. The enrichment thus obtained is comparable with that obtained in separations in large scale electromagnetic separators.

## LITERATURE CITED

[1] C. P. Keim, Ann. Rev. Nucl. Sci. 1, 263 (1952).

[2] A. M. Rodin, Report Acad. Sci. USSR, 1950.

[3] K. G. Ordzhonikidze and G. N. Zubarev, The Relative Occurence of Germanium and Palladium Isotopes (Paper given at the All-Soviet Scientific-Technical Conference on the Application of Radioactive and Stable Isotopes), Moscow, 1957.

[4] C. P. Keim, J. Appl. Phys. 10, 1255 (1953).

Received December 19, 1956

BLANK
PAGE

# ATOMIC ENGINES FOR SHIPS

V. V. Lakhanin

In recent years, work dealing with the application of atomic energy for ship propulsion has been conducted in a number of countries (USSR, USA, Norway, Japan, and others), and the conditions required for realizing it have been analyzed. It has been established that the power of atomic-powered vessels should be sufficiently large – not less than 10,000 HP – and the speed of atomic-powered freighters (18-21 knots) should be considerably greater than that of similar conventional vessels (12-15 knots). Steam or gas turbines will be employed in atomic-powered vessels. At the present time, it is more advantageous to utilize the dual loop cooling system with a steam turbine installation and a thermal reactor, water moderated and cooled. Projects dealing with the creation of a high-temperature reactor with gaseous coolant are under way for future realization of the advantages of the gas turbine installation. The weight of the atomic vessel installation should be less than the total weight of a conventional vessel installation and fuel supply. Calculations indicate that the atomic vessel can be as economical as the conventional vessel.

## General Characteristics of Atomic Vessels

Due to economic considerations, at the present time only large ocean-going atomic-powered vessels are being designed and constructed: ice breakers, large tankers (with a displacement from 30,000 to 80,000 tons), submarines, etc. In this connection, of great importance is the problem of the minimum and most economical power of atomic vessel installations, which is associated with the problem of expanding the types and sizes of vessels suitable for the installation of atomic engines.

Up to the present time, the lower limit has been 10,000 HP, in which connection a tendency became apparent of reducing it to 3,000 HP (order of power of river vessels) [1] - [10].

The proposed speeds of atomic vessels varies within the limits (for freighters) of 18-21 knots [1]-[10], whereas the speed of similar vessels with conventional engines is 12-15 knots. An increase in speed of 40-50% will greatly decrease the round trip time and, as a result, increase the commercial value of vessels.

The utilization of atomic engines in ships permits of considerable increase in the endurance without refuelling (from tens of days for conventional vessels to hundreds of days for atomic vessels), and extensive voyages, in turn, are advantageous from the point of view of atomic engines – in this case the reactor can operate a long time at a constant level, whereas with frequent halts of the vessel it must operate at disadvantageous variable levels with nonproductive heat dissipation during vessel halts, since the danger of occurrence of "iodine sinks" (poisoning of the reactor by the fission products) which are caused during reactor shutdown dictates the necessity for maintaining the reactor at power.

In general, it is possible to improve the reactor operating level during frequent vessel halts and to avoid

nonproductive heat dissipation, but under the condition that the reactor have an excess reactivity sufficient for compensation of the reactor poisoning by the fission products during a halt, and this requires the use of a highly enriched, expensive fuel.

For ice breakers, in addition to extensive endurance without refuelling, an important characteristic is the ratio of the vessel power to the displacement, i.e., the horsepower per ton of displacement. This ratio is called the specific power [3]. For conventional ice breakers the specific power varies within the limits of 1.1-2.0 HP/ton, and for the atomic ice breaker it attains 2.75 HP/ton.

TABLE 1

Comparative Economic Characteristics of Conventional and Atomic Tankers

| Expenditures and income | Tanker with conventional power installation | | Tanker with atomic power installation | |
|---|---|---|---|---|
| | millions of dollars | % | millions of dollars | % |
| Cost of hull and equipment | 7.50 | 70.2 | 8.16 | 76.5 |
| Cost of power installation | 3.18 | 29.8 | 8.30 | 77.5 |
| Total construction expenditures | 10.68 | 100.0 | 16.46 | 154.0 |
| Amortization and insurance | 0.671 | 29.7 | 1.094 | 48.2 |
| Salaries, repairs, maintenance in ports | 1.011 | 44.8 | 1.063 | 47.1 |
| Fuel expenses | 0.578 | 25.5 | 1.104 | 48.7 |
| Total annual operating expenses | 2.260 | 100.0 | 3.261 | 144.0 |
| Annual income | 3.880 | 100.0 | 3.900 | 100.5 |
| Annual profit | 1.620 | 100.0 | 0.639 | 39.4 |

Only preliminary data are available in the literature relative to the cost of atomic vessels. For example, the cost of an atomic cruiser (USA) is $87,000,000 ($18,000,000 of this amount represents the cost of the reactor equipment); $43,000,000 has been alloted for the construction of an atomic freight and passenger vessel [5], etc.

Table 1 presents data [1] on the cost of construction and operation of two tankers utilizing conventional and atomic fuel with approximately the same annual productivity (290,000 tons), at a transportation cost of $7.77 per ton for the conventional tanker, and $11.15 for the atomic tanker. It follows from Table that at the present time the cost of the atomic vessel and fuel is higher than the corresponding cost of the conventional vessel power installation and fuel.

It is pointed out in reference [1] that the economy of the atomic tanker can be greater due to the greater cargo capacity, and also due to greater productivity as a result of increase in speed.

## Atomic Installations for Ships

At the present time, there is little published data on ship reactors and cooling systems. Certain data are presented in Table 2.

In references [2], [11]-[13] are discussions mainly of five atomic installations which, in the opinion of the authors, can be employed in vessels:

1) Dual loop, heterogeneous, thermal reactor system with presurized water;

2) Single loop, heterogeneous, thermal reactor system with boiling water in the core;

3) Dual loop, homogeneous, thermal reactor system;

4) Three loop, heterogeneous, thermal or intermediate reactor system with graphite moderator and sodium coolant;

5) Single loop, heterogeneous, thermal reactor system with helium coolant.

TABLE 2

Some Data on Foreign Atomic Installations for Ships

| Vessel | Reactor | Coolant | System | Main engine |
|---|---|---|---|---|
| Submarine "Nautilus" (USA) | Heterogeneous, thermal, with pressurized water | Water | Dual loop | Steam turbine; parameters of steam at turbine inlet: $P$=17,58 kg/cm$^2$ $t$=219° C |
| Submarine "Sea Wolf" (USA) | Heterogeneous, intermediate, Sodium coolant and graphite moderator | Sodium | Three loop | Steam turbine |
| Proposed Norwegian tanker | Heterogeneous, pressurized heavy water | Heavy water | Dual loop | Steam turbine, parameters of steam at turbine inlet: $P$=30,6 kg/cm$^2$ $t$=234° C |
| Proposed passenger and freight vessel (USA) | Heterogeneous, pressurized water | Water | Dual loop | Steam turbine |

Steam turbines are employed in the first four systems, and a gas turbine in the last system. Certain shipbuilding specialists [2], [11]-[13] consider the last system to be the most advantageous, since pure helium is not activated in the reactor, which facilitates shielding design. In comparison with the steam turbine installation, the weight and size of the gas turbine installation is less [11], [14] and the efficiency is greater (38-42%). Nevertheless, the advantages of the gas turbine installation are doubted by many authorities [15]. The objections raised consist of the following: 1) steam turbines, and also reactors with pressurized water, are better understood, less expensive and more reliable; 2) helium is scarce and expensive; 3) high temperature reactors with a gaseous coolant have not been fully developed; 4) the efficiency values presented above for the gas turbine installation can be attained only when the gas temperature at the turbine inlet is at least 760°C. The minimum temperature values which assure the advantages of gas turbines are 600-650°C, whereas reliable operation of a reactor with gaseous coolant can be attained when the temperature of the gases at the outlet is approximately 400°C. In this case, the efficiency of gas turbine installations is lower than that of steam turbine installations.

The efficiency of dual loop systems, in which a reactor with pressurized water is used, is greatly affected by the amount of pressure, since the latter determines the parameters of the steam at the turbine inlet. At the present time, such reactors are operated at a pressure of 100-140 atmospheres, absolute. In this connection, it is possible to obtain in the second loop saturated steam under a pressure of 28-60 atmospheres, absolute, or superheated steam under a pressure of 10-26 atmospheres, absolute. Consequently, the steam temperature decreases if an individual steam superheater is not used with conventional fuel when superheated steam is employed, and in certain cases this results in a lower efficiency as compared with the system of utilizing saturated steam under a greater pressure.

When saturated steam is used, it is necessary to employ intermediate drying or heating of the steam. For purposes of explanation, the diagram below presents four methods of heat removal and the thermodynamic cycles for them in i,s-coordinates [16], [17].

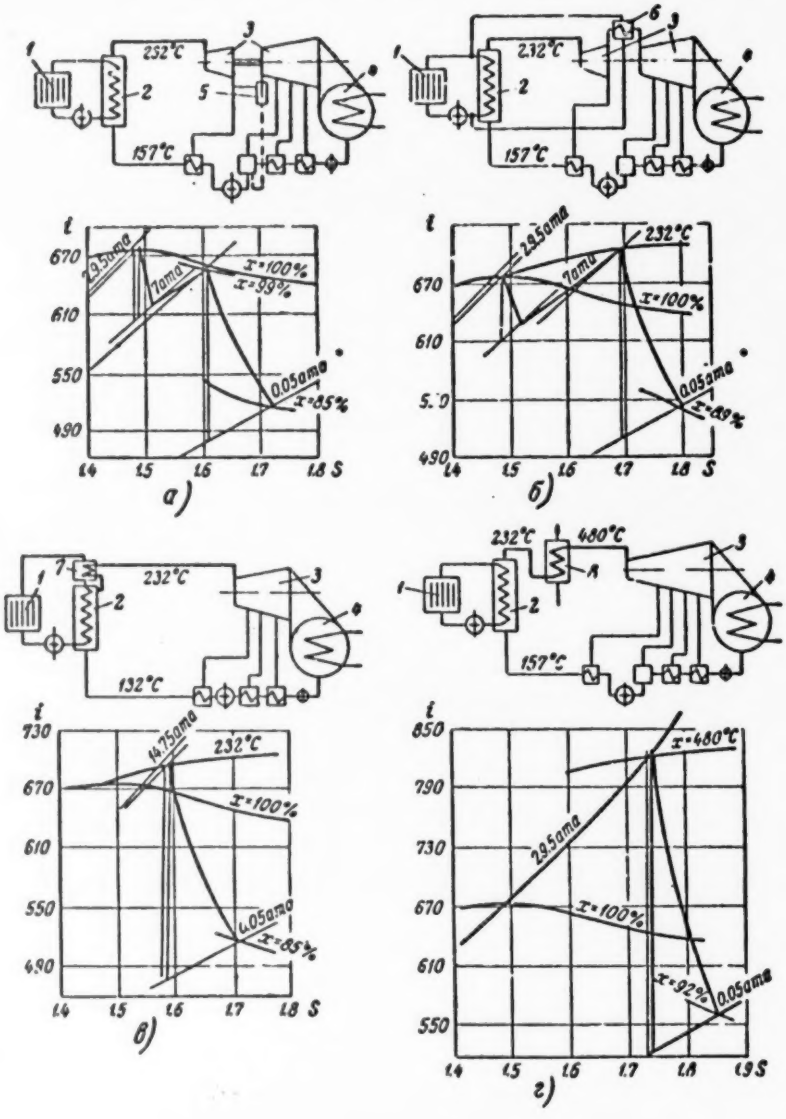


Dual loop systems of atomic installations

a) saturated steam with intermediate separation; b) saturated steam with intermediate superheating; c) superheated steam at lower temperature; c) high temperature superheated steam obtained in an individual superheater operated by the combustion of conventional fuel; 1) reactor; 2) heat exchanger; 3) turbine; 4) condenser; 5) separator for removing moisture from steam; 6) intermediate steam superheater; 7) steam superheater 8) steam superheater employing conventional fuel.

* ["ama" = atmospheres, absolute .]

In all four cases, the initial temperature in the second loop is taken to be 232°C. A pressure of saturated steam of 29.5 atmospheres, absolute, corresponds to this temperature. For the methods utilizing superheated steam, one-half that pressure – 14.75 atmospheres, absolute-is the accepted value. In the version which has an individual conventional fuel steam superheater, the steam, which is under a pressure of 29.5 atmospheres, absolute, is superheated in the superheater to 480°C. A regenerative steam power cycle with steam extraction for feed water heating is employed in all cases.

Calculations show that systems a and b (utilizing saturated steam) have an efficiency of 27.8%, system c (utilizing superheated steam at lower temperature) – 24.3%, and system d (utilizing high temperature superheated steam) – 32.3%.

Thus, improved saturated steam cycles at a lower pressure can be more advantageous than the superheated steam cycle. Reference [15] points out the definite advantage of the system with high superheating obtained by combustion of conventional fuel (see d in the figure).

Finally, mention should be made of the weight of atomic installations for ships. If a comparison is made of two ships of the same total displacement, one atomic-powered and the other conventional, the weight of their hulls, crews and supplies may be considered to be the same. With regard to the mechanisms, fuel and cargo capacity, their total weight is the same in both cases, but due to the smaller weight of the nuclear fuel the cargo capacity of the atomic-powered ship is greater than that of the conventional ship [15], [17].

## LITERATURE CITED


[1] Shipbuilding and Shipping Record 88, 199 (1956).

[2] K. Maddocks, Shipbuilder and Marine Engine-builder 63, 306 (1956).

[3] Shipbuilding No. 1, 11 (1957).

[4] Directives of the Twentieth Congress of the Communist Party dealing with the sixth five-year plan for developing the national economy of the USSR for 1956-1960. Published by "Pravda," 1956, p. 8.

[5] The Motor Ship XXXVII, 393 (1957).

[6] Shipbuilding and Shipping Record 88, 93 (1956).

[7] Shipbuilding and Shipping Record 88, 130 (1956).

[8] I. Cockcroft, Atomics Engineering and Technology 7, 241 (1956).

[9] Shipbuilding and Ship Record, 87, 372 (1956).

[10] I. Cockcroft, Shipbuilding and Shipping Record 87, 280 (1956).

[11] K. Maddocks, Shipbuilding and Shipping Record 86, No. 25 (1955).

[12] K. Maddocks, Shipbuilding and Shipping Record 86, No. 26 (1955).

[13] K. Maddocks, The Motor Ship XXXVI, No. 430 (1956).

[14] Witzke and S. A. Maverstick, The Motor Ship, XXXV, 188 (1954).

[15] The Motor Ship XXXVI, 514 (1956).

[16] Engineering 181, 78 (1956).

[17] Atomics Engineering and Technology 7, 97 (1956).

[18] L. M. Nogid, "Theory of Ship Design," Shipbuilding Industry Publishing Office, 1955, p. 44.


Received March 23, 1957

BLANK
PAGE

# THE USE OF RADIOACTIVE ISOTOPES FOR DETERMINATION OF SATURATED VAPOR PRESSURE

An. N. Nesmeyanov

A short survey of methods and apparatus arrangements used for measurement of vapor pressure by means of radioactive isotopes, is given here. A description is given of vapor pressure determination by the static method, through the direct measurement of radioactivity in the vapor by a counter, or through the determination of activity by radiographic and chemical means. Work on measurement of vapor pressure along the lines of the boiling point method and the jet method, is presented. On the basis of two works, the method of Langmuir in the variant of vaporization of matter from a thin wire and vaporization from a crucible, is discussed. The vapor pressure of liquid metals and of components of liquid alloys is derived from the activity of the condensate. A variation of this method is described, in which the vapor pressure is determined from the activity of part of the condensate. Integral (with collection of all vapor), and differential (with collection of only part of the vapor phase) variations of Knudsen's method are presented, as well as the results of measurement of vapor pressure of elements and components of alloys by means of radiometric analysis of condensate. In the last section a description is given of measurements of vapor pressure by the method of isotope exchange.

A table is given of relative sensitivity of vapor pressure measurement by the various methods.

It is essential to know the pressure of saturated vapor for calculation of the thermodynamic properties of matter.

The most accurate values of thermodynamic properties may be obtained from the dependence of vapor pressure on temperature over wide temperature intervals, particularly in the range of low vapor pressures.

Under ordinary temperatures, vapor pressures of solid materials, in particular of metals and their alloys, are measured in small fractions of millimeters of mercury column.

Various methods are used for measurement of saturated vapor pressures: static, boiling point, dynamic (method of inert gas stream), Langmuir's (evaporation from an exposed surface), Knudsen's effusion method, and the method of isotope exchange. The greatest errors in any one of these methods are incurred in measuring the temperature, as well as from the use of insufficiently pure substances.

To increase accuracy or sensitivity of measurements, radioactive isotopes are used. In that case the accuracy of results depends also on the accuracy of measurement of radioactivity. Here it is important that the isotope being used be radiochemically pure; a high chemical purity of the substance used for measurement is less essential.

1. The static method. The static method has two basic variations. The first variation includes the direct measurement of vapor pressure in a given space, in equilibrium with the condensed phase, by means of a mercury, ionization, quartz or other type of manometer.

This variation of the method was used [1] for determination of vapor pressure of solid white phosphorus by means of $P^{32}$ (Fig. 1); of phosphor pentaflouride [2], and of liquid zinc [3], contaminated with $Zn^{65}$ (Fig. 2).

For measurement of the vapor pressure, the substance under examination is placed in an enclosed space held at constant temperature and in which a high vacuum has been drawn. The pressure is determined from the radioactivity of the vapor measured with a counter. This method makes it possible to measure easily and with great accuracy, changes of radioactivity as functions of temperature, and to find the heat of vaporization within the measured temperature interval. For conversion to absolute values of vapor pressure it is essential to know the vapor pressure at one of the temperatures [1], or to find the conversion coefficient from activity to number of molecules with the aid of geometric correction factors and of radiation absorption factors [2]. The latter course is very complex, therefore it is better to calibrate the instrument to a substance with known activity and containing the subject isotope.

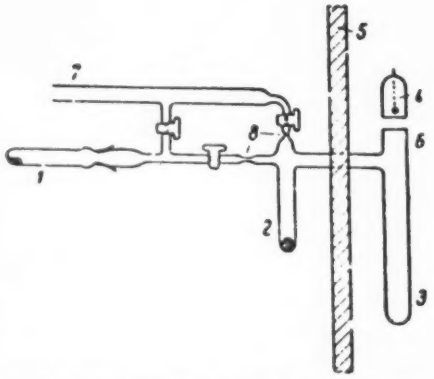


Fig. 1. Diagram of the apparatus of Dainton and Kimberley [1] for determination of vapor pressure of phosphorus.
1) red phosphorus; 2) white phosphorus; 3) sampling test tube; 4) counter; 5) shielding wall; 6) thin window; 7) to vacuum; 8) separation points.

An original variation of the static method was developed [4] for the determination of polonium vapor pressure. It is suitable for determination of vapor pressure of other $\alpha$-emitters. The polonium was placed in a cylindrical appendage of a spherical glass vessel, which was evacuated. Polonium vapors filled the sphere until equilibrium pressure was reached. The quantity of polonium in the spherical volume was determined by the number of $\alpha$-particles $\nu$, incident on 1 $cm^2$ of the inside surface of the sphere. These particles were registered on a photoemulsion, which was examined under a microscope, and the number of tracks counted. The following equation was used for calculations:

$$P = \frac{3kT}{\lambda t r}\,\nu, \qquad (1)$$

where $k$ – Boltzmann constant; $T$ – absolute temperature; $t$ – exposure time; $\lambda$ – decay constant, and $r$ – sphere radius.

To account for change of radioactivity with time, the decay correction factor $(1-e^{-\lambda t})$ was introduced into the denominator. Vapor pressure at room temperature turned out to be $5 \cdot 10^{-15}$ mm Hg.

At exposures up to 30 days time, it was possible to measure record low vapor pressures by this method. Polonium vapor pressure at room temperature turned out to be $5 \cdot 10^{-15}$ mm Hg. However, if there is no equilibrium between the vapor and condensate, erroneous results may be obtained. In addition, the assumption that the vapor consists of polonium atoms is doubtful.

In the second variation of this method [5], the number of gas molecules in a known volume, at a given temperature, is determined. The radioactive substance under examination is placed in a glass vessel 1, 2 (Fig. 3), (connected to the vacuum system), which is evacuated, melted off, and is placed in a furnace at constant temperature. After sufficient time has elapsed to establish equilibrium between the vapor and condensed phases, the vessel is melted at the neck 3, into two parts, while still in the furnace. Next the upper part of the vessel 1, is exposed and flushed with a solvent, following which, the quantity of radioactive material is determined from the activity of the resulting solution. Knowing the volume of the vessel, the quantity and molecular weight of the material, it is easy to determine the saturated vapor pressure by Clapeyron's equation.

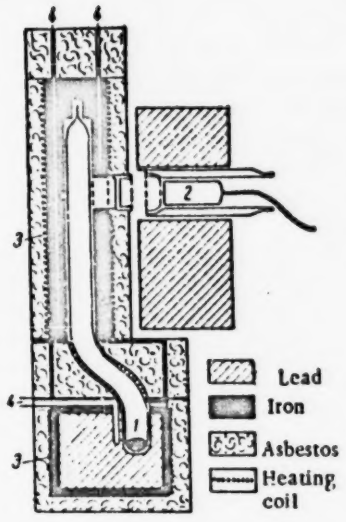


Fig. 2. Diagram of the apparatus of Groatto and Riccoboni [3] for measurement of vapor pressure. 1) glass or quartz vacuum tube containing the experimental substance; 2) counter; 3) heating pads; 4) leads for thermocouples.

The above method can yield results of high accuracy, but it is very laborious, and in addition the highest experimental temperature can not exceed the melting point of quartz. Obviously, this limitation applies to the first variation of the static method as well.

2. The boiling point method. A liquid boils when external pressure equals the pressure of its saturated vapor. This phenomenon is widely used for determination of vapor pressure of substances and metals that boil readily under lowered pressure. The substance under investigation is placed in a vessel that is reduced to the desired pressure, which is measured by a manometer. Then the temperature is raised to the boiling point, which is determined by various methods which introduce an initial error into the results. This method was adapted [6] for determination of vapor pressure of zinc. Zinc, containing $Zn^{65}$, was placed in the lower part (Fig. 4) of a bent quartz tube 2, which terminates in a U shaped condenser, 1. The end of the tube containing the molten zinc was located in a copper block that was electrically heated. The rest of the tube, up to the condenser, was within spirally wound electric heating elements and thermal insulation, which prevented vapor condensation on the walls of the tube. At the center of the horizontal section of the tube was a length that could be heated quickly at any time. 9. The vertical and horizontal sections of the tube were separated by a perforated barrier 7. The tube was connected to the vacuum system and to an argon gas cylinder through an adapter, 10. The system was evacuated, degassed, and filled with argon to a predetermined pressure. After this the metal in the tube was rapidly heated to 10 to 15° below the boiling point. Beyond this the heating was done at a rate of 0.3° per minute, then the heating of the central length of tubing was cut and the radioactivity of the condensate forming on the walls was measured by the counter 6, over definite time intervals. The slope of activity versus time, breaks at the boiling point. Both theoretically and in practice it was shown [7] that in the presence of the perforated diaphragm, which creates a resistance to the flow of vapor, the point of change of slope is sharply defined; there is an upper limit to the perforation size at which the change of slope is still sharp and the character of the change depends on the velocity near the boiling point. The authors obtained good results over a wide temperature range.

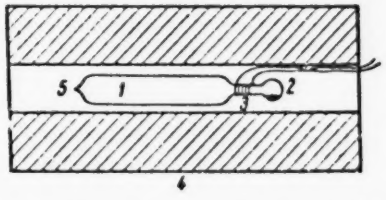


Fig. 3. Apparatus of Nesmeyanov and Iofa [5] for measurement of vapor pressure by the static method. 1,2) glass or quartz tube with subject material; 3) parting point; 4) furnace; 5) parting point from vacuum system.

3. Dynamic method (gas jet method). A gas jet that is inert in relation to the subject substance is directed over a sample of the substance which is heated to a predetermined temperature, thus carrying off vapors of the substance. The rate of vapor removal depends on the rate of flow of gas. Data obtained from tests at various velocities, extrapolated to zero velocity, allow the calculation of saturated vapor pressure by the equation

$$P = P_1 \frac{n}{n + n_1}, \qquad (2)$$

where P – vapor pressure of the subject substance; $P_1$ – total pressure of inert gas and vapor; n – number of mols of the subject substance carried off by $n_1$ mols of inert gas.

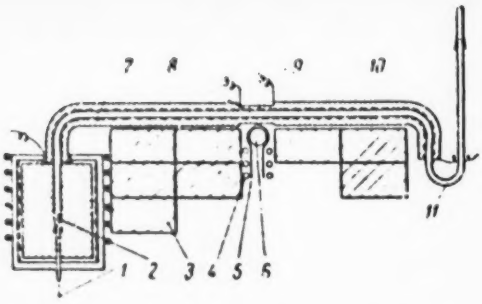


Fig. 4. Diagram of the equipment of Smirnov and Detkov [6] for determination of vapor pressure by the boiling point method.
1) thermocouple; 2) metal in quartz tube; 3) lead block; 4) cooler; 5) counter shield; 6) counter; 7) perforated barriers; 8) location of temporary vapor condensation; 9) heating system for temporary condensation tube length; 10) adapter to the vacuum system; 11) vapor condensation region.

The quantity of vaporized substance is determined by weight loss of original sample or by the quantity of condensate. In the latter case, radioactive tracers can be used successfully. Recently this method was used [8] for determination of partial pressures of a solution of bromine, including $Br^{82}$, in carbon tetrachloride. A stream of air was passed over the bromine solution. Next, the mixture of gases was passed through a vessel enclosing the counter, and arrived in the condenser. The quantity of condensate, through which the vapor pressure was determined, was measured by a counter for changes in radioactivity, against external pressure and volume of mixed gases passed through.

4. Langmuir's method (evaporation from an exposed surface). The quantity of material that evaporates in unit time from a square centimeter of exposed surface of sample in vacuum, is determined by the relationship derived by Langmuir,

$$G = \alpha P \sqrt{\frac{M}{2\pi RT}}, \qquad (3)$$

where G – rate of evaporation in $g/cm^2$ sec; P – vapor pressure in $dyne/cm^2$; M – molecular weight; R – gas constant in ergs/degree; T – absolute temperature; $\alpha$ – dimensionless coefficient of vaporization, which determines the portion of surface from which evaporation actually occurs. Although this coefficient is taken equal to unity in the vast majority of cases, this assumption may introduce serious errors in the calculations.

The quantity of evaporated material can be determined from the weight of condensate through comparison of its activity with the specific activity of the original substance which contains the radioactive trace element.

Vapor pressure of strontium oxide including some $Sr^{89}$, that had been deposited on a platinum wire, was determined by this method [9]. The platinum wire was heated, in vacuum, by electric current flow. The temperature of the strontium oxide on the wire was measured by an optical pyrometer. The vapors of strontium oxide condensed out on the walls of the glass vessel in which the wire was contained, and from which the strontium oxide was washed out by an acid salt solution. The strontium content in the solution was determined by potentiometric titration, by weight method and by radioactivity.

This apparatus was not perfected, since after every exposure it became necessary to break the glass vessel. In addition, the surface of vaporizing substance did not measure accurately. A more perfected apparatus was used [5] for determination of vapor pressure of cadmium and zinc solids (Fig. 5) containing $Cd^{113}$ or $Zn^{65}$. The metal was electroplated onto a ceramic tube that had been coated with silver. The tube was fitted over an iron or molybdenum wire 2, which served as heating element 3, and was connected to molybdenum terminals cast into a base adapter. A glass dome with a cooling shroud 8, was fitted over the base adapter, after which, the dome was evacuated. The temperature was measured through the thermocouple 5, whose hot junction was fastened in a recess in the ceramic tube at the metal surface. The error in temperature reading incurred through conduction of heat through the thermocouple must be considered. Often, one of the most important sources of error in Langmuir's method is the inequality of temperature between the bulk of the metal and the metal surface. At conclusion of the experiment the condensate was washed out of the glass dome, and the quantity of metal present was determined by the radioactivity of the solution.

During the past few years another variation of Langmuir's method has been widely adopted. A cylinder or ring made of the metal under investigation, is heated under vacuum by high frequency currents. Since a large mass of metal is used for the experiment, the radioactive tracers can obviously be used by their deposition onto a ring or cylinder made of another inert material.

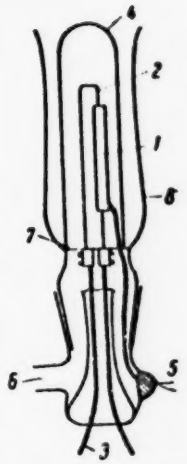


Fig. 5. Diagram of Nesmeyanov's, Priselkov's and Chernorotov's apparatus [5] for measurement of vapor pressure of zinc and cadmium solids by Langmuir's method.

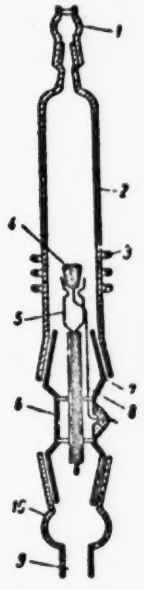


Fig. 6. Diagram of apparatus of Lyubimova and Granovskaya [10] for determination of vapor pressure of liquid metals by Langmuir's method.
1) adapter with quartz window; 2) condenser; 3) high frequency coil of induction furnace; 4) crucibles containing metal; 5,7) crucible holding base; 6) coupling adapter; 8) thermocouple; 9) to the vacuum system; 10) adapter.

Langmuir's method was also adopted for determination of vapor pressure of liquid silver [10] and of partial vapor pressures of the constituents of alloys of silver and lead, and iron and phosphorus [11], silicon, sulphur [12] and chrome [13] with corresponding employment of $Ag^{110}$, $P^{32}$, $S^{35}$, $Fe^{59}$, and $Cr^{51}$. Evaporation took place from an exposed metal surface in a crucible. The crucible was fixed in the base of a glass apparatus, the upper part of which, was a glass dome (Fig. 6). The base of the apparatus and the dome were joined through an adapter 7. The apparatus was connected to a vacuum system 9. The metal in the crucible was heated by induction coil 3. The temperature was measured by a thermocouple 8, that was lead from below, to the bottom of the crucible. The evaporating metal gathered on the surface of the dome 2. The quantity of evaporated metal was determined by the radioactivity of the condensate. As in all the other variations of Langmuir's method, there is present an inaccuracy in determination of exposure time since no methods for isolating the condensation dome from the vapors during heating up and cooling down of the crucible are available. In addition there is an inaccuracy in the determination of metal surface area, which under the action of high frequency currents, assumes a spherical shape. All these errors are accounted for by special experiments.

Of interest is the work [14] in which evaporation was conducted in a vacuum with exposed surface of a solid metal disc, and the condensate was collected on a receiving disc (target), made of another metal, located parallel to the first disc and at some distance from it. Having adapted the law of nondependence of molecular flow distribution on the nature of the vaporizing substance to the case of evaporation from a flat source, the authors made use of the relationship that gives the fraction of molecular current falling on the target,

$$k = \frac{1}{2l^2}\left[r^2 + \sqrt{(h^2+l^2+r^2)^2 - 4l^2r^2} + \right. \\ \left. + \sqrt{(h^2+l^2)^2}\right], \qquad (4)$$

where $l$ – radius of sample; $r$ – radius of target and $h$ – distance from sample to target.

The quantity $k$ may be found by experimental methods through the relationship of quantity of substance, condensing on the target, to the loss of weight of the sample. A check showed good coincidence of experimental and calculated values of $k$.

Vapor pressure of cobalt including $Co^{60}$ and of iron including $Fe^{59}$ was determined through the formula

$$P = \frac{I}{\beta_0 kSt}\sqrt{\frac{2\pi RT}{M}}, \qquad (5)$$

where $t$ – exposure time in sec; S – area of sample in cm²; $\beta_0$ – activity of one gram of the initial metal sample; I – measured activity of the condensate.

In using the formula it was assumed that the evaporation coefficient was equal to unity, and vapor condensation is complete on the target. The apparatus held a large quantity of targets distributed similar to the arrangement shown in Fig. 7. This allowed the acquisition of many readings without disturbing the vacuum.

A fault of this variation is the probable nonuniformity of induction heating of the metal surface.

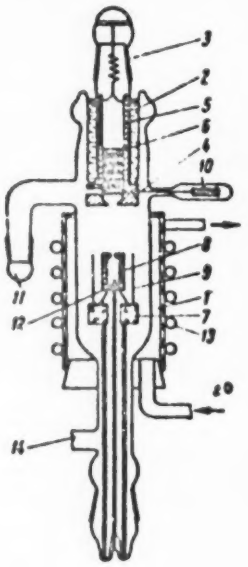


Fig. 7. Schematic diagram of apparatus for determination of vapor pressure by the differential effusion method.
1) cooler shroud; 2) dewar flask with liquid nitrogen; 3) adapter; 4) collimator; 5) cell containing targets; 6) targets; 7) effusion chamber holder; 8) effusion chamber; 9) screen; 10) manipulator; 11) target receiver; 12) thermocouple; 13) high frequency induction heater; 14) to vacuum system.

5. Knudsen's effusion method (flow of vapor through a small aperture to vacuum). This method is based on the relationship derived by Knudsen expressing the quantity of vapor passing by effusion* through an ideal (with infinitely thin walls) small aperture into a vacuum:

$$g = At(P - P_1)\sqrt{\frac{M}{2\pi RT}}, \qquad (6)$$

where $P - P_1$ – difference of vapor pressures on either side of the aperture in dyne/cm²; A – area of effusion aperture in cm²; $t$ – time of effusion in sec; R – gas constant in ergs.

The experiment is run so that in the volume on one side of the aperture, the vapor pressure is established, and on the other side – a vacuum, $P_1 = 0$.

Vaporization takes place through a tangible opening, out of a cylindrical chamber. Both the opening and the chamber offer resistance to the flow of vapor, which is determined from the relationship of their diameter and height. Resistance of the effusion cell is, as a rule, small, and it can be neglected. The resistance of the aperture is characterized by Clausing's coefficient, K, which represents the relationship between the number of molecules passing through the effusion aperture and the number of molecules entering it. The vapor pressure, considering K, is determined from the formula

$$P = \frac{g}{KAt}\sqrt{\frac{2\pi RT}{M}}. \qquad (7)$$

In essence, the method should yield accurate results in the case of a current of molecules established through the effusion aperture, that is, when the aperture dimensions are smaller than the mean free path of the molecules (in practice the pressure must be below $10^{-4}$ mm Hg.) and there is equilibrium of pressure in the effusion chamber. The values of K, A and $t$ may be easily determined with great accuracy. The most considerable errors are introduced into the measurements in the case of temperature determination. The value of M in vapors is difficult to determine, and the available methods do not yield consistent results; therefore the value of M is, in most cases, assumed to equal the weight of a single molecule. The effusion chamber material must not react with the vapors of the material under test. The condensation of the vapors must be complete on the receiver.

* The slow flow of gas through a small aperture is called effusion.

The effusion method may be conducted in one of two variations. The first – integral method – is based on the determination of total quantity of material passing through the effusion aperture in time t. It may be determined through weight loss of material in the effusion chamber, or through the amount of condensate. In the latter case, the use of radioactive tracers increases the sensitivity of the method considerably.

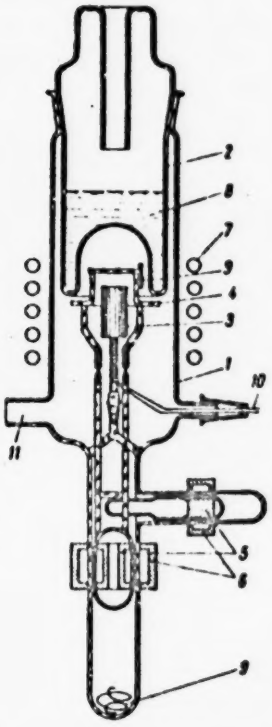


Fig. 8. Schematic diagram of the apparatus of Priselkov and Nesmeyanov [30] for determination of vapor pressure by the integral effusion method.
1) basic shell; 2) condensing dome; 3) effusion chamber; 4) protective cover; 5) holders; 6) electromagnets; 7) induction coil; 8) liquefied air; 9) small spring; 10) thermocouple; 11) to the vacuum system.

The second, differential, variation of the method has been developed during the past years [15], [16] and has received wide acceptance. The sensitivity of this method is considerably below that of the integral method, since only a part of the effusion flow is collected.

The apparatus used by various researchers do not vary basically, although the apparatus of Hall [17] is essentially different in design from the apparatus of other authors. The general scheme of these apparatuses is shown in Fig. 7.

A small central portion of the molecular ray, detached by the collimator 4, condenses on the flat metallic targets 6, which are cooled by liquid nitrogen 2. By means of the manipulator 10, the discs may be replaced without disturbing the vacuum in the apparatus. In the vast majority of cases, heating was done by high frequency currents through an induction coil, 13, that was fitted over the glass or quartz apparatus. After conclusion of a series of exposures, the apparatus is disassembled and the activity of the condensate on the discs is measured with a counter. For calculation of vapor pressure the formula (7) is used, including a factor that accounts for the fraction of molecular current passing through the collimator,

$$\frac{D^2 + 4h^2}{D^2}, \qquad (8)$$

where D – diameter of collimator aperture and h – distance between effusion aperture and collimator.

Inadequate calibration of the apparatus can introduce considerably larger errors into the results than in reference [14]. In addition, in the case of β-emitters, it is essential to maintain nearly the same weight of condensate on the target disc in all experiments.

By means of this method the following were measured:

Americium vapor pressure [18], which was determined by Rayleigh's law from the vapor pressure over a dilute solid solution of americium in plutonium; the results agree well with later [19] direct determination;

Uranium vapor pressure [20], which was determined from fission product activity that was obtained by irradiation of uranium in a nuclear reactor;

Gold ($Au^{198}$) vapor pressure, from solid solutions of gold in copper [17];

Vapor pressure of halogen compounds of tri-valent plutonium and americium [21], [22], dioxide of plutonium [23], dioxide of uranium [24], beryllium oxide ($Be^{7}$) [25], calcium ($Ca^{45}$) [26], silver ($Ag^{110}$) [17], iron ($Fe^{59}$) [27], cobalt ($Co^{60}$) [28], and alloys of silver ($Ag^{110}$) with gold [29].

Investigations of the vapor pressure of silver [5] by the differential method, showed that the inaccuracies mentioned earlier can be aggravated by the action of a high frequency field which disturbs the molecular current.

The integral effusion method was first developed for inductive heating (determination of vapor pressure of solid calcium ($Ca^{45}$) and strontium ($Sr^{89}$) [30], Fig. 8 and 9), and later for common heating [31] (determination of vapor pressure ($Sb^{125}$) - solid antimony).

In all the experiments the vapor condensate was collected on a receiver, was washed off it, and the radioactivity of the resulting solution was determined by a counter. The devices 4,5,6 (Fig. 8), that allow cutting off the flow of molecules while the chamber is being heated to temperature and while it is being cooled, improve the accuracy of measurements considerably, and the ability to collect all the condensate is an advantage possessed by this apparatus over the apparatus of the differential variety. The vapor pressures of solid zinc and cadmium ($Zn^{65}$, $Cd^{113}$•) [32], arsenic ($As^{76}$), copper, silver and gold ($Cu^{64}$, $Ag^{110}$, $Au^{196}$) [33] were determined by this method.

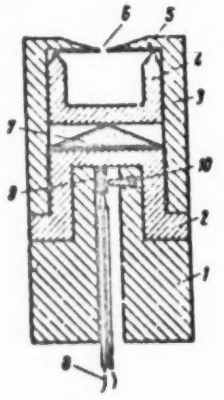


Fig. 9. Effusion chamber for apparatus of Priselkov and Nesmeyanov (see Fig. 8).
1) base; 2) lower plug; 3) cover; 4) insert, 5) diaphragm; 6) diaphragm aperture; 7) pressure cone; 8) thermocouples; 9) hot junction; 10) set screw.

Of greater interest are the experiments in connection with measurement of vapor pressures of the components of metal alloys and of mixed crystals of various salts. Alloys of antimony and zinc, arsenic and zinc and cadmium, and zinc and cadmium, which included eutectics and chemical links, were investigated.

The investigations showed that there exist two types of alloys that form chemical links.

In the first type the vapor pressure, measured for each component individually, varies. At evaporation, decomposition of the chemical links (ZnSb, $Zn_3Sb_2$) takes place at the surface of the alloy, and it behaves like a solid solution. The vapor pressure of zinc changes over the entire range of concentration, proportionally to its mol fraction in the alloy, and the vapor pressure of antimony in all alloys is near the vapor pressure of pure antimony. Apparently, the surface layers of crystalline substances can behave independently of the mass of the substance under conditions of evaporation, and in the surface layer of the antimony-zinc system there occurs a dissociation of the antimony-zinc link and the rapid expulsion of the more volatile zinc causes a surface enrichment in antimony. Oppositely, alloys of the second type (chemical links and zinc and cadmium with arsenic) do not decompose under evaporation, and the vapor pressures measured for each of the components individually, yield identical results. The heat of dissociation of these links is higher than the heat of evaporation, while for alloys of antimony and zinc, the heat of dissociation is lower.

The vapor pressure of eutectic alloys [34] (Zn-Cd; KCl-NaCl) is equal to the vapor pressure of the pure components.

The investigation of vapor pressures of components of solid solutions of metals [33] and of potassium chloride and rubidium chloride [35] demonstrated the suitability of the method for study of the thermodynamics of solid solutions. Diagrams of vapor pressure vs. composition for the system gold-silver, gold-copper, exhibit negative departures from Rayleigh's law. The complex nature of the curves for the system KCl-RbCl indicates changes of linkage in the crystal lattice. The results show agreement with the equation of Gibbs-Duhanand with the data obtained by other authors and other methods.

The integral effusion method was also used in the work [36] on vapor pressure of solid zinc with $Zn^{65}$. The results were entirely satisfactory.

6. The isotope exchange method. This method [37], [38] is based on the measurement of rate of exchange of molecules through the gaseous phase between two samples of a substance in a vacuum that are of identical chemical composition and different isotope composition.

The following cases of exchange are possible:

a) the samples are located opposite each other,
b) the samples are located in one plane,
c) the samples are separated by a diaphragm with small aperture.

The rate of isotope exchange at any given temperature is determined by the speed of evaporation and the speed of diffusion of the molecules into the body of the sample. The relationships that determine the dependence of evaporation rate and of diffusion coefficient on time are the solutions of the diffusion equation with boundary conditions given by the evaporation process. This solution may be given either as an equation containing the Gaussian probability integral [37], [39], [40] or, converting to a more simplified expression, by conversion of the probability function into a series [38].

For samples located in one plane, the final equation may be given in the following form:

$$I = \frac{\alpha K G b S_2}{c^3}\left(v^3 - \frac{4}{3}\cdot\frac{v^3}{\sqrt{\pi}} + \frac{1}{2}v^4 - \right.$$
$$\left. - \frac{8}{15}\cdot\frac{v^5}{\sqrt{\pi}} + \cdots\right), \qquad (9)$$

where

$$v = c\sqrt{t} = \frac{\alpha K G}{\rho}\sqrt{\frac{t}{D}}; \quad b = \frac{\beta_0 S_1}{S_1 + S_2};$$

I is the activity of the initially inactive sample, in counts/sec; $\alpha$ is the dimensionless coefficient of evaporation; K is the dimensionless Clausing coefficient; G is the rate of evaporation in g/cm² sec.; $\rho$ is the density in g/cm³; $\beta_0$ is the specific activity of the initially radioactive sample in counts/sec/g; $S_1$ is the area of the radioactive sample in cm²; $S_2$ is the area of the inactive sample in cm²; t is the time of exchange in sec. D is the diffusion coefficient in cm²/sec.

In practice the measurements are made within a time interval such that one of two first terms of the equation are sufficient. In the case of location of the sample surfaces in one plane, the rate of transfer increases and the formula (9) assumes a form with which, for samples of equal areas, it is essential to replace G by 2G. If the exchange time is low, then all terms of the series except the first, may be discarded and the formula takes the form that gives a linear relationship between activity and time.

For the case in which the radioactive sample is much lower in area than the inactive sample, and the surfaces of the samples are opposite each other, still another solution can be used [41] in which the linear terms of activity vs. time are greater.

The solution of the exchange problem in the case of samples whose surfaces are situated opposite each other, without expansion of a series, reduces to the following two expressions [38]:

$$A = \sqrt{\frac{t'}{\pi}} + \frac{1}{4}e^{t/t'}\left[1 + \Phi\left(2\sqrt{t'}\right)\right] - \frac{1}{4} \qquad (10)$$

and

$$I = \frac{\beta_0 \rho S_2}{h}\left\{h\sqrt{\frac{Dt}{\pi}} + \frac{1}{4}\exp\left(4h^2 Dt\right) \times \right.$$
$$\left. \times \left[1 - \Phi\left(2h\sqrt{Dt}\right)\right] - \frac{1}{4}\right\}, \qquad (11)$$

where A is a dimensionless function of $t'$ characterizing the amount of radioactive isotope collected; $t' = h^2$; $h = \frac{G\alpha K}{\rho D}$; $\Phi$ is the probability integral.

To determine rate of evaporation by formulas (10) and (11) it becomes necessary to use a graphic method. First a curve of the theoretical relationship of A to $t'$ is drawn on a log-log graph, then the relationship of log I to log $t$ is found from experimental results. The second curve is drawn with the first, and from this the values of $t'$, h and D are found.

The method of isotope exchange allows the simultaneous determination of the rate of evaporation and coefficient of diffusion by means of determination of the change in radioactivity of the originally inactive sample as a function of time at constant temperature. Since the chemical composition of the samples does not change with time, this method is suitable for measurement of partial pressures of components over alloys. The basic difficulty in the method is the necessity for determination of the evaporation coefficient $\alpha$.

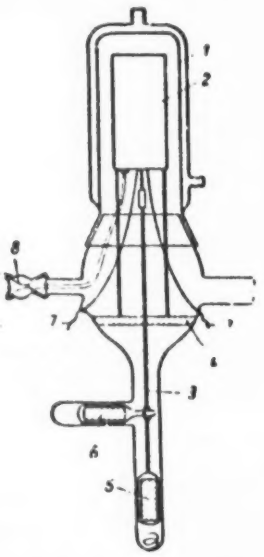


Fig. 10. Schematic diagram of apparatus of Nesmeyanov et al., [43] for measurement of saturated vapor pressure by the method of isotope exchange. 1) removable dome with cooling device; 2) heating oven with exchange chamber; 3) shade center line axis; 4) oven base; 5,6) retainers; 7) molybdenum electrodes; 8) thermocouples.

When the samples are separated by a space that has large resistance to vapor flow [42], or by a diaphragm with a small aperture [38], [39], then in the region of each sample saturated vapor is formed. From experiments at various temperatures on the relationship of log I to 1/4 it is possible to find the heat of evaporation. For determination of absolute value of rate of evaporation, the exchange must be made through a diaphragm with a known aperture area S. For the calculation it is possible to make use of the Equation (9), replacing $\frac{S_1 G}{S_1 + S_2}$ by $2GS/S_2$. In this experimental set up, the growth of activity occurs linearly over a relatively long time.

Figs. 10 and 11 give schematic diagrams of the set up and of the chamber for measurement of evaporation rate and coefficient of diffusion by means of the isotope exchange method [43]. The metallic exchange chamber, including a shade that separated the samples during heating of the chamber to predetermined temperature, was placed inside a glass or quartz vacuum chamber. The chamber was heated by means of a high frequency induction coil, or by a miniature resistance heating oven, fitted inside the vacuum chamber. The discs were exposed for definite periods of time under constant temperature. The radioactivity of the originally inactive sample was measured as was the specific activity of the initial sample.

The rates of evaporation of solid silver [38] were also measured using $Ag^{110}$ and solid bismuth [43] (up to $4 \cdot 10^{-11}$ mm Hg) with $Bi^{210}$. The rates of evaporation of zinc ($Zn^{65}$) and cadmium ($Cd^{113}$•) [44] were measured in a similar apparatus but with diaphragm having a calibrated aperture.

The results proved to fall near previously published data that had been obtained by other methods.

In the determination of rates of evaporation of silver ($Ag^{110}$) from alloys of silver, gold [31], tin and lead [45], a simplified method was used. Metal discs (radioactive and inactive) of equal area were placed on top of each other and were separated by an air space by means of mica spacer rings. Such packs were placed in the evacuated space in the oven and were kept there a predetermined time, after which the activity of the originally inactive sample was measured.

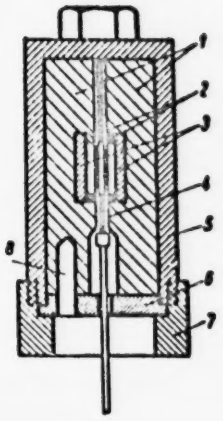


Fig. 11. Exchange chamber for apparatus of Nesmeyanov et al.
1) Insert; 2) support rings; 3) samples; 4) shade; 5) chamber shell; 6) cover; 7) nut; 8) thermocouple recess.

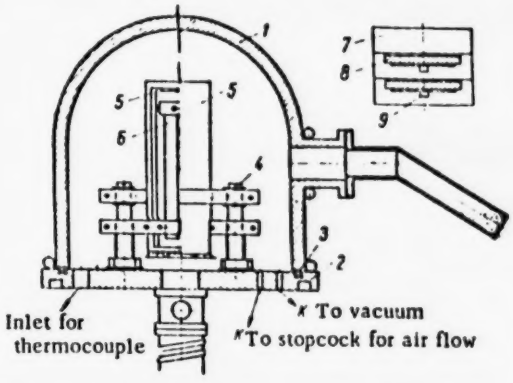


Fig. 12. Diagram of the apparatus of Ivanov and Matveeva for determination [46] of vapor pressure by the isotope exchange method.
1) copper dome; 2) steel plate; 3) rubber seal; 4) current supply electrodes, cooled by water; 5) molybdenum screen; 6) molybdenum heater; 7) corundum cups; 8) inactive sample (target); 9) radioactive sample.

A more complicated method was used in work [41] conducted for determination of evaporation rates of iron from iron-chromium alloys, with the use of $Fe^{59}$. Ten corundum cups 7 (Fig. 12) were filled with the metal samples; a small radioactive one 9- in the recess and a large inactive one 8- on the recessed shoulder over the small sample. Each cup contained alloys of different composition. The cups were fixed inside a container which was placed inside a molybdenum resistance oven 6 under a vacuum dome. Exposure was conducted for a predetermined time, following which the activity of previously inactive samples was measured. The rate of evaporation and vapor pressure were determined from the activity.

• • •

In all the above considerations it was assumed that all isotopes of an element have equal saturated vapor pressures. However this is only approximately true, and it is necessary to multiply the vapor pressure by a coefficient

$$f = \sqrt{\frac{M_i}{M_e}}, \qquad (12)$$

where $M_i$ is the molecular (atomic) weight of the simplest isotope molecule, and $M_e$ is the molecular (atomic) weight of the molecule of the natural isotopic mixture.

| Methods | Pressure mm Hg |
|---|---|
| Langmuir's | $10^{-12}$ |
| Knudsen's (integral) | $10^{-9}$ |
| Knudsen's (differential) | $10^{-7}$ |
| Isotope exchange | $10^{-12}$ |
| Nesmayanov, Iofa (static) | $10^{-7}$ |

The sensitivity figures for the various methods of measuring vapor pressure with a 10% counting effectiveness for a sample of 1 curie activity are given in the table.

The use of radioactive isotopes is particularly practical for measurement of saturated vapor pressures of metals and their alloys.

## LITERATURE CITED

[1] F. S. Dainton and H. M. Kimberley, Trans. Faraday Soc. 46, 912 (1950).

[2] F. D. Rosen and W. Davis, Rev. Sci. Instruments 24, 349 (1953).

[3] U. Groatto and L. Riccoboni, La Chimica e L'Industria 37, 538 (1955).

[4] J. S. Auslander and I. I. Georgescu (Report No. 1090, presented at the International conference on peaceful uses of atomic energy, Geneva, 1955).

[5] A. N. Nesmeyanov, Measurement of vapor pressure of solid substances in binary alloys. Collection of papers presented at the All-Union Conference on the uses of radioactive and stable isotopes, Vol. 2, Metallurgy and Metalworking, Izd. AN SSSR (in publication).

[6] M. V. Smirnov and S. N. Detkov, Annals of Acad. of Sci. USSR 98, 777 (1954).

[7] S. N. Detkov, Journal of Phys. Chem. 31, 83 (1957).

[8] C. Barthel and M. Dode, Bull. Soc. Chim. France, 1312 (1954).

[9] G. E. Moore, H. W. Allison and I. D. Struthers, J. Chem. Phys. 18, 1572 (1950).

[10] A. P. Lyubimov and A. A. Granovskaya, Journal of Phys. Chem. 27, 10 (1953).

[11] A. P. Lyubimov and A. A. Granovskaya, Journal of Phys. Chem. 27, 1437 (1953).

[12] A. A. Granovskaya and A. P. Lyubimov, Uses of radioactive isotopes in metallurgy, GITI, 1955, p. 66.

[13] A. P. Lyubimov and A. A. Granovskaya, Uses of radioactive isotopes in metallurgy, GITI, 1955, p. 95.

[14] M. P. Matveeva, I. A. Popov and L. I. Ivanov,Quotation from book by I. S. Kulikov and I. A. Popov, Uses of radioactive isotopes in metallurgy, p. 127 GITI, 1956.

[15] S. C. Carniglia and B. B. Cunningham, J. Amer. Chem. Soc. 77, 1502 (1955).

[16] D. H. Tomlin, Proc. Phys. Soc. 67B, 787 (1954).

[17] H. M. Schadel and C. E. Birchenall, J. Metals 188, 1134 (1950).

[18] T. E. Phipps, G. W. Sears, R. L. Seifert and O. C. Simpson, Vapour Pressure of Plutonium (Report No. 735, presented at the International Conference on the peaceful uses of atomic energy, Geneva, 1955).

[19] N. D. Erway and O. C. Simpson, J. Chem. Phys. 18, 953 (1950).

[20] E. G. Rauh and R. J. Thom, J. Chem. Phys. 22, 1414 (1954).

[21] L. D. Hall, J. Chem. Soc. 73, 757 (1951).

[22] T. E. Phipps, G. W. Sears, R. L. Seifert and O. C. Simpson, J. Chem. Phys. 18, 713 (1950).

[23] S. C. Carniglia and B. B. Cunningham, J. Amer. Chem. Soc. 77, 1451 (1955).

[24] R. J. Ackerman, ANL – 5482, Sept. 14, 1955.

[25] T. E. Phipps, G. W. Sears and O. C. Simpson, J. Chem. Phys. 18, 724 (1950).

[26] N. D. Erway and L. K. Seifert, J. Electrochem. Soc. 98, 83 (1951).

[27] Yu. V. Kornev, Annals of Acad. of Sci. USSR 93, 467 (1953).

[28] Yu. V. Kornev and V. N. Golubkin, Annals of Acad. of Sci. USSR 99, 565 (1954).

[29] Yu. V. Kornev and E. Z. Vaintaikin, Journal of Phys. Chem. 30, 1540 (1956).

[30] Yu. A. Priselkov and A. N. Nesmeyanov, Annals of Acad. of Sci. USSR 95, 1207 (1954).

[31] A. N. Nesmeyanov and B. Z. Iofa, Annals of Acad. of Sci. USSR 98, 993 (1954).

[32] A. N. Nesmeyanov, B. Z. Iofa, A. A. Strelnikov and V. G. Firsov, Journal of Phys. Chem. 30, 1250 (1956).

[33] A. N. Nesmeyanov, L. A. Smakhtin and V. I. Lebedev, Annals of the Acad. of Sci. USSR 112, 700 (1957).

[34] A. N. Nesmeyanov and L. A. Sazonov, Zh. N. Kh. 2, 946 (1957).

[35] A. N. Nesmeyanov and L. A. Sazonov, Zh. N. Kh. 2, 1183 (1957).

[36] I. D. McKinley and L. E. Vanu, J. Chem. Phys. 22, 1120 (1954).

[37] A. N. Nesmeyanov, V. I. Lozgachev and N. F. Lebedev, Annals of Acad. of Sci. USSR 102, 307 (1955).

[38] A. N. Nesmeyanov, N. F. Lebedev, V. I. Lozgachev and E. G. Chudinov, The method of isotope exchange for measurement of rate of evaporation and diffusion coefficient of metals. Session of Acad. of Sci. of USSR on the peaceful uses of atomic energy, 1-5 June 1955 (Session of the division of technical sciences) Izd. AN SSSR, 1955, p. 79.

[39] A. A. Zhukhovitsky, Methods of investigation of diffusion by means of radioactive isotopes. Session of the Acad. of Sci. of USSR on peaceful uses of atomic energy, 1-5 June 1955 (Session of the division of technical sciences) Izd. AN SSSR, 1955, p. 101.

[40] A. A. Zhukovsky, M. E. Yanitskaya and S. M. Kryukov, Journal of Phys. Chem. 29, 1338 (1955).

[41] L. I. Ivanov, I. S. Kulikov and M. N. Matveeva, Bull. Acad. Sci. SSSR, Div. of Tech. Sci. No. 8 (1955).

[42] A. A. Zhukhovitsky, M. E. Yanitskaya, S. M. Kryukov and A. G. Galitsin, Annals of Acad. of Sci. USSR 102, 127 (1955).

[43] A. N. Nesmeyanov, B. Z. Iofa and B. Karasev, Annals of Acad. of Sci. USSR 112, 882 (1957).

[44] A. N. Nesmeyanov and L. M. Iyicheva, Journal of Phys. Chem. (in print).

[45] A. A. Zhukhovitsky and M. E. Yanitskaya, Annals of Acad. of Sci. USSR (in print).

[46] L. I. Ivanov and M. P. Matveeva, A new apparatus and method for measurement of elasticity of metal vapor, II-57-17/4. VNIITEI of State Tech. USSR and Acad. of Sci. USSR, 1957.

Received June 19, 1957

BLANK
PAGE

# THE DEFINITION OF THE ROENTGEN IN THE "RECOMMENDATIONS OF THE INTERNATIONAL COMMISSION ON RADIOLOGICAL UNITS, 1953"

S. N. Ardashnikov and N. S. Chetverikov

The contradictions found in the definitions of the roentgen as a unit of X- and γ-radiation are expounded and criticized. The definition accepted in the USSR of the roentgen as the unit of physical dose ($\frac{OST}{VKS}$ 7623) differs from those in the International Recommendations and of the Congresses (Stockholm 1928 and Chicago 1937), where the roentgen is considered as the unit of dose, and not the physical dose. This has occasioned much confusion as to the physical content of the phenomena which the roentgen was intended to measure. An attempt was made in the 1953 Recommendations to resolve these difficulties, but this cannot be considered successful. The basic fault in the definition of the roentgen, which is that it "measures the amount of X- or γ-radiation" is retained. The definition given in the Recommendations of the amount of radiation as the time-integral of the intensity leads to the concept of the amount of radiation as being a flux density at a point, i.e., it adds a third variant to the dose concept, which further confuses the issue. The paper presents the requirements which the definitions of the basic units for measuring ionizing radiations – the roentgen and its equivalents – must satisfy.

The concept of the roentgen as the unit of physical radiation dose was attached to the All-Union standard unit of X-radiation ($\frac{OST}{VKS}$ 7623) prepared by I. V. Poroikov in 1934, the following entry stemming from this:

| Name | Symbol | Definition | Ratio to basic unit | Dimensions |
|---|---|---|---|---|
| Unit of physical radiation dose<br>1. Roentgen | r | The physical dose of X-rays which produces charges each of one electrostatic unit in magnitude per $cm^3$ of irradiated volume in air at O°C and normal atmospheric pressure when ionization is complete; | 1 | $L^{-1}MT^{-2}$ |

Note. By complete ionization is understood the complete use of the radiation energy to produce ionization.

Since this definition differs from the generally accepted definitions in the International Recommendations we must pause over the concepts on which the definition is based. By physical dose is meant the ratio of the absorbed energy to the mass of the irradiated substance (here air) or to its volume if it contains air at NTP.*

* "The physical dose is D. It is the absorbed X-ray energy per unit volume of irradiated medium. D = dW/dv, where dv is a volume element ($L^{-1}MT^{-2}$)". ($\frac{OST}{VKS}$ 6350).

By absorption of energy ($\frac{OST}{VKS}$ 7770) we should understand "the transformation of the energy in the incident X-rays into other forms of energy when the rays pass through any medium."

This implies that 1) the roentgen in the physical dose unit for X-rays; 2) the medium in which the energy transformation occurs is air; 3) measurement is made of the total charge due to ions of one sign produced in the air, and finally 4) measurement of ion charge relates not to the whole volume of air in which ionization occurs but to one restricted to the primary X-ray beam, i.e., to the irradiated volume.

This definition (as the unit of physical dose) differs from the original one accepted at the 2nd International Radiological Congress in 1928 (Stockholm) and from the various modifications in the Recommendations of subsequent Congresses. The definition accepted at the above Congress was that "the international unit of X-radiation is the amount of X-rays which produces in an ionization chamber at 0°C and 760 mm Hg a conductivity, such that the charge measured in terms of the saturation current is one electrostatic unit when the secondary electrons are completely utilized and the wall effects are eliminated" ($\frac{OST}{VKS}$ 7623).

In this definition it still remains unclear what is the physical essence of what the roentgen measures and what is understood by the term "amount of rays", as Porotkov, Krongauz, Shekhtman, etc, have repeatedly emphasized.

This obscurity is retained in the later definition accepted at the 5th Congress in Chicago in 1937, where the term "amount of radiation" replaced "amount of rays". The roentgen is "the quantity of X- or $\gamma$-radiation such that the associated corpuscular emission per 0,001293 g of air produces, in air, ions carrying one electrostatic unit of quantity of electricity of either sign" [1].

When the two definitions are compared a very important difference appears in the basis to which the measured quantity of radiation is referred. While in the first (Stockholm) definition this is the ionized air (ionized volume) the Chicago definition speaks of the volume of air in which the corpuscular emission occurs, i.e., to the measurement volume, so, strictly speaking, these definitions relate to units with essentially different physical characteristics. The definition given in OST agrees with the Chicago one as regards the fact that both have in view the transformed energy referred to the irradiated volume. The advantage of the OST definition is that it uses the physical dose concept, defined precisely in OST (see above) instead of the unclear "amount of radiation" or "rays".

But more recently the strict physical dose definition given to the roentgen in OST has not been adhered to in discussing units in the USSR literature [2-9], and it has been replaced either by the term "dose," with another meaning, or the two concepts and terms are not differentiated, or else the term "physical dose" is assigned the meaning given to "dose." By "dose" is usually meant the amount of energy absorbed in acts of ionization and excitation referred to the volume (mass) in which they occur.

In general the "physical dose" concept as defined in $\left(\frac{OST}{VKS}\right)$ 6350) has no currency abroad. The roentgen [1,10, etc.] is as a rule taken as being the unit of dose.

An instance of the contradictions in the physical significance of the roentgen concept can be drawn from the Recommendations of the Internation Commission. In the 1950 Recommendations it is proposed to express the dose as "the amount of energy absorbed per unit mass in ergs per gram of irradiated meterial at the site in question", it being specially emphasized that by "absorbed energy" is meant energy communicated to the substance by ionizing particles. The Commission (§ 4) also considers that the roentgen should also from then on be considered as the unit of X- or $\gamma$-rays or dose.

This interchange of terms has caused confusion as to the physical content of the phenomena the roentgen was designed to measure.

The most evident cause of confusion as to the physical content of the phenomena the roentgen was designed to measure is the introduction of the so-called "physical equivalent" of X-radiation computed from the relation between the amounts of X- or $\gamma$-radiation per roentgen and the corpuscular emission producing one unit of electrostatic charge. A simple calculation shows that in 1 $cm^3$ of ionized air there are formed $1/(4{,}8 \cdot 10^{-10}) = 2{,}08 \cdot 10^9$ elementary charges. Since on average 33 ev are required to produce one ion pair with X- and $\gamma$-rays the total energy requirement per roentgen is $2{,}08 \cdot 10^9 \cdot 33$ ev / $cm^3$ = 0,11 erg /$cm^3$.

The physical equivalent concept has led many to deduce (incorrectly) that the roentgen, as unit of physical dose, is the amount of radiation energy absorbed per $cm^3$ of air, i.e., to equate the roentgen and its mechanical equivalent (1 r = 0.11 ergs/$cm^3$), thus omitting the difference of principle between the roentgen as a measure of corpuscular emission in the irradiated (measurement) volume and the energy absorbed by ionization in the ionized volume.

The 7th International Radiological Congress in Copenhagen (July, 1953) saw an attempt by the International Commission to resolve this problem [7]. But before turning to the definition of 1953 we must pause over some accessory concepts of which the significance is often felt to be unclear.

An energy flux is usually specified by relative parameters giving 1) the ratio of the amount of energy passing through a section to the area of the section, i.e., the mean flux density W/S; 2) the ratio of the amount of energy passing through the whole of the given area to the time of flow, i.e., the mean intensity W/t; 3) the ratio of the amount of energy passing through the given area in a given time to the area of the section and the time interval, i.e., the mean flux intensity W/St.

If we assume the energy flux through the section to be distributed continuously in space and time and reduce the area of our section and the time of observation without limit, then in the limit the mean values go over to the exact relative characteristics of the flux, taking the form of the derivatives dW/dS, dW/dt and $d^2W/dSdt$ at the given point and instant.

Let us follow some simplified schematic path of the radiation from the source up to the instant when the charge measured by an electrometer is produced. The energy flux emitted by the source reaches the object at an intensity which has been weakened on the way. The intensity from a point source falls off according to the inverse square law and in accordance with the attenuation in the intervening medium (between source and measurement point).

The amount of radiation or incident energy can be specified by the density or intensity of the flux. If the density is taken as the derivative of the energy with respect to the area of section (as in the 1953 Recommendations, § 2, i.e. as a point function) it is more convenient to extend the density (or intensity) measurement to the whole irradiated volume. We must then allow for the changes in radiation energy which occur both before and after the flux reaches the irradiated object. By taking into account as completely as possible the factors which determine the energy reaching each point in our object we can determine the density (intensity) of the incident energy at all points in the object, i.e., find dW/dS and $d^2W/dSdt$ as point functions. By multiplying these by dv and dividing by $\underline{v}$ we get the mean density (intensity) of the flux within our object. Let us term these the volume density and volume intensity. In essence it does not matter whether the radiation falls on the object from one or several directions, or even from all sides, since only the absolute values are of interest. If they are made up of fluxes of various directions they are summed at every point.

Some of the energy reaching the object is there transformed to corpuscular emission. The emitted energy in turn is distributed between ionization and excitation. These effects can be used to measure the energy at the ionization stage (in the ionization volume) or at the emission stage (in the irradiated or measurement volume).

The concepts of the interaction of radiation with matter used here have been given before [13], the authors then expressing the dose as

$$D = F \cdot \epsilon_c \cdot \epsilon_u,$$

where F is the primary energy flux in ergs/$cm^2$, $\epsilon_c$ being the fraction of this flux transformed to particle ionization energy per g of material, $\epsilon_u$ being the fraction of this energy transferred to a biological or other object.

In our presentation F corresponds to the incident energy, $\epsilon_c$ to the emitted, and $\epsilon_u$ to the absorbed.

Let us consider the situation as regards the 1953 Recommendations in the light of the above. These Recommendations leave the previous (1937) definition of the roentgen in force but attempt to specify the physical nature, and even the dimensions, of the "amount of radiation."

In § 1 of the 1953 Recommendations the radiation intensity is defined as "the amount of energy passing

through unit area in unit time". In § 2 the " amount of radiation" is defined as the "integral of the intensity with respect to time".

Since the intensity is expressed as a second derivative, $dW/dS\,dt$, its integral with respect to time is the first derivative, $dW/dS$, i.e., the flux density at a point, or as a limiting concept the derivative is here a point function. But in § 2 it is again stated that the quantity is "the total amount of energy passing through unit area". This is in poor agreement with the derivative concept, which is always essentially a relative quantity, while the "total amount of energy" although restricted to 1 $cm^2$, must be considered an absolute quantity. The 1953 Recommendations clearly relate the roentgen concept to the measurement of the energy passing through some cross-section, but we can then neither consider the transformation nor the absorption of the energy since neither can pass through a cross-section.

We are naturally led to wonder what is the energy measured in roentgens and where the cross-section lies (above the point) in relation to which the flux density is measured.

According to the submission of the International Commission the roentgen is henceforth intended to measure incident energy (i.e., the radiation reaching the object) and moreover at some point in the object at which the flux density has its mean value over the whole irradiated body. Still greater clarity would be produced by using the "volume density" concept of irradiation (see above) which would eliminate the dependence of this quantity on the direction of radiation incidence.

In the 1953 Recommendations the roentgen is not related to energy transformation or absorption processes, since in § 3 a special unit – the rad – is proposed to measure energy absorption ("dose of absorbed radiation"), being 100 ergs per g irradiated matter. Thus we must differentiate the "dose" measured in roentgens from the "absorbed dose" measured in rads, although § 13 speaks of "dose measurement in roentgens or rads" as though these units were in lesser degree adequate.

Thus in order to clearly delimit the concepts of the energy absorbed by corpuscular emission and that absorbed by ionization and excitation the 1953 Recommendations give yet a third variant of the dose concept (see § 7 and also §§ 1 and 2) as the density of "incident" energy. They also pose, but do not finally resolve, the problem as to the content of the roentgen concept.* This all gave an impetus to the discussion of the definition of the roentgen.

To demonstrate the extensive disagreement over this let us consider the definitions of roentgen given at various times by different authors.

Gray [15] maintained the repesentation of the roentgen as the unit of incident energy in a paper at the special symposium concerned with the problem of passing from the roentgen to the rad.

Yudin [16, 17] put forward three interpretations of the roentgen concept: 1) as a unit of energy incident on 1 $cm^2$, which corresponds to the 1953 Recommendations; 2) as the unit of physical dose in any medium, i.e., the unit of energy absorbed in 1 g of any substance, air being only a typical medium; 3) as the unit of dose of energy absorbed from X- or $\gamma$-rays, the energy being taken in relation to 0.001293 g of air. The latter corresponds to the one generally used in the dosimetry of ionizing radiations in practice.

Tikhodeev [18] correctly states that Yudin's three variants are different interpretations of at least two completely different physical quantities, and not of a single unit. He is evidently inclined to the first.

Poroikov [19] has adopted a peculiar but sound position on this topic, proposing to consider the roentgen the unit of ionization producted by radiation, i.e., of the physical effect directly related to the charge recorded by an electrometer. An analogous I unit (Ionization Unit) was proposed by the British Committee on Radiolo-

* The contradictions as regards the definitions of the roentgen in the 1953 Recommendations were sharply criticized by one of the participants in the discussion on the Recommendations – the Dutchman Somerwil, who dealt with this in a letter to the British Journal of Radiology [14]. He wrote "according to the definition (in the Recommendations) a number of quanta of radiation appears to be no more quantity of radiation. Only a number of quanta per $cm^2$ is allowed to be called a quantity; consequently this number of quanta = a quantity x an area ... Quantity of radiation ought to be defined as the time and surface integral of intensity, but this having been done, the roentgen is not a quantity of radiation."

gical Units, but was not accepted by the International Commission.

Quimby and Laurence [20] introduced the term "exposure or dose" as relating solely to the radiation itself, without regard to what occurs at the measurement point, i.e., whether the body absorbs or passes the radiation. Exposure, absorption and ionization are three very different physical effects and should be distinguished clearly (p. 138). Exposure is not a measure of the energy of the radiation, but is only its ability to ionize air under certain specified conditions. The exposure (dose) is measured by the ionization produced by the radiation (p. 140).* The internal contradictions in these concepts are clear of themselves. Gorshkov adopted an exactly opposite position on the nature of the roentgen; he considers that the roentgen is not an amount of $\gamma$-radiation in the strict sense of the word. According to Gorshkov the roentgen does not deal with the number of photons, with the total energy of the photon beam, with a photon quality or with the photon intensity (see the 1953 Recommendations), but only with the amount of ionization produced by secondary electrons. But Gorshkov has in mind dose as generally conceived (the energy absorbed by the ionization effect) but subscribes to the OST dose definition, where not absorption but transformation of energy in the irradiated volume is considered.

Shekhtman [7] correctly states that the definitions given by the 1953 Recommendations leaves unclear what should be understood by amount of radiation or dose of X- and $\gamma$-rays. But the same lack of clarity occurs in the definitions of the roentgen he proposes.

Roberts [22], dealing with the practical application of the 1953 Recommendations, devotes most attention to the relations between the "roentgen" and "rad" units. He envisages difficulties only in measuring doses directly in rads and in transforming doses in air to those in other media; he forgets the basic difficulty: the conceptual differences between roentgen and rad.

It is clear from this review that the various definitions and explanations of the roentgen contain many unclear points, tacit assumptions and even non sequiturs; this was not avoided in the 1953 Recommendations of the International Commission on Radiological Units. A fresh radical reconsideration of this basic radiological unit is undoubtedly required. The definition of the roentgen must state with exhaustive clarity: 1) what the roentgen measures; ionizing capacity of the radiation, amount of ionization, or amount of energy; 2) if it measures energy, then of what kind; energy reaching the irradiated object (incident), or that absorbed in corpuscular emission, or that absorbed by acts of ionization and excitation; 3) whether the measurement is absolute or with respect to the mass, to the volume or to the area; 4) if to the mass or volume, then to what of these; the irradiated volume in which the corpuscular emission occurs or the "ionization volume", in which the ionization and excitation occur; 5) since the quantity measured directly is not of interest to us, being a more or less remote effect (a charge), its relations and coefficients must be stated exactly in a general mathematical formula and in tables attested by the Commission, so it is possible with appropriate accuracy to determine the quantity from dosimetric measurements.

This is the current state of that basic radiological unit the roentgen. This is not the sole debatable point. It was long ago recognized that there was a need for an All-Union Commission on Radiological Units which would take over the responsibility for selecting, approving and introducing basic radiological units into the dosimetry of ionizing radiations. We are still very far from solving the cardinal problem of dosimetry – the direct quantitative determination of the physical effect produced in the irradiated material under given irradiated material under given irradiation conditions; this could be considered as solved if we could say that the irradiated substance received a dose of so many ergs per gram and that this energy was distributed along the charged particle tracks at the rate of so many electron-volts per centimeter. The way to the solution of the difficult problem can be made much shorter and easier if a more rigorous and profound approach to the introduction of the basic elements of current radiometry is adopted.

We are deeply indebted to E. A. Liberman for discussions of the questions dealt with in this paper.

## LITERATURE CITED

[1] D. E. Lea, Action of radiations on living cells, Cambridge, 1946, p. 6-7.

[2] L. A. Sena, Units for measuring physical quantities, State Tech. Press, 1948, p. 127.

[3] A. V. Beklemishev, Dimensions and units of physical quantities, State Tech. Press, 1954, p. 235.

* As in original – Publisher's note.

[4] K. K. Aglintsev. Dosimetry of ionizing radiations. State Medical Press, 1950, p. 213.

[5] K. K. Aglintsev. Fundamentals of ionizing radiation dosimetry. State Medical Press, 1954, p. 107.

[6] Ya. L. Shekhtman. Dosimetry of radiations from radioisotopes. (Symposium on "Labelled atom methods in biology", ed. A. M. Kuzin) Izd. MGU, 1955, p. 221.

[7] Ya. L. Shekhtman. Trans. Inst. Biophysics AN SSSR, 1, 122-135, 1955.

[8] L. B. Kelrim-Markus and U. Ya. Margulis. A brief outline of the physical bases of radiology. (Symp. "Biological actions of radiations and the pathology of radiation sickness"). State Med. Press, 1954, pp. 40-41.

[9] L. V. Poroikov. Measurement of X-rays. State Tech. Press, 1950, p. 124.

[10] W. V. Mayneord. Acta of the International Union against Cancer II, No. 3, 271 (1937).

[11] Recommendations of the International Commission on Radiological Units (London, 1950), Radiology 56, No. 1, 117-119 (1951).

[12] Recommendations of the International Commission on Radiological Units (Revised at the Seventh International Congress of Radiology, Copenhagen, 1953), Radiology 62, No. 1, 106-109 (1954).

[13] L. D. Marinelli and L. S. Taylor. Radiation Biology, Ed. by A. Hollaender 1, 1954, p. 145.

[14] A. Somerwil, Brit. J. Radiol. 27, No. 319, 412 (1954).

[15] L. H. Gray. Brit. J. Radiol. 29, No. 343, 355 (1956).

[16] M. F. Yudin. Measurement technique. 1, 18-19, 1956.

[17] M. F. Yudin. Measurement technique. 1, 31-36, 1956.

[18] P. M. Tikhodeev. Measurement technique. 1, 15, 1956.

[19] L. V. Poroikov. Measurement technique. 1, 20-23, 1956.

[20] E. H. Quimby and G. C. Laurence. Radiology 35, No. 2, 138-139 (1940).

[21] G. V. Gorshkov. The γ-rays from radioactive substances. Izd. LGU, 1956, p. 128.*

[22] J. E. Roberts, Brit. J. Radiol. 28, No. 336, 682 (1955).

Received August 23, 1956

* ["LGU" = "Leningrad State University."]

# LETTERS TO THE EDITOR

## PARTICLE BUNCHING IN A TRAVELING-WAVE LINEAR ACCELERATOR

G. I. Zhileiko

A traveling-wave linear accelerator can be used to obtain extremely short pulses of accelerated electrons. In a number of cases [1] the bunching capacity of the accelerator itself is found to be insufficient so that a system of preliminary bunching is introduced. The presence of a current of accelerated particles leads to a reduction in the amplitude of the electric field; this effect tends to inhibit electron bunching in the accelerator.

Below we consider electron bunching in an accelerator under the following assumptions: 1) an electron bunch of angular length $2\Delta\varphi_{inj} < 30°$ where $\varphi_{max} = \varphi_s + \Delta\varphi_{inj}$ and $\varphi_{min} = \varphi_s - \Delta\varphi_{inj}$ is introduced into the accelerator at equilibrium phase $\varphi_s$; 2) the amplitude of the phase oscillations is small ($\Delta\varphi < 15°$); 3) the accelerator parameters vary slowly along its length (in a distance equal to one oscillation wavelength in the apertured (disc-loaded) wave guide the phase velocity is not increased by more than 10% and the amplitude of the accelerating field is not reduced by more than 5-10%. Using these assumptions we analyze the longitudinal electron oscillations about the equilibrium phase [2], [3]; assuming that $\varphi_s$ = const we obtain the equation*

$$\frac{\Delta\varphi_{inj}}{\Delta\varphi_{out}} = \sqrt[4]{\frac{\beta^3_{out} m_{k\cdot out} E_{z\,out}}{\beta^3_{inj} m_{k\cdot inj} E_{z\,inj}}} \cos\varphi_s, \qquad (1)$$

where $\Delta\varphi_{out}$ is the angular duration of the particle bunch at output of the accelerator; $\beta = \frac{v}{c}$; $\underline{v}$ is the particle velocity; $\underline{c}$ is the velocity of light; $m_{corr} = \frac{m_0}{(1-\beta^2)^{3/2}}$.

Using Eq. (1) we can determine the angular duration required at injection in order to achieve a given bunch length at the output $\Delta\varphi_{out}$.

In Eq. (1) the quantity $E_z$ can be given by the expression

$$E_z = e^{-\alpha z}\sqrt{\frac{P_0 - IU(1+\rho)}{z\Gamma}}, \qquad (2)$$

where $\alpha$ is the attenuation factor in the accelerator wave guide; $\underline{z}$ is the longitudinal coordinate; $P_0$ is the power flux at the input of the wave guide (z = 0); I is the current of the particle beam; U is the kinetic energy of the particles; $\rho = \alpha z + \alpha^2 z^2$; $\tau$ is a constant; $\Gamma = \frac{1}{2\pi E_z^2}\int_s E_r H_\varphi\, ds$ is a function which depends on the wave guide geometry and the phase velocity ($\underline{s}$ is the area of the cross section over which there is an interaction in the wave guide).

Eq. (2) is obtained by integrating the power-balance differential equation for the accelerator wave guide. In carrying out this procedure it is assumed that $\alpha Z < 1$.

* [Here and elsewhere "k" in subscript ≡ "corrected." – ed.]

Using Eq. (2) we find

$$\frac{E_{z\,out}}{E_{z\,inj}} = e^{-\alpha z} \sqrt{\frac{\Gamma_{inj}}{\Gamma_{out}}\left(1 - \frac{I'U_{out}}{P_0}\right)}. \tag{3}$$

Eq. (1) now assumes the form

$$\frac{\Delta\varphi_{inj}}{\Delta\varphi_{out}} = e^{-\frac{\alpha z}{4}} \sqrt{\frac{\beta^2_{out}(U_{out}+U_0)}{\beta^2_{inj}(U_{out}+U_0)}} \times \sqrt{\frac{\Gamma_{inj}}{\Gamma_{out}}\left(1 - \frac{I'U_{out}}{P_0}\right)}, \tag{4}$$

where $I' = I(1+\rho)$; $U_0$ is the rest energy of the electron.

On the basis of Eq. (4) the following conclusions can be reached:

1. When the wave guide is loaded by the beam current the ratio $\frac{\Delta\varphi_{inj}}{\Delta\varphi_{out}}$ is reduced. In other words, if $\Delta\varphi_{inj}$ is fixed, $\Delta\varphi_{out}$ increases with increasing particle current. This factor manifests the effect of the current on particle bunching in the accelerator.

2. The quantity $\frac{\Delta\varphi_{inj}}{\Delta\varphi_{out}}$ increases with the ratio $\frac{\Gamma_{inj}}{\Gamma_{out}}$.

3. There is an optimum value of the final electron energy $U_{out}$ for which the maximum possible bunching is obtained with a given particle current and power $P_0$.

4. The allowable value of $\Delta\varphi_{inj}$ is reduced as the wall losses in the wave guide increase (the term $\frac{I'U_{out}}{P_0} = \frac{U_{out}}{P_0} I(1+\alpha z+\alpha^2 z)$ and the factor $e^{-\frac{\alpha z}{4}}$).

Using Eq. (4) we can determine the required angular bunch length which must be achieved by the preliminary buncher.

It can also be shown that it is necessary that the quantity $\Gamma$ vary in a specific way if optimum particle bunching is to be achieved. It should be noted, however, that even a considerable increase in the ratio $\frac{\Gamma_{inj}}{\Gamma_{out}}$ does not yield a large gain in bunching [cf. Eq. (4)]. Thus, in the Stanford University accelerator (U.S.A.) [2] the quantity $\frac{\Gamma_{inj}}{\Gamma_{out}} \approx 132$. All other things being equal, as compared with $\frac{\Gamma_{inj}}{\Gamma_{out}} = 1$ this value increases the ratio $\frac{\Delta\varphi_{inj}}{\Delta\varphi_{out}}$ by only a factor of 1.85. To achieve this value of $\frac{\Gamma_{inj}}{\Gamma_{out}}$ a great number of engineering difficulties must be overcome.

The quantity $\frac{\Gamma_{inj}}{\Gamma_{out}}$ can be very different in different types of apertured wave guides which are suitable for electron acceleration. For instance, the value of $\frac{\Gamma_{inj}}{\Gamma_{out}}$ can be estimated using the formulas given in Ref. [4].

If it is assumed that the energy of the accelerated particles is not less than 1 Mev, while $\beta_{inj} = 0.5$ ($U_{inj} \approx 80$ kev), Eq. (4) can be simplified

$$\frac{\Delta\varphi_{inj}}{\Delta\varphi_{out}} = 1.68\, e^{-\frac{\alpha z}{4}} \sqrt{\frac{\Gamma_{inj}}{\Gamma_{out}}\left(1 - \frac{I'}{P_0}U_{out}\right)\left(\frac{U_{out}+U_0}{U_0}\right)^3}. \tag{5}$$

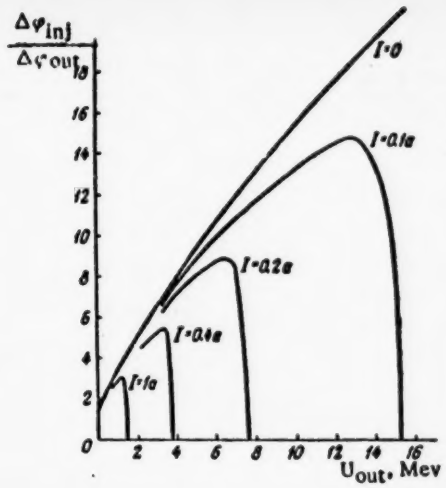


Fig. 1. The ratio $\frac{\Delta\varphi_{inj}}{\Delta\varphi_{out}}$ has a function of the final electron energy $U_{out}$ for various beam currents $I_0$ ($P_0$ = 2 megawatts, $\alpha z$ = 0.25).

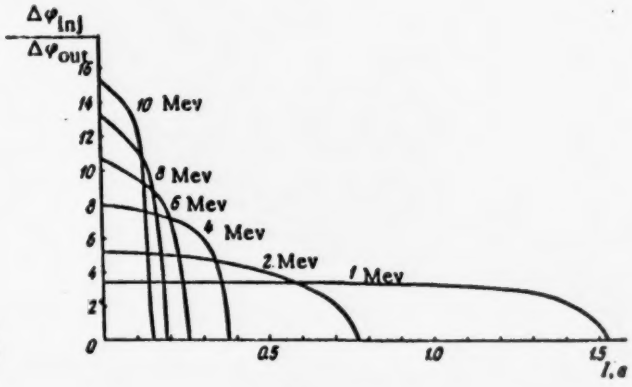


Fig. 2. The ratio $\frac{\Delta\varphi_{inj}}{\Delta\varphi_{out}}$ as a function of beam current I for various final electron energies ($P_0$ = 2 megawatts $\alpha z$ = 0.25).

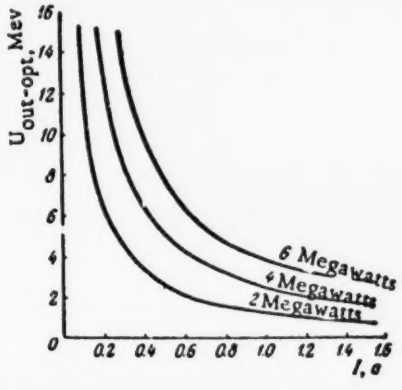


Fig. 3. The optimum value of the final electron energy $U_{out\ opt}$ as a function of $\alpha$ beam current I at various powers $P_0$ ($\alpha z$ = 0.25).

We now consider certain examples in which $\frac{\Delta\varphi_{inj}}{\Delta\varphi_{out}}$ is determined for various given values of $\alpha$, z, $\Gamma$, I and $U_0$.

If the phase velocity in the wave guide is increased from 0.5 c to c by increasing the diameter of the apertures the function $\Gamma$ remains virtually constant. We will assume $\alpha z$ = 0.25. Then Eq. (5) can be written in the form

$$\frac{\Delta\varphi_{inj}}{\Delta\varphi_{out}} \approx 1{,}58 \sqrt[8]{\left(1-\frac{1{,}31\,I}{P_0}U_{out}\right)\left(\frac{U_{out}+U_0}{U_0}\right)^8}. \quad (6)$$

Now it is easy to determine the magnitude of $U_{out}$ for which a maximum value of the ratio $\frac{\Delta\varphi_{inj}}{\Delta\varphi_{out}}$ is obtained.

$$U_{out\ opt} = \frac{1}{7}\left(\frac{6P_0}{1{,}31\,I}-U_0\right). \quad (7)$$

In Fig. 1 are shown the relations between $\frac{\Delta\varphi_{inj}}{\Delta\varphi_{out}}$ and $U_{out}$ for $P_0$ = 2 megawatts as calculated from Eq. (6). The curves in Fig. 2 show the dependence of $\frac{\Delta\varphi_{inj}}{\Delta\varphi_{out}}$ on the magnitude of the beam current for different final particle energies. The curves in Fig. 3 show the dependence of the optimum final energy on beam current. By optimum final particle energy we are to understand the energy at which the maximum value of the ratio $\frac{\Delta\varphi_{inj}}{\Delta\varphi_{out}}$ is achieved for a given particle current.

## LITERATURE CITED

[1] H. Motz, Trans. IRE AP-4, No. 3, 374 (1956).

[2] J. C. Slater, Rev. Mod. Phys., 20, 473 (1949).

[3] M. Chodorow et al., Rev. Sci. Instr. 26, 134 (1955).

[4] R. G. Mirimanov and G. I. Zhileiko, Electronics and Electron Physics 2, 137 (1957).

Received March 19, 1957

# RADIOMETER-ANALYZER FOR FIELD USE

G. R. Tolbek, V. V. Matteev, and R. S. Shlyapnikov

In carrying out geological surveys at radioactive-ore sites it is extremely desirable to be able to assay the radioactive ores directly at the deposit.

In a number of papers [1] - [3] it has been shown that the nature of the energy spectra of $\gamma$-radiation from radioactive elements of the uranium and thorium series makes it possible to carry out such a determination.

According to the theory given in Ref. [3] the equation for $\gamma$-rays, emitted by a rock which contains elements of the radioactive families of uranium and thorium is of the form:

$$N^{\Gamma}=aR_{Ra}+bR_{Th}$$

for the total $\gamma$-ray spectra and

$$N^{\gamma}=a\varkappa_{Ra}R_{Ra}+b\varkappa_{Th}R_{Th}$$

for $\gamma$-rays with energies above a given value, where a and b are constants which characterize the rock and the instrument, $R_{Ra}$ and $R_{Th}$ are the radium and thorium content of the rock, $N^{\Gamma}$ is the counting rate for all $\gamma$-quanta, $N^{\gamma}$ is the counting rate for $\gamma$-rays with energies higher than a given value, and $\varkappa = N^{\gamma}/N^{\Gamma}$.

It follows from these equations that

$$\left.\begin{aligned} R_{Ra}&=\frac{N^{\Gamma}\varkappa_{Th}-N^{\gamma}}{a(\varkappa_{Th}-\varkappa_{Ra})},\\ R_{Th}&=\frac{N^{\gamma}-N^{\Gamma}\varkappa_{Ra}}{b(\varkappa_{Th}-\varkappa_{Ra})}. \end{aligned}\right\} \qquad (1)$$

The relative thorium and uranium content of radioactive ores can be characterized by the quantity

$$\vartheta=\frac{R_{Th}}{R_{Ra}+R_{Th}}, \qquad (2)$$

where $R_{Th}$ is the thorium content and $R_{Ra}$ is the radium content, which is proportional to the uranium content at radioactive equilibrium between uranium and radium. Substituting Eq. (1) in Eq. (2) we obtain an expression for $\vartheta$ in terms of measurable quantities

$$\vartheta=\frac{\varkappa-\varkappa_{Ra}}{\frac{b}{a}(\varkappa_{Th}-\varkappa)+\varkappa-\varkappa_{Ra}}, \qquad (3)$$

where $\kappa = N^{\gamma}/N^{\Gamma}$ for a given deposit and the ratio b/a is easily determined experimentally and remains constant in all measurements.

The considerations given above apply when radioactive equilibrium obtains between the thorium and uranium ores and when the relative spectral composition of the $\gamma$-radiation is independent of the matter in the rock.

As a rule thorium ores are in equilibrium under natural conditions. In a number of uranium ores equilibrium may not obtain; however, we shall assume that equilibrium does, in fact, exist.

It has been shown in Ref. [4] that the $\gamma$-radiation spectrum changes slightly in passage through a layer of matter. However, if the detection instrument is surrounded by a layer of material having a high atomic number (thickness 1-2 mm) which intercepts a large part of the $\gamma$-quanta with energies of approximately 200-300 kev the reading of the instrument is practically independent of the chemical composition and thickness of the material above the ore deposit and these effects can be neglected.

The detection and analysis of the spectral composition of $\gamma$-radiation can be realized by various methods; of these the most convenient for field use are the scintillation method and a method in which a threshold spectrometer, using a Geiger-Müller counter is used, as suggested by Bothe. The latter method has been used in the present work because it is more reliable and simpler.

In the instrument being described here the role of the fixed radiator of the Bothe scheme is played by the walls of the counters which make up the system. Using this disposition of the counters, all the secondary electrons (rather than only a small part incident in a rather narrow solid angle) produced by the counter and the fixed radiator are used. This is an advantage over the apparatus. The detection unit of the instrument is the system of Geiger-Müller counters, consisting of the one central counter which is surrounded by a ring of six counters. Coincidences between the central counter and the ring which surrounds it are detected. This system, equivalent to 6 Bothe systems, has high sensitivity and can be used, comparatively weak fields of $\gamma$-radiation. If, in addition, we record coincidences between any neighboring pairs of counters in the external ring, this system becomes the equivalent of twelve pairs of counters, connected in a Bothe system. A system of this kind has the maximum possible efficiency for detection of coincidences for a given number of counters.

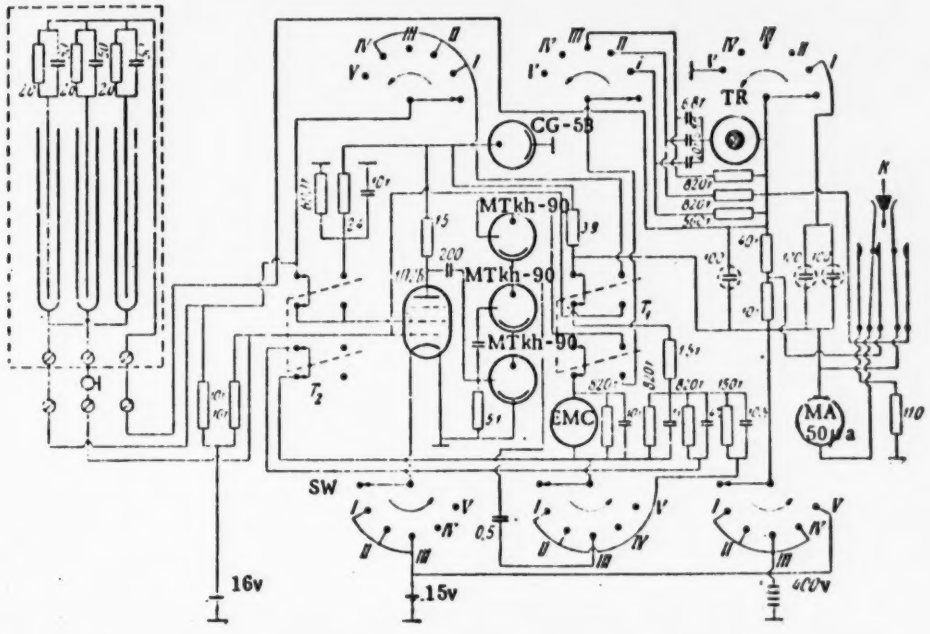


Fig. 1. Schematic diagram of the instrument. The range switch is in the "off" position; the toggle-switch $T_1$ is in the "Analyze" position; the toggle-switch $T_2$ is in the "Count Coincidences" position.

However, in view of the fact that a system of the second kind requires a more complicated electronic system, the authors have used the first version. In order to obtain the highest resolution

$$\left(\text{the ratio } \eta = \frac{\varkappa_{Th}}{\varkappa_{Ra}} = \frac{N^{\gamma}_{Th} N^{\Gamma}_{Ra}}{N^{\Gamma}_{Th} N^{\gamma}_{Ra}}\right)$$

with reasonably high detection efficiency of soft $\gamma$-radiation, it is generally necessary to use secondary-electron energy discrimination. The required discrimination is realized by the choice of appropriate filters.

The experiments have shown that the best resolution with satisfactory coincidence efficiency is obtained with a filter fabricated from materials with low atomic number. Hence the absorption filters were made from aluminum.

The experimental data on the choice of aluminum-filter thickness are given in the Table.

| Thickness of aluminum filter, mm | $\varkappa_{Ra}$ % | $\varkappa_{Th}$ % | $\eta=\frac{\varkappa_{Th}}{\varkappa_{Ra}}$ |
|---|---|---|---|
| 0 | 33 ±1 | 48±1 | 1,45±0.1 |
| 0.4 | 16 ±1 | 29±1 | 1,81±0.2 |
| 0.8 | 11.5±1 | 26±1 | 2,26±0.3 |
| 1.0 | 10 ±1 | 20±1 | 2,0 ±0.3 |

It is obvious from the table that the best resolution is obtained with an aluminum-filter thickness of 0.8 mm.

The detection unit of the radiometer-analyzer comprises 6 type STS-5 counters. The central counter is located in an aluminum cylinder with a wall thickness of 0.8 mm. The detection unit is surrounded by a removable lead shield 1 mm thick with an intermediate filter of aluminum 1-2 mm in thickness.

Other types of counters can also be used in the instrument. However, halogen counters are most suitable since the operating voltage in these tubes is only 400 volts and the pulses from these counters are sufficient for transmission by cable without amplification.

When halogen counters are used special care must be taken since some counters have a high inherent noise level.

A schematic diagram of the instrument is shown in Fig. 1. Two types of measurements can be carried out with this radiometer-analyzer: 1) detection of $\gamma$-radiation and determination of its intensity (in prospecting); 2) analysis of the spectral composition of $\gamma$-radiation for determination of the nature of the deposits. The choice of operation is controlled by the toggle-switch $T_1$.

When the instrument is used as a prospecting radiometer the counter pulses are fed to the control grid of a 1P2B tube. The pulses, amplified by this tube, are shaped in a circuit in which MTKh-90 thyratons are used. The shaped current pulses are averaged in an integrating circuit connected to the anode circuit of the thyraton. The current in the integrating circuit, which is proportional to the pulse-containing rate, is measured with a microammeter.

The microammeter scale can be changed by the scale-selector push button K.

The total $\gamma$-radiation intensity range is divided into four scales: I) 100 $\mu$r/hr, II) 250 $\mu$r/hr, III) 2,000 $\mu$r/hr, IV) 15,000 $\mu$r/hr. The choice of appropriate range is made by the range switch which changes the capacity of the condenser in the thyratron circuit.

Two measurements are required in an analysis of the spectral composition of $\gamma$-radiation: a determination of the coincidence counting rate $N^{\gamma}$ and the counting rate for the pulses from the central counter $N^{\Gamma}$.

To determine the coincidence counting rate $N^{\gamma}$ the pulses from the counters in the outer ring are applied to the screen grid of the 1P2B tube while the pulses from the central counter are applied to the control grid. A blanking voltage of 10-20 volts is applied to both grids. Pulses will appear in the anode circuit of the tube only when counter-pulses appear simultaneously on the control grid and screen grid.

In measuring the counting rate $N^{\Gamma}$ the 1P2B is operated as a pentode using the switch $T_2$.

The pulses from the anode of the 1P2B* tube are applied to a relaxation circuit containing MTKh-90 thyratrons and an electromechanical counter (EMC).

As an extra convenience the instrument has a telephone receiver (TR); an idea of the radiation intensity can be obtained from the clicks in the receiver.

In analyzing radiation intensities (above 500 μr/hr) the instrument makes use of a scaler storage system, which uses the MTKh-90 thyratrons (position III of the range switch). The scaling operation is carried out by the same thyratrons which are used for pulse shaping.

The instrument also has provision for monitoring the voltage of the battery supply (position V of the range switch).

A general view of the instrument is shown in Fig. 2.

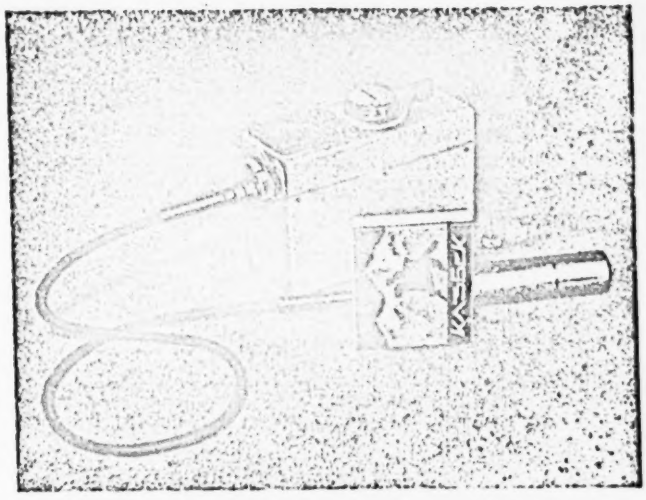

Fig. 2. External view of the instrument.

The weight of the instrument is 2.5 kg, the overall dimensions are 200 x 135 x 180 mm. The power supply of the instrument consists of a dry plate-battery (initial voltage 420 volts; capacity of 50 ma-hrs) and a type 1 KS UZ filament battery with a capacity of 3 amp-hours. These batteries guarantee continuous operation of the instrument for 100 hours.

The diameter of the external pickup unit is 37 mm, the cable length is 1.5-2 meters.

This field radiometer-analyzer is designed for uranium and thorium prospecting and evaluation of the radioactive-ore content (for ores containing more than 0.01% radioactive elements) at the site.

This instrument can measure γ-intensities ranging from 3 to 15,000 μr/hr and can be used to analyze the γ-radiation at intensities from 50 to 5,000 μr/hr.

The spectrometer specifications of the instrument, determined with pure uranium and thorium ores, are

$$\kappa_{Ra} = (12 = 1)\%,$$

$$\kappa_{Th} = (25 \pm 1)\%.$$

Experience with the instrument under field conditions have shown that it can be used for relatively rapid and reliable determinations of the nature of radioactive deposits. The instrument can also be used in various processes in which radioactive isotopes are involved.

*[1P2B: 5-contact socket, $E_f$ = 1.25 v, $I_f$ = 0.05 amp, $E_p$ = + 45 v, $I_p$ = 0.6 ma, $E_{c1}$ = 2v, $E_{c2}$ = + 45 v, $I_{c2}$ = = 0.25 ma, $g_m$ = 500 μ mho, $\Gamma_p$ = 3.60 kohms, $R_l$ = 50 kohm, $P_{out}$ = 0.01 w.]

## LITERATURE CITED

[1] W. Bothe and W. Rolhörster, Z. f. Naturwiss 16, 1045 (1928).

[2] C. Lapointe, Can. Min. and Metal. Bull. 460, 465 (1950).

[3] G. R. Golbek, V. V. Matveev and R. S. Shlyapnikov, Research in Geology, Chemistry and Metallurgy. (Report presented by the Soviet Delegation to the International Conference on the Peaceful Use of Atomic Energy, Geneva 1955) Izd. Akad. Nauk SSSR 1955, p. 40.

[4] B. V. Matveev, A. D. Sokolov and R. S. Shlyapnikov, J. Atomic Energy 4, 57 (1956).*



Received December 19, 1956


# FLOW-RATE METER WITH RADIOACTIVE PICKUP UNIT


N. S. Korshunov and M. V. Khatskevich


The use of radioactive isotopes makes it possible to construct measurement instruments which have a number of important advantages [1]-[3].

Interesting results have been obtained with the use of radioactive cobalt, in conjunction with an ordinary rotation-type meter [4], in carrying out remote flow-rate measurements on small flows of gases and liquids.

At present rotation type meters are widely used in remote flow-rate measurements; these instruments employ electromagnetic-induction units. It has been shown in practice that instruments of this type are not suitable for measuring small flow-rates (from 0.2 up to 2 liters/hr). Moreover, the sensitivity of these devices is poor and can be increased only by the introduction of complicated electronic circuits and good stabilization. It is not always feasible to make the rotation tube of the instrument of a non-magnetic material nor to make it structurally complicated. These shortcomings can be avoided in a radioactive remote flow-rate meter (RRFM).

A schematic diagram of the device is shown in Fig. 1. A gamma source is placed on a float in the flow-tube. The position of the float is determined by the difference current in a differential ionization chamber connected, for example, to an SP amplifier. The amplifier scale is calibrated in flow-rate units. As desired, the signal from the dc amplifie. can be fed to an automatic recorder or to a control system.

The $\gamma$-radiation source is $Co^{60}$ in the form of a metal wire 0.7-0.8 mm in diameter. The source intensity is of the order of 2-5 $\mu$ curies. A piece of this wire is placed on a teflon float. The rotation tube can be fabricated from any material which meets the engineering requirements.

The construction of the differential ionization chamber is shown in Fig. 2. The chamber consits of four coaxial cylinders and is filled with air at atmospheric pressure. Cylinder 1 is the collector; cylinder 2 is the high-voltage electrode and is cut in two; a voltage of 200 volts, but of opposite sign, is applied to each half at 3; cylinders 4 and 5 are the walls of the chamber.

The inner cylinder contains the rotation tube, which is held in place by rubber gaskets. The collector and high-voltage electrodes are supported by plexiglas insulators 6. All outputs from the electrodes also come through the insulators. Ring 7 is a guard ring and braces the insulator 6; it is connected to a frame screw 8.

The frame of the chamber is fastened to the two supports 9 by collars 10. The chamber can be moved vertically by the lead screw 11 and crank 12, thus making it possible to vary the flow-rate range.

The mathematical relation between the differential current in the chamber and the position of the radioactive float is given by the following expression:

* See C. B. Translation.

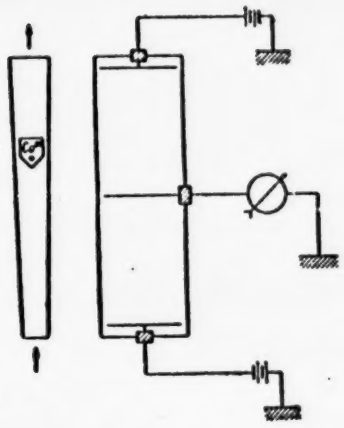

Fig. 1. Schematic diagram of the radioactive flow-rate meter.

$$\Delta I = -2\pi K\left\{R\left(\tan^{-1}\frac{H-Z}{R}+2\tan^{-1}\frac{Z}{R}-\tan^{-1}\frac{H+Z}{R}\right)-\right.$$
$$-r\left(\tan^{-1}\frac{H-Z}{r}+2\tan^{-1}\frac{Z}{r}-\tan^{-1}\frac{H+Z}{r}\right)-$$
$$\left.-\frac{1}{2}\left[(H-Z)\ln\frac{(H-Z)^2}{(H-Z)^2+R^2}+2Z\ln\frac{Z^2+r^2}{Z^2+R^2}-\right.\right.$$
$$\left.\left.-(H+Z)\ln\frac{(H+Z)^2+r^2}{(H+Z)^2+R^2}\right]\right\},$$

where K is a proportionality factor.

The remaining terms in the formula are obvious from Fig. 3. Analysis shows that when Z = 0, $\Delta I = 0$, that is to say, the chamber current vanishes when the $\gamma$-active float is at the center of the chamber. The function f(Z) is an odd function, that is, $f(-Z) = -f(Z)$; consequently the differential-current curve is symmetric about the origin.

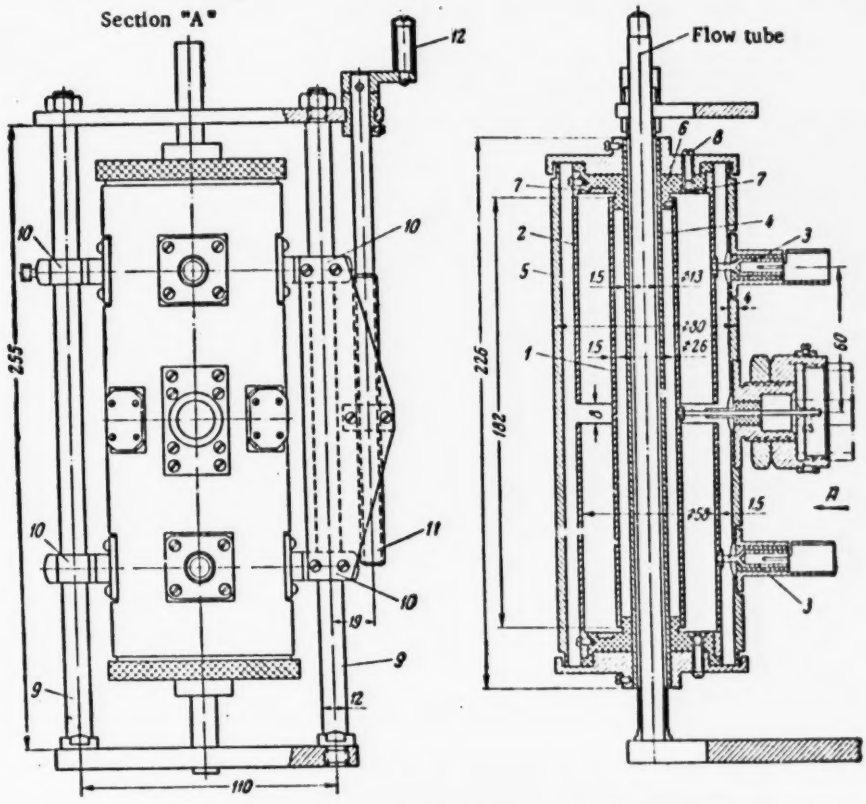


Fig. 2. Construction of the chamber of the flow-rate meter. 1,2) electrodes; 3) inputs; 4,5) cylinders; 6) insulator; 7) ring; 8) screw; 9) support; 10) collar; 11) lead screw; 12) crank.

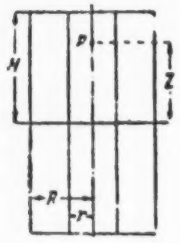


Fig. 3. Diagram for formula given in text.

In Fig. 4 are shown curves of $\Delta I = f(Z)$. One of these 2 is computed from the formula; the other 1 is the experimental curve. The function is essentially linear over a limited region. Thus, the flow-rate meter can be used with a linear scale. Because of the high sensitivity of the differential chamber the position of the float can be determined to better than 0.5 mm.

The radioactivity flow-rate meters of the type described here are made in two models: one with a linear float range of 100 mm (RDR-1-100) and one with a range of 50 mm (RDR-2-250). The flow-rate range in each case is determined by the particular flow tube which is used and the float parameters. Experience under laboratory conditions using a flow-rate meter with a range of 0.015 to 0.06 liters/hr with carbon tetrachloride and a unit with a range of 0.222 liters/hr with water indicates that the errors in flow-rate determination are less than ± 2.5%.

Similar instruments have been used at semi-industrial installations. In this case the pickup unit was separated from the control panel by a distance of 20 meters. The instruments operated satisfactorily. The errors were never greater than 2.5%.

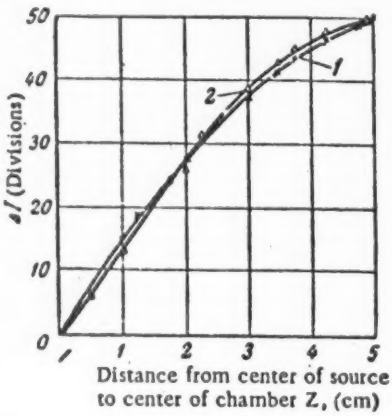


Fig. 4. Calibration curves for the radioactive flow-rate meter.

A device for automatic control of small flows, based on a flow-rate meter with a radioactive float, has been developed. The elements of this device were developed at the R A T, Academy of Sciences, USSR. A system of this kind makes it possible to maintain a given liquid flow-rate in the range from 0.5 to 3 liters/hr. The time required to establish this flow-rate is 50-60 seconds.

## LITERATURE CITED

[1] N. I. Shteibok, Usp. Fiz. Nauk 4, 231 (1954).

[2] G. G. Iordan, Instrument Design 1, 4 (1956).

[3] M. B. Neiman, Measurement Technique 1, 10 (1955).

[4] N. S. Korshunov, Author's patent certificate No. 01971.

Received February 9, 1957

# TEMPERATURE DEPENDENCE OF THE EFFECTIVE RESONANCE ABSORPTION INTEGRAL

I. V. Gordeev, V. V. Orlov, and T. Kh. Sedelnikov

The effective resonance absorption integral for neutron absorption by a resonance absorber uniformly interspersed in a moderator, is computed from a formula given in Ref. [1]

$$I_{eff} = \int_0^\infty \sigma_r(E) \frac{\Sigma_s}{\Sigma_s + \Sigma(E)} \frac{dE}{E}, \qquad (1)$$

where $\Sigma(E) = \rho[\sigma_r(E) + \sigma_{sa}(E)$ is the macroscopic resonance cross section; E is the neutron energy; $\sigma_r(E)$ is the resonance absorption cross section; $\sigma_{sa}(E)$ is the resonance scattering cross section; $\rho$ is the number of atoms of the absorber in 1 $cm^3$; $\Sigma_s$ is the macroscopic cross section for potential scattering in the medium.

A knowledge of the effective resonance integral makes it possible to compute the resonance escape probability for neutrons from the formula $\varphi = \exp\left(-\frac{\rho I_{eff}}{\zeta \Sigma_s}\right)$, where $\zeta$ is the mean logarithmic neutron energy loss per collision.

Eq. (1) applies in those cases in which either the absorption cross section is small ($\Sigma_r << \Sigma_s$) or the resonance absorption occurs in a narrow energy interval ($\Delta E_{eff} << \zeta E$).

In this case the width of the "danger zone" $\Delta E_{eff}$ is defined from the condition $\Sigma > \Sigma_s$ within the energy interval $\Delta E_{eff}$.

We consider $I_{eff}$ for an isolated resonance such that the total resonance integral is the sum of the resonance integrals for separate resonances. Furthermore, we neglect interference between potential and resonance scattering. If $\Gamma\gamma$, $\Gamma_n$, $\Gamma = \Gamma\gamma + \Gamma_n$ are respectively the radiative, neutron and total widths of the resonance in question, then $\sigma_r = \frac{\Gamma\gamma}{\Gamma}\sigma$, when the energy dependence of the resonance cross section $\sigma(E)$ is given by the Breit-Wigner formula

$$\sigma(E) = \sigma_0 \sqrt{\frac{E_0}{E}} \frac{1}{1 + x^2}, \tag{2}$$

where $x = \frac{E - E_0}{\Gamma/2}$; $\sigma_0$ is the resonance cross section at $E = E_0$; $E_0$ is the energy of the resonance level.

If the nuclei in the absorber undergo thermal motion, the observed cross section itself has an energy dependence because of the Doppler effect. To determine the energy dependence of the observed resonance cross section we must take an average (for a given neutron energy in the laboratory coordinate system) over the possible relative velocities of the neutron and absorbing nuclei. Carrying out this procedure (Cf. Ref. [2]):

$$\begin{gathered}\sigma_a(x, \xi) = \sigma_0 \Psi(x, \xi), \\ \Psi(x, \xi) = \frac{\xi}{2\sqrt{\pi}} \int_{-\infty}^{\infty} e^{-\frac{\xi^2}{4}(x-y)^2} \frac{dy}{1 + y^2}, \\ \sqrt{\frac{E_0}{E}} \sim 1, \quad \xi = \Gamma/\Delta, \quad \Delta = 2\sqrt{\frac{kTE_0}{A}},\end{gathered} \tag{3}$$

where k is the Boltzmann constant; T is the temperature of the medium in °K (it is assumed that the temperature of the medium T is higher than the Debye temperature of the absorber $\Theta$).

The function $\Psi(x, \xi)$ can be related to the real part of a complex function:

$$W(x^*, y^*) = u(x^*, y^*) + iv(x^*, y^*),$$

namely

$$\Psi(x, \xi) = \xi \frac{\sqrt{\pi}}{2} u(x^*, y^*),$$

where $x^* = \xi/2x$; $y^* = \xi/2$;

$$u(x^*, y^*) = \frac{1}{\pi} \int_{-\infty}^{\infty} \frac{y^* e^{-t^2} dt}{(x^* - t)^2 + y^{*2}}.$$

Values of the quantity $\underline{u}(x^*, y^*)$ as a function of $x^*$, $y^*$ are given in the tables in Ref. [3].

As a result of the averaging process the resonance line becomes wider but the absorption at the center of the line is reduced. Under these conditions the true resonance integral

$$I_R = \int_0^\infty \sigma_r(E)\frac{dE}{E}$$

is not changed but $I_{eff}$ increases because of the increased width of the "danger zone" $\Delta E_{eff}$.

Substituting the expressions given above in Eq. (1) and neglecting small changes in $\Gamma_n(E)$ and $\frac{1}{E}$ over the narrow interval $\Delta E_{eff}$, we find

$$I_{eff} = \frac{\Gamma_\gamma}{2E_0}\frac{\Sigma_s}{\rho}\int_{-\infty}^{\infty}\frac{\Psi(x,\xi)\,dx}{\Psi(x,\xi)+\frac{\Sigma_s}{\rho\sigma_0}}. \qquad (4)$$

Without serious error the integration with respect to $\underline{x}$ in Eq. (4) can be extended to the limits $(-\infty, \infty)$ since when

$$x > x_{eff} = \frac{\Delta E_{eff}}{\Gamma/2}$$

the expression under the integral sign falls off rapidly.

As is apparent from Eq. (4), for a given resonance the effective resonance integral, because of the parameters $\xi(T)$, depends on the temperature of the medium T and the cross section for potential scattering per nucleus of the absorber $\sigma_s = \frac{\Sigma_s}{\rho}$. With a very dilute absorber $(\rho \to 0)$ $I_{eff} \to I_R = \frac{\pi}{2}\frac{\sigma_0\Gamma_\gamma}{E_0}$, since

$$\int_{-\infty}^{\infty}\Psi(x,\xi)\,dx = \pi.$$

In the general case it is convenient to write $I_{eff}$ in the form of a product

$$I_{eff} = I_R f\left(\xi, \frac{1}{a}\right).$$

where $\frac{1}{a} = \frac{\Sigma_0}{\Sigma_s}$, $\Sigma_0 = \rho\sigma_0$ and the quantity $f < 1$ characterizes the self-shielding of the resonance due to the large absorption cross section and the large scattering cross section.

When $T = 0$ $(\xi = \infty)$ the Doppler effect vanishes and $\psi \longrightarrow \frac{1}{1+x^2}$, whence

$$f\left(\infty, \frac{1}{a}\right) = f_\infty\left(\frac{1}{a}\right) = \frac{1}{\sqrt{1+\frac{1}{a}}}.$$

Hence it is convenient to write

$$I_{eff}\left(\xi, \frac{1}{a}\right) = I_R f_\infty\left(\frac{1}{a}\right)\eta\left(\xi, \frac{1}{a}\right). \qquad (5)$$

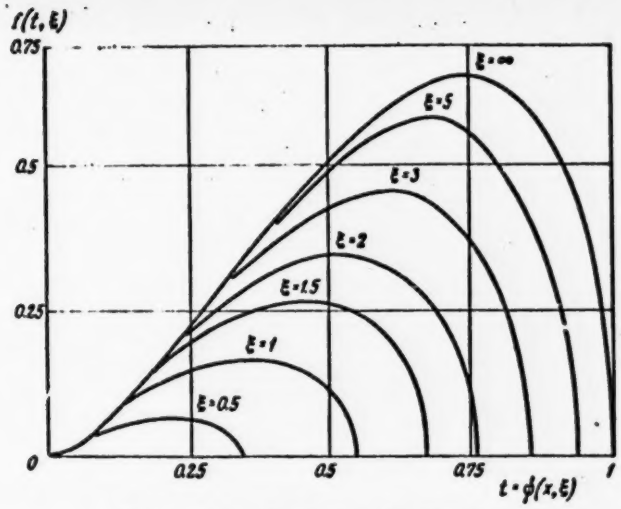


Fig. 1. Curves for the function f(t, ξ).

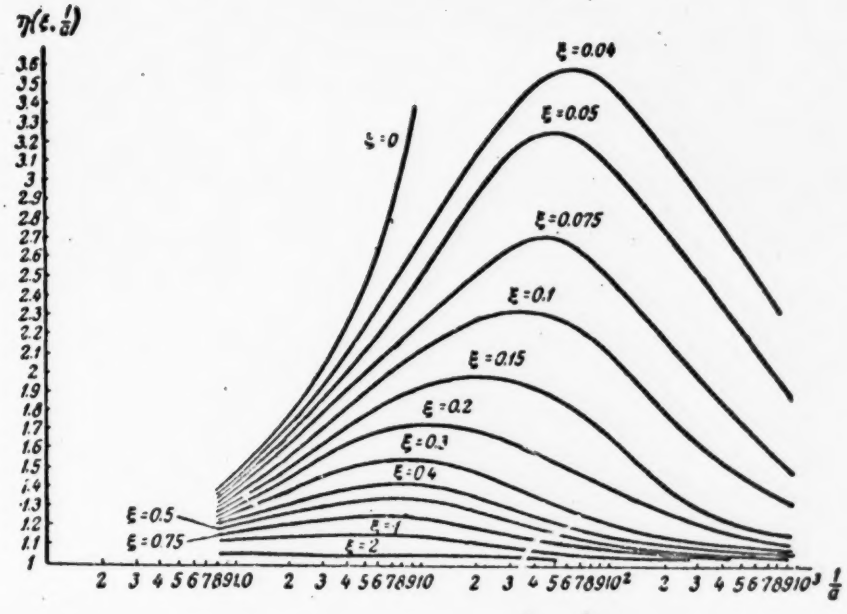


Fig. 2. Curves for the function $\eta\left(\xi, \frac{1}{a}\right)$

where

$$\eta\left(\xi, \frac{1}{a}\right) = \frac{2}{\pi}\sqrt{1+\frac{1}{a}}\int_0^\infty \frac{\Psi(x,\xi)}{1+\frac{\Psi(x,\xi)}{a}}\,dx. \tag{6}$$

Thus, the quantity $\eta\left(\xi, \frac{1}{a}\right)$ characterizes the temperature dependence of $I_{eff}$. In particular, when $T = 0$, $\eta\left(\infty, \frac{1}{a}\right) = 1$. For

$$T \to \infty (\Delta \to \infty, \xi \to 0) \quad \eta\left(\xi, \frac{1}{a}\right) \to \sqrt{1 + \frac{1}{a}},$$

so that $f \to 1$, that is, to say the resonance cross section becomes so small that there is no self-shielding of the resonance. When

$$x\xi^3 \ll 1, \Psi(x, \xi) \sim \frac{\sqrt{\pi}}{2} \xi \exp\left(-\frac{[x^2\xi^3}{4}\right),$$

i.e., the resonance cross section assumes a purely Doppler form. If the condition $\xi/a < 1$ is satisfied, the main contribution to the integral in Eq. (6) is due to values of $x$ which satisfy the condition $x\xi^2 << 1$. In this case

$$\eta\left(\xi, \frac{1}{a}\right) = \sqrt{1 + \frac{1}{a}} \sum_{n=0}^{\infty} \frac{(-1)^n}{\sqrt{n+1}} \left(\frac{\sqrt{\pi}}{4} \xi a^{-1}\right)^n.$$

In the general case numerical integration must be employed. It is convenient to introduce the variable $y = \frac{x}{x_{eff}}$, where $x_{eff}$ is determined from the condition $\Psi(x_{eff}, \xi) = a$. Then

$$\eta = \frac{2}{\pi} \sqrt{\frac{1}{a} + 1}\, x_{eff} \int_0^{\infty} \frac{\Psi(y x_{eff}, a)}{1 + \frac{\Psi}{a}}\, dy,$$

where the integral is approximately equal to 1 and shows very little change with variations in $a$ and $\xi$.

In the computations it is also convenient to introduce the variable $z = \frac{1}{1+y}$. Then

$$\eta = \frac{2}{\pi} \sqrt{1 + \frac{1}{a}}\, x_{eff} \int_0^1 \frac{\Psi\left(x_{eff} \frac{1-z}{z}, \xi\right)}{1 + \frac{\Psi}{a}} \frac{dz}{z^2}.$$

Another method of integration is the following. In the integral $I_{eff} = \int_{-\infty}^{\infty} F(\Psi)\, dx$, where F is an arbitrary function which falls off rapidly as $\Psi \to 0$ ($x \to \pm \infty$), we may make a substitution of variables $t = \Psi(x, \xi)$. Thus

$$I_{eff} = \int_0^{\Psi(0, \xi)} F(t) \frac{dt}{f(t, \xi)},$$

where $f(t, \xi) = \frac{\partial \Psi / \partial x}{\Psi}$.

The function $\Psi'(\Psi, \xi)$ can be given in terms of the following series:

$$\Psi'_x = -4x^*(y^*)^2 e^{-(x^*)^2} \sum_{n=0}^{\infty} \frac{'I_n(y^*) - I_{n-1}(y^*)}{n'},$$

where

$$y^* = \frac{\xi}{2}, \quad x^* = \frac{x\xi}{2}, \quad I_n(y^*) = \frac{y^*}{2n+1}[1 - 2y^* I_{n-1}(y^*)], \quad 'I_0(y^*) = \frac{\sqrt{\pi}}{2} e^{(y^*)^2}[1 - \Psi(y^*)].$$

When

$$\xi \to 0 \quad f(t, \xi) \simeq \xi t \sqrt{\ln \frac{\Psi(0, \xi)}{t}}, \quad \Psi(0, \xi) = \xi I_0(\xi/2);$$

for $t \to t_{max}$, $f(t, \xi) \simeq (2y^*)^{3/2} (L_0 - L_1)^{1/2} \sqrt{t_{max} - t}$; for $t \to 0$, $f(t, \xi) \simeq 2t^{3/2} \sqrt{1 - t}$.

Curves of the functions $f(t, \xi)$ and $\eta\left(\xi, \frac{1}{a}\right)$ are given in Figs. 1 and 2. The curve for the function $f(t, \xi)$ is purely illustrative. To determine the temperature dependence of the effective resonance absorption integral the curve for the function $\eta\left(\xi, \frac{1}{a}\right)$ must be used.

## LITERATURE CITED


[1] Glasstone and Edlund, Elements of Nuclear Reactor Theory, IL Moscow, 1954.

[2] A. Akhiezer and I. Pomeranchuk, Some Problems in Nuclear Theory, State Tech. Press, Moscow (1950).

[3] V. N. Faddeeva and N. M. Terentev, Tables of Values of the Probability Integral for Complex Arguments. Edited by Acad. V. A. Fok, State Tech Press (1954).



Received March 18, 1957

# ANALYTICAL DETERMINATION OF RADIOACTIVE CESIUM AS PHOSPHOTUNGSTATE

Vikt. I. Spitsyn, and N. B. Mikheev

Radiochemical analysis of solutions containing fission products involves considerable difficulties. The perchlorate [1] and bismuth iodide [2] methods are used for analytical determination of radioactive cesium.

Our proposed method for separation of radioactive cesium is based on selective precipitation of cesium as the phosphotungstate [3]. Other elements, apart from potassium and rubidium, are not coprecipitated. Because of the extremely low solubility of cesium phosphotungstate (0.0034 millimole/liter), losses of cesium due to solubility may be disregarded in the analysis.

The following solutions are used for the analytical determination of radioactive cesium:

1) cesium chloride solution containing 7 g/liter; when necessary, CsCl may be replaced by an equivalent amount by $CsNO_3$;

2) sodium phosphotungstate solution containing 5.5 g of $Na_3H_4[P(W_2O_7)_6] \cdot 19\ H_2O$ in 100 ml of 5% $NHO_3$;

3) 15% NaOH solution;

4) 15% KOH solution;

5) 0.1% solution of ferric nitrate, $Fe(NO_3)_3$.

## Analytical Procedure

A sample of solution containing fragment elements, but free from the main bulk of uranium salts (the uranium content must not exceed 0.1 g/liter) is put into a centrifuge tube 10 ml in capacity. 0.5-1 ml of concentrated nitric acid and 1 ml of cesium chloride solution is added to the solution. The resultant liquid is mixed thoroughly and heated on the water bath. 1 ml of sodium phosphotungstate solution is then added to the contents of the tube; a precipitate of cesium phosphotungstate is formed as a result. To recrystallize the precipitate the tube is heated on the water bath for 10 minutes. After cooling, the cesium phosphotungstate precipitate is centrifuged off, and the supernatant liquid is decanted. To wash the cesium phosphotungstate precipitate, 5-10 ml of 10% nitric acid solution is added to the tube. The precipitate is stirred thoroughly in the liquid, after which the suspension is centrifuged again and the solution decanted. The precipitate is washed three times. For additional purification, reprecipitation is necessary. For this, 1 ml of 15% caustic soda solution is added to the washed cesium phosphotungstate precipitate; this decomposes the latter to give soluble sodium phosphate and tungstate. To the solution 2-5 mg of sodium dihydrogen phosphate, $NaH_2PO_4 \cdot H_2O$, is added, followed by dropwise addition of concentrated nitric acid. Nitric acid is added until a white precipitate of cesium phosphotungstate, which does not dissolve when the tube is shaken, is formed. After this 0.5 ml of sodium phosphotungstate solution is added to the liquid. The contents of the tube are mixed and heated for 10 minutes on the water bath. The tube is cooled, the cesium phosphotungstate precipitate is separated by centrifugation, and the liquid is rejected. The reprecipitation of cesium phosphotungstate is carried out twice.

The precipitate is dissolved in 1 ml of 15% caustic potash solution. The alkaline solution is quantitatively transferred into a measuring flask. The volume of the flask is so chosen that convenient samples for activity determinations can be taken after the dilution. To the alkaline solution 5-10 ml of water and 1 ml of 0.1% ferric nitrate solution are added. This precipitates ferric hydroxide, which carries remaining traces of other radioactive

isotopes down with it. The liquid in the flask is shaken vigorously. The solution is then made up to the mark with distilled water. For activity determinations, the ferric hydroxide precipitate must be separated off by filtration, sedimentation, or centrifugation before sampling.

If radioactive rubidium isotopes are present in the solution, they are determined together with the radiocesium. Contamination of the separated radiocesium with other fragment elements (strontium, ruthenium, rare earth elements, zirconium, and niobium), for the same initial radioactivity of each of these isotopes and radioactive cesium, is less than 0.003%.

The course of the analysis is not affected by the presence of salts of sodium, magnesium, alkaline earth elements, less than 10 g of potassium per liter, or of chlorides, nitrates, sulfates, and acetates.

## LITERATURE CITED

[1] L. E. Glendenin and C. M. Nelson, Radiochemical Studies: The fission products 3, 1642 (1951), New York, Toronto, London.

[2] H. B. Evans, Radiochemical Studies: The fission products 3, 1646 (1951), New York, Toronto, London.

[3] Handbuch der analytischen Chemie, Teil 2 Bd. 1-a, 91, 200 (1944) Berlin.

Received April 30, 1957

# ENERGY LEVELS IN $Tm^{169}$

S. A. Baranov, R. M. Folevoi, Iu. F. Rodionov and G. V. Shishkin

A natural mixture of ytterbium isotopes was exposed to slow neutrons in the RFT [1] reactor for a month. During the course of the thirty days following irradiation the ytterbium was purified and the other rare-earth elements removed by chromatography. The radioactivity from the $Yb^{169}$ sample prepared in this way ($T_{1/2}$ = = 30.6 days [2]) was studied by means of a double-focussing $\beta$-spectrometer [3], a scintillation spectrometer and a proportional counter filled with heavy gases (Ar, Kr).

Special attention was paid to the soft part of the electron spectrum and the soft $\gamma$-radiation from $Tm^{169}$. In the first case, using the $\beta$-spectrometer, the following conversion lines were observed: K–63.13 kev, $M_1$-N–8.42 kev, and $L_1$-M–20.74 kev. In the studies with the proportional counter, in which x-ray and soft $\gamma$-radiation were observed, the lines of the corresponding atomic transitions were found: $L_{\alpha 1}$, $L_{\beta 1}$, $K_{\alpha_{2,1}}$, $K_{\beta_{3,1}}$ (transition energies of 7.18, 8.10, 15.4 and 57.5 kev respectively); $\gamma$-transitions in the $Tm^{169}$ nucleus at energies of 21.74 and 63.13 kev were also observed.

The final results obtained by means of the three methods indicated above yield the following thirteen $\gamma$-transitions in $Tm^{169}$: 8.42 (M1+E2); 20.74 (M1); 63.13 (E1); 93.62 (0.9M1+0.1E2); 109.67 (M1); 118.20 (E2); 130.48 (E2); 156?; 177.21 (0.75M1+0.25E2); 197.97 (M1); 240.6 (E1?); 260.8 (E1?); 307.7 (E2) kev. The multipole assignments are shown in brackets.*

The observed $\gamma$-rays lead us to the following assignment of energy levels in $Tm^{169}$: 8.42, 118.20, 138.90, 316.06, 379.19, and 472.8 kev.

The ground state of $Tm^{169}$ has spin $I_0 = 1/2$ [6]. Hence, if we take account of the multipole assignments of the $\gamma$-transitions indicated above, the levels with energies of 8.42, 118.20 and 138.90 kev may be assigned to rotational levels having spins of $3/2\pm$, $5/2\pm$ and $7/2\pm$ respectively. The levels with energies of 316.06, 379.19 and 472.8 kev may be assigned spins of $7/2\pm$, $7/2\mp$ and $9/2\mp$. The nature of these levels requires further investigation. Apparently the first may be ascribed to single-particle level.

If we write the Bohr-Mottelson formula [7] for the energy levels of a nucleus with $I_0 = 1/2$ in the form

$$E_I = E_0 + \frac{\hbar^2}{2J}[I(I+1) + a(-1)^{I+1/2}(I+1/2)] + \\ + A[I(I+1/2) + a(-1)^{I+1/2}(I+1/2)]^2$$

and neglect second order terms, using the values for the rotational energy levels in $Tm^{169}$ it is possible to determine $a$, $\frac{\hbar^2}{2J}$ and $E_0$. The following values of these quantities are obtained:

$$a = -0{,}763, \quad \frac{\hbar^2}{2J} = 12{,}457 \text{ кэв}, \quad E_0 = -18{,}474 \text{ кэв}.$$

* The multipole assignments were obtained by comparing the experimental and theoretical conversion coefficients. The theoretical values were obtained by interpolation and extrapolation of the values given by Sliv and Band [4] and Rose [5].

The quantity A is found to be + 0.032 kev.

The results presented here are in good agreement with those obtained by other authors [8]–[14].

## LITERATURE CITED


[1] Reactor Theory and Design (Report presented by the Soviet Delegation to the International Conference on the Peaceful Use of Atomic Energy, Geneva 1955) Izd. Akad. Nauk SSSR 1955, p. 49.

[2] J. M. Cork, M. K. Brice, D. W. Martin, L. C. Schmid and R. G. Helmer, Phys. Rev. 101, 1041 (1956).

[3] S. A. Baranov, A. F. Malov and K. N. Shliagin, Instruments and Experimental Techniques 1, 1 (1956).

[4] L. A. Sliv and I. M. Band, Tables of Coefficients for Internal Conversion Gamma-Radiation, Izd. Akad. Nauk SSSR (1956).

[5] M. E. Rose, Beta- and Gamma-Ray spectroscopy ed. by K. Siegbahn, Amsterdam, 1955.

[6] K. N. Linderberger and A. Steudel, Naturwiss. 42, 41 (1955).

[7] A. Bohr and B. R. Mottelson, Beta- and Gamma-Ray Spectroscopy, ed. by K. Siegbahn, North-Holland Publishing Company, Amsterdam, 1955.

[8] D. S. Martin, E. N. Jensen, D. J. Hughes and R. T. Nikols, Phys. Rev. 82, 579 (1951).

[9] J. M. Hollander, J. Perlman and G. T. Seaborg, Revs. Mod. Phys. 25, 469 (1953).

[10] S. A. E. Johansson, Phys. Rev. 100, 835 (1955).

[11] S. D. Kolcki and A. M. Kolcki, Bull. Inst. Nucl. Sciences "Boris Kidrich" 6, No. 89 (1956).

[12] J. W. Mihelich, T. J. Ward and R. P. Jacob, Phys. Rev. 103, 1285 (1956).

[13] A. Bisi, S. Terrani and L. Zappa, Nuovo Cimento IV, 758 (1956).

[14] E. H. Hatck, F. Boehm, P. Marmier and J. W. M. Du-Mond, Phys. Rev. 104, 745 (1956).


Received April 15, 1957

# ON THE ENTRAINMENT OF RESIDUAL GAS BY A STREAM OF VAPOR FLOWING INTO A VACUUM

V. D. Burlakov

It has been noted that the condensate that is produced when metals are purified by vacuum distillation is contaminated with oxygen and nitrogen from the residual air in the vacuum chamber even in the case of a high vacuum. The quantity of absorbed gases is sometimes greater than would be expected from the pressure as a result of adsorption on condensing layers. As an explanation it has been suggested that a molecular beam or stream of distilled metal entrains, in the direction of the condensation surface, atoms of the gas in the space between the evaporation and condensation surfaces. The result is the formation of a dense "gas layer" close to the condensation surface, so that the condensate is saturated with oxygen and nitrogen. The gases either combine chemically with the condensing metal or are dissolved in it.

In order to test this hypothesis experiments have been performed on the evaporation of mercury with $Hg^{203}$ vapor as the residual gas. Mercury enriched with $Hg^{203}$ was placed in the branch tube R of a continuously evacuated glass vessel (Fig. 1). On the opposite side a filled cigar-shaped vessel S was inserted through a ground glass joint; it included a small reservoir F filled with nonradioactive mercury. The mercury in the branch R and in the reservoir F could be heated to different temperatures, for which purpose R was placed in a Dewar filled with water or oil heated to a certain temperature. S was also filled with water or oil heated by a nichrome coil. The source R served to maintain equilibrium mercury pressure in the apparatus; this pressure corresponded to room temperature when the temperature in R and F was not below room temperature. The source F provided a beam or stream of mercury atoms which condensed on the top inner surface of the main vessel.

The counter $N_2$ located near the condensation of the stream from F recorded the variation of gamma radioactivity of the condensate. For the purpose of recording the radiation background another counter $N_1$ was placed at one side, outside of the region reached by the stream from F.

These experiments revealed a very rapid enrichment of the condensate with radioactive atoms. It could be concluded that the stream of vapor "pumps" the radioactive mercury from R by entraining radioactive atoms, which are in random motion, in the direction of the condensation surface.

In Fig. 2 the curves recorded by means of counter $N_2$ show the dependence of the radioactivity on time when the temperature of the mercury in R was 40°C, for various temperatures of F. The figure shows that the rate of increase of radioactivity with higher mercury temperature in the source F, although the two curves for the highest temperatures deviate from this rule. It is characteristic that in almost all of the experimental curves linear increase of radioactivity is attained after a short time. Some curves are distinguished by slower increase at the very beginning; this represents a certain time needed to establish some kind of equilibrium. The causes of these characteristics of the temperature and time dependence of the experimental curves could not be determined because of the difficulty of estimating the effect of contamination of the mercury surface in R and F on the rate of evaporation.

The results obtained with radioactive mercury were confirmed by supplementary experiments in which diffusion pump oil was evaporated from the source F while the radioactive mercury in R was at room temperature. From the reduction in size of the mercury droplets in R it was possible to observe visually the pumping effect of the stream of oil vapor issuing from F at 150° and 250°C. However in this case the counters $N_2$ and $N_1$ did not record the increase of radioactivity because the mercury entrained by the stream of oil vapor did not

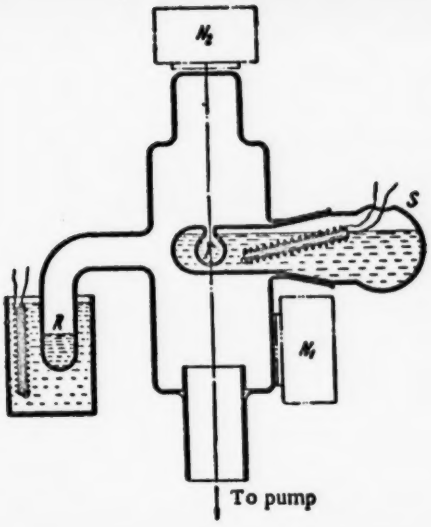


Fig. 1. Diargram of apparatus for evaporating mercury.

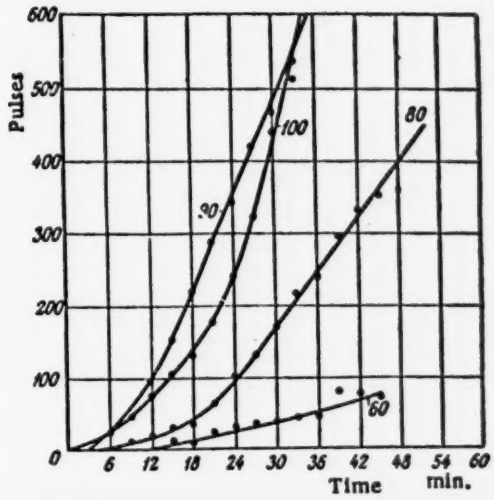


Fig. 2. Increase of radioactivity of the condensate resulting from entrainment of $Hg^{203}$ (the "residual gas") by the vapor stream. The mercury temperature in source R was 40°C. The mercury temperature (°C) in source F is indicated on the curves.

condense on the vessel wall. In further exerpiments R contained nonradioactive mercury at room temperature and the pumping effect of the vapor stream from F was determined from the reduction of the weight of the mercury. Since the mercury was not condensed on the wall these experiments can be regarded as a proof that a stream of oil vapor entrains mercury atoms from the volume of the vessel (the "residual gas") to form a dense layer of mercury vapor (at the condensation surface) which is subsequently pumped out by the diffusion pump.

These experiments confirmed the hypothesis of pumping action of a stream of evaporating metal with the formation near the condensation surface of a dense layer of residual gas which can interact with the condensate.

The author is grateful to Academician K. D. Sinel'nikov of the Ukrainian Academy of Sciences for suggesting the problem and for a discussion of the results, and also to Candidate in physico-mathmethical sciences A. P. Kliucharev for assistance in the experiments.

Received April 23, 1957

# AN IMPROVED PROCESS FOR THE CAUSTIC SODA DECOMPOSITION OF MONAZITE

G. A. Meerson, G. E. Kaplan and T. A. Uspenskaia

The basic raw material for the production of thorium and its compounds is a monazite concentrate. Monazite is a phosphate of rare earths and sometimes of thorium. Some investigators believe that the monazite contains thorium in the form of a silicate.

Until recently monazite was processed throughout the world mainly with sulfuric acid. This method is simple and also insures practically complete extraction of the mineral; but one of its defects is the fact that all of the phosphoric acid goes into the solution together with the rare earths and thorium.

Caustic soda methods of treating monazite (fusion with NaOH [1], treatment with a solution of NaOH [2], baking with soda [3]) with the precipitation of phosphorus in the form of trisodium phosphate were suggested a fairly long time ago but only the sulfuric acid method is used industrially. Caustic soda methods have recently begun to attract attention again [4-11], and in the USA [12] and some other countries they have been used industrially.

In 1952 a plant was put into operation in India for the treatment of 1500-3000 tons of monazite annually by an alkali method [6]. Since 1949 thorium salts have been produced in Brazil through the treatment of 2000 tons of raw material annually by an alkali method [13]. The method used in the USA [4] decomposes monazite in a 45% solution of NaOH at 138°C; the hydrated deposit is dissolved in hydrochloric acid, after which the chemical thorium concentrate is precipitated by partial neutralization of the solution and the rare earth hydroxides are separated from the filtrate by further neutralization of the solution. Trisodium phosphate is separated from the alkalis by evaporation; the solution of residual caustic soda is used for later operations.

The extraction of the monazite is sufficiently complete only when the concentrate is very finely pulverized (95.5% - 325 mesh), which is usually associated with high mechanical losses of the concentrate and is also expensive. It is also believed to be necessary to use a large excess of caustic soda (about 150% of the weight of the concentrate).

Soviet investigators are working on the improvement of caustic soda methods of processing monazite [14]. The authors of the present paper have worked out a method of decomposition under optimum conditions similar to those established by other workers [4] -- a 650 g/liter concentration of the caustic soda solution at 130°. For the purpose of intensifying the process and avoiding preliminary pulverization of the concentration, as well as the reduction of the consumption of caustic soda, the minerals were chemically decomposed in a heated ball mill, as in the method used for the processing of tungsten concentrates [15, 18]. The action of the balls on the mineral accelerates the reaction by breaking the film of insoluble precipitates which are formed in chemical decomposition and which cover the mineral grains.

The experiments were conducted with samples of concentrates containing 90-95% of monazite from different deposits. The principal components were as follows: 60-70% combined rare earth and thorium oxides and 25-27% of phosphorus pentoxide. The crushed particle size of the initial concentrates was 1 to 5 mm.

One-hundred gram batches of concentrates were decomposed in steel ball mills of 1.5 liter capacity loaded with balls of 0.8 cm diameter weighing 1.5 kg. The drums were revolved at about 75% of the critical speed in an air thermostat heated electrically to a set temperature. When the breakdown was completed the

TABLE

Results of the Two-Stage Treatment of a Concentrate by a Caustic Soda Solution

| | Amount of original material, kg | Weight of residue, % of weight of raw material | Quantity of rare earths and thorium in residue, % of content in raw material | Extraction of rare earths and thorium in the solution, % of content in raw material |
|---|---|---|---|---|
| First treatment of the concentrate (10 batches) | 4.0 | 11.1 | 6.2 | 93.8 |
| Second treatment of 10 residues from the first treatment | 0.445 | 1.7 | 0.1 | 99.9 |

hydroxide deposits were treated with hot water to remove the sodium phosphate and were then dissolved in hydrochloric acid. The degree of decomposition was determined from the thorium and rare earth content in the undissolved residue.

The first experiments studied the effect of prolonged treatment. The results showed that maximum decomposition is attained under the given conditions within four hours. This regime was used in subsequent experiments.

The next series of experiments studied the effect of different amounts of caustic soda. The leaching results showed (see the figure) that the extraction exceeds 99.5% when the consumption of caustic soda is 150-200% of the weight of the original concentrate. When the quantity of NaOH is reduced to 75-100% the extraction of rare earths and thorium is reduced by 1.5-3.5%. When the NaOH amounts to 50% of the weight of the concentrate the residue not dissolved in the hydrochloric acid contains 15-20% of the rare earths and thorium in the raw material.

A two-stage method was experimented with for the purpose of reducing the quantity of NaOH. In the first stage decomposition of the concentrate proceeded in NaOH amounting to 75% of the weight of the raw material. The resulting hydroxides were dissolved in hydrochloric acid and the undissolved residues (particle size 10-15 microns) from ten batches were combined and subjected to a second treatment by a solution of NaOH in a heated ball mill. The NaOH solution comprised 150% of the weight of the residues, which was very much more than the theoretical requirement for secondary decomposition. The second stage therefore produced practically complete decomposition.

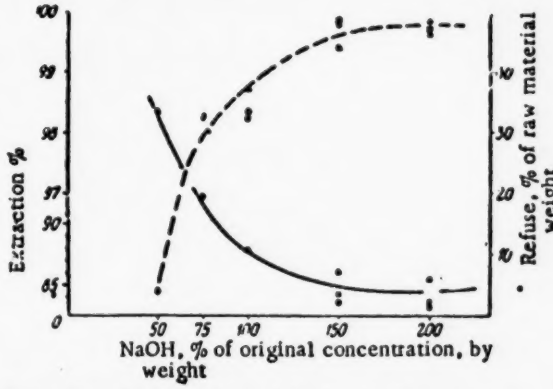


Extraction of rare earths and thorium and percentage of refuse after treatment, as a function of consumption of NaOH.

– – – – extraction; ——— refuse; ●○ – sample No. 1; ■□ – sample No. 2; ▲△ – sample No. 3; ◆◇ – sample No. 4.

The alkali from the secondary decomposition was used for the following primary decomposition of the concentrate. The combined consumption of caustic soda in both stages was 75-80% of the weight of the concentrate. The alkali solutions could be evaporated for removal of the trisodium phosphate, and the solution of excess caustic soda could be reemployed for decomposition of the concentrate.

The present investigation has showed that the decomposition of a monazite concentrate by a caustic soda solution in heated ball mills results in practically complete extraction of the mineral (by a two-stage process) without the need for pulverization, and that the consumption of caustic soda is about half what is required in the oridnary method of caustic soda decomposition.

## LITERATURE CITED


[1] W. Buddens and L. Preussner, et al., D.R.P. –95061 (1896).

[2] Dr. von Helmolt and Dr. Remse, D. R. P. –315371 (1918–1919).

[3] C. R. Böhm, Chem. Ind. 29, 450 (1906).

[4] A. E. Bearse et al., Chem. Eng. Prog. 50, No. 5, 235 (1954).

[5] The South African Mining and Eng. Journal 65, No. 3225, 573 (1954).

[6] Chem. Eng. News 31, No. 681, 1550 (1953).

[7] Chem. Age 64, No. 1652, 378 (1951).

[8] Industrie Chimique 450, 30 (1955).

[9] Northern Miner 41, No. 36, 26 (1954).

[10] The Industrial Chemist 30, No. 358, 555 (1954).

[11] Chem. Eng. News 32, 41 (1954).

[12] O. N. Carlson et al., "The metallurgy of thorium and its alloys" (Report No. 556 of the USA at the International Conference on the Peaceful Uses of Atomic Energy).

[13] P. Krumholz, "Extraction of thorium and uranium from Brazilian monazite" (Report No. 133 of Brazil at the International Conference on the Peaceful Uses of Atomic Energy).

[14] G. E. Kaplan, T. A. Uspenskaya, K. V. Orlov and V. M. Sadovnikova, "Investigations in Geology, Chemistry and Metallurgy" (Reports of the Soviet delegation at the International Conference on the Peaceful Uses of Atomic Energy), Acad. Sci. USSR Press, 1955, p. 105.

[15] G. A. Meerson and N. M. Yakobi, GIREDMET (State Rare Metals Research Institute), 1951.

[16] A. N. Nadolsky, Dissertation, Mintsvetmetzoloto (Ministry of Nonferrous Metals and Gold), 1954.

[17] G. A. Meerson and R. A. Pavlyuk, Trans. Mintsvetmetzoloto, 1956.

[18] G. A. Meerson and N. N. Khavsky, Nonferrous Metals (U.S.S.R.) No. 3, 41 (1957).


Received June 10, 1957

# X-RAY STUDY OF THE ELONGATION OF IRRADIATED URANIUM RODS

I. V. Batenin and B. V. Sharov

The literature [1,2] contains studies of the growth in size of uranium specimens as a result of irradiation in a reactor. A relation was found between the degree of perfection of the [010] texture of unirradiated uranium specimens in the direction of rolling and the radiation-induced growth. It was assumed that the texture is preserved during irradiation.

If the growth of uranium specimens in a reactor depends only on the perfection of the [010] texture, other conditions remaining unchanged, it is evident that in irradiated specimens greater elongation should correspond to more perfect [010] texture in the direction of elongation. It was of interest to test this hypothesis.

An x-ray study was made of the texture of uranium rods which were lengthened by irradiation. $CuK_\alpha$ radiation was used in apparatus for the roentgenography of highly radioactive materials [3]. The specimens were rods of natural and 2% enriched uranium produced by the same process but showing differences when irradiated in the FTR reactor (Table 1).

TABLE 1

| No. of specimen | % elongation | % depletion |
|---|---|---|
| 1 | 0 | 0.07 |
| 2 | 12.5 | 0.07 |
| 3 | 15 | 0.1 |
| 4 | 25 | 0.07 |
| 5 | 180 | 0.1 |

Specimens Nos. 3 and 5 were cut from the same rod, the parts of which lengthened differently during irradiation.

Specimens about 15 mm long were cut from rods of about 3 mm diameter; these were polished in the direction of the axis. The work-hardened surface layer was removed by etching. Before each x-ray exposure the oxide layer on the surface of the specimens was etched in hot concentrated nitric acid. The radioactivity of the specimens was between 25 and 120 microcuries depending on their size. The x-ray photographs were taken in the angular range $\vartheta = 15\text{-}60°$.

Analysis of the x-ray photographs showed that the structure of specimen No. 1 was an almost isotropic grain distribution, as the diffraction line intensities were almost in agreement with theoretical calculations.

Specimens Nos. 2-5 showed considerable rearrangement of line intensities, thus providing evidence of texture in the metal. Study of the diffraction line intensities shows a considerable [010] texture component in the direction of the rod axis. The degree of perfection of the [010] texture increases with the radiation-induced growth. As is shown in Ref. [1], the growth of uranium specimens obeys the experimental law

$$\frac{\ln \frac{l + \Delta l}{l}}{\%\ \text{depletion}} = G,$$

where $\frac{l + \Delta l}{l}$ is the relative elongation and G is a function of the texture and temperature during irradiation.

The temperature was kept constant during the irradiation of all specimens; therefore a definite value of the "growth coefficient" can be ascribed to each.

Fig. 1 shows portions of the x-ray photographs placed in the order of increasing G. These provide qualitative evidence that G increases with degree of perfection of the [010] texture. This follows from the different relative intensities of the (002), (021) and (110) lines.

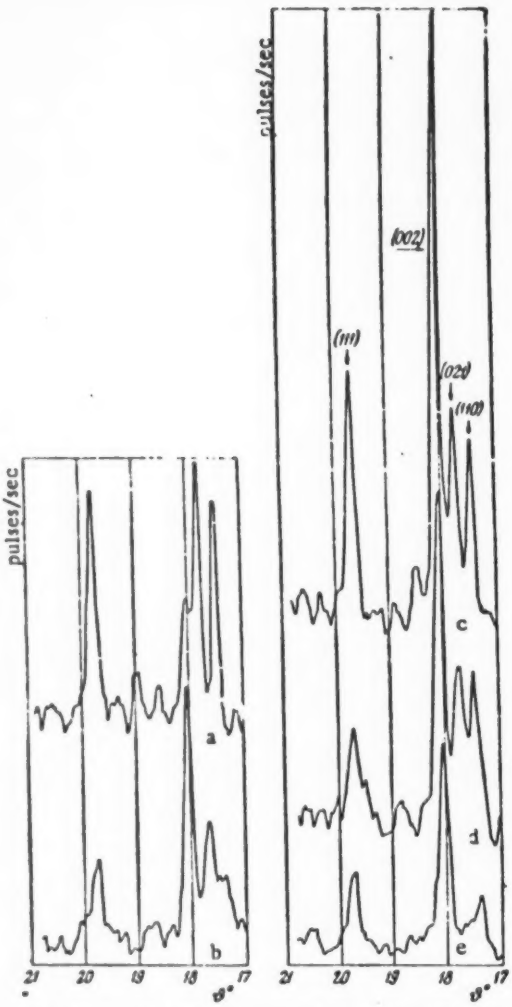


Fig. 1. Portions of the x-ray photographs of specimens after irradiation.
a) specimen No. 1, G = 0, elongation 0; b) specimen No. 3, G = 140, elongation 15%; c) specimen No. 2, G = 168.5, elongation 12.5%; d) specimen No. 4, G = 319, elongation 25%; e) sample No. 5, G = 1030, elongation 180%.

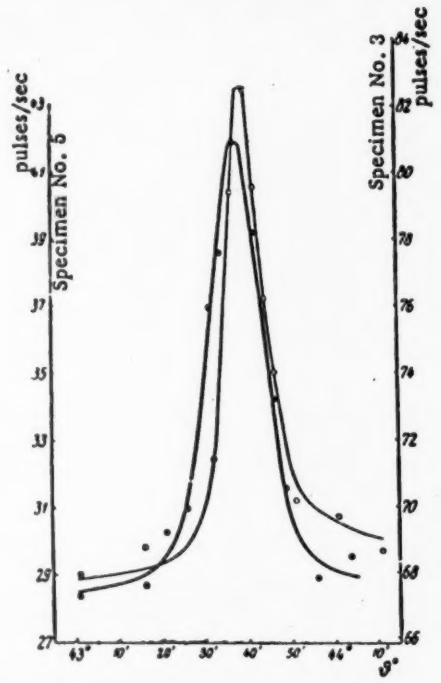


Fig. 2. X-ray photograph of (114) line O – specimen No. 3; ● – specimen No. 5.

The likelihood of accidental changes of the relative intensities of the lines because of inaccurate mounting of the specimens or instability of the apparatus was eliminated by several repetitions of the x-ray photographs.

It is also of great interest to measure stresses of the second kind in the material. For this purpose we measured the widths of the (131) lines of specimens Nos. 1,2,4 (Table 2) and of the (114) lines of Nos. 3 and 5 (Fig. 2).

For greater accuracy the x-ray photographs of the lines were taken at several points. Since stresses of the second kind broaden the diffraction lines it might be expected that the greatest line breadth would be obtained from untextured specimen No. 1. In actuality Table 2 and Fig. 2 show the reverse: the line breadth increases with radiation-induced growth.

The cause of this effect apparently lies in the elimination of stresses which exceed the tensile strength of the metal in both the untextured specimen and in the specimens with a small degree of texture perfection through inelastic deformation with twinning and the formation of microcracks. This was confirmed by a metallographic study of the structure and by data on the mechanical strength of the material.

TABLE 2

| No. of specimen | % elongation | Line breadth in arbitary units |
|---|---|---|
| 1 | 0 | 10 |
| 2 | 12.5 | 10 |
| 4 | 25 | 18 |

Thus variation in the technological process of manufacture can lead to inhomogeneities in the structure of the rods. Differences in the texture of different rods and of different parts of a single rod result in different growth under irradiation and in different stressed states.

In conclusion we wish to thank N. F. Pravdyuk and V. A. Mitropolevsky for assistance with the preparation of the specimens.

## LITERATURE CITED

[1] S. C. Payne and C. Kittel, The Metallurgy of Nuclear Power and the Effect of Radiation on Materials (Report of Foreign Scientists at the International Conference on the Peaceful Uses of Atomic Energy) Metallurgizdat, 1956, p. 642 (Russian translation).

[2] S. F. Pew, ibid, p. 668.

[3] I. V. Batenin and B. V. Sharov, PTE No. 3, 59 (1956).

Received April 23, 1957

BLANK
PAGE

# SCIENTIFIC AND TECHNICAL NEWS

## AT THE JOINT INSTITUTE FOR NUCLEAR RESEARCH

R. M. Lebedev

From May 15 to 18, 1957 the second meeting of the Scientific Council of the Joint Nuclear Research Institute took place at Dubno. The members of the Scientific Council who were present represented 11 countries which are members of the Institute.

Professor D. I. Blokhintsev, director of the Joint Institute, opened the meeting by congratulating the Council, Professor V. I. Veksler and the staff of the High Energy Laboratory on the successful start of operation of the proton synchrotron. The meeting discussed matters connected with the starting of the 10-Bev proton synchrotron, the scientific work of the Laboratory, the planning of new objectives of the Institute and the development of international scientific cooperation.

Operation of the Proton Synchrotron. Professor V. I. Veksler, director of the High Energy Laboratory reported on the starting adjustment of the accelerator and the difficulties which had to be overcome by the staff. The synchrotron was put into operation in two stages. In the first stage the various units of the accelerator were adjusted; in the second stage combined operation was started. *

It was necessary to adjust the five principal units of the accelerator: the electromagnet power supply, the time-varying magnetic field, the vacuum system, the high-frequency system and the system of injection and extraction of orbital particles.

Adjustment of the power supply system was directed by N. I. Pavlov; K. V. Chekhlov directed the adjustment of the high-frequency system. The difficulties which had to be overcome, in the adjustment of the magnet for example, are shown by the fact that to insure the homogeneous field required for stable proton acceleration about 100,000 magnetic measurements were made.

After the planned parameters of the separate units had been attained the staff proceeded to the very complicated task of starting the accelerator to test the combined operation of all units. This was done in three stages. In the first stage 9-Mev charged particles were injected, with a constant magnetic field of ~ 140 oersteds and provision for a few revolutions of the particles. In the second stage the particles were injected subject to a magnetic field increasing in time. In the third stage the high-frequency voltage was turned on and synchrotron acceleration of the protons was achieved. From the time of the complete start, which was directed by L. P. Zinovev, until the projected energy of 10 Bev was reached only two months elapsed, which is a very short time for the starting of accelerators of this type.

At the conclusion of his report Professor Veksler projected photomicrographs of nuclear disintegrations ("stars") produced by 9-Bev protons in emulsion nuclei.

Scientific work of the Institute's laboratories. It was the aim of the Council to become acquainted with the scientific work of the laboratories during the previous half year and to discuss and confirm future plans.

Professor Veksler in his report on the High-Energy Laboratory spoke of the preparation and conduct of research with the proton synchrotron. The principal task of the laboratory research staff was the development of methods for recording and investigating the behavior of high-energy particles. Several groups of the basic research division devoted themselves to this problem under the direction of Candidate in physico-mathematical

* This accelerator was described previously (Soviet J. Atomic Energy 1, 4, 22 (1956)). [C. B. Translation, p. 469.]

science I. V. Chuvilo. The departments of electronics, nuclear emulsions and diffusion and bubble chambers have recently developed some highly original techniques. A group led by Professor Van Gan-Chan is working on a large propane bubble chamber. Following a suggestion of K. D. Tolstov the staff of his department have worked with Professor A. I. Shalnikov to develop methods of depositing heavy hydrogen and deuterium on the surface of photographic emulsions. These plates will make it possible to study elementary interactions between particles of practically any energy and the nuclei of hydrogen and deuterium.

Original methods are being developed by the pellicle stack department under the direction of M. I. Podgoretsky. E. N. Matveev, M. N. Medvedev and others have developed methods of producing plastic scintillators of practically any size and are investigating their characteristics. The electronics department continues to develop original methods of discriminating particles in the 5-Bev range, for the detection and study of new particles, especially antihyperons.

In presenting the research program of his laboratory to the Scientific Council Professor Veksler reported that the primary aim will be the search for new particles and new types of interactions and the detailed study of the properties of elementary particles. At the same time the development of new techniques will be continued, involving a large liquid hydrogen chamber, pulsed magnetic fields for experiments with nuclear emulsions, apparatus for the automatic scanning of emulsions and films, and the production of particle beams.

The work of the Laboratory for Nuclear Problems was reported on by its director, Doctor of physico-mathematical sciences V. P. Dzhelepov. Since 1949 this laboratory has used a synchrocyclotron to accelerate protons to 680 Mev. The extraction of many beams of protons, neutrons, positive and negative pions, polarized nucleons etc., has made it possible to conduct studies of great diversity. Dr. Dzhelepov stated that at the beginning of 1957 the chief engineer of the laboratory, B. I. Zamolodchikov, had directed work which increased the operating time of the accelerator from 96 to 140 hours weekly. Further increase of the efficient utilization of this accelerator will result mainly from increased beam intensities.

Dr. Dzhelepov also reported in detail on the work done during the past half year; the pertinent papers will be published in the near future. The principal lines of investigation in the laboratory were as follows:

1. Elastic polarized and unpolarized nucleon-nucleon scattering at 600-660 Mev. (Departments of V. P. Dzhelepov, M. G. Meshcheryakov and G. R. Poze).

2. Pion production by polarized and unpolarized nucleons. (Departments of M. G. Meshcheryakov, V. P. Dzhelepov and R. M. Sudyaev. Similar studies were made by the group of A. G. Meshkovsky of the Academy of Sciences, USSR).

3. Pion production by pions. (This work was done mainly by the department of B. M. Pontecorvo as well as by that of V. M. Sidorov). The Laboratory for Nuclear Problems has recently obtained meson beams of 310 Mev and high intensity (up to 1300 mesons/cm$^2$-sec), thus making it possible to study the production of mesons by mesons near the threshold.

4. Pion scattering by nucleons, including polarization effects. Pontecorvo's group investigated elastic and exchange scattering at 307 and 335 Mev. The phase analysis of these experiments which took account of s and p waves showed the need for including d waves. Work in this direction will continue.

5. Interactions between high-energy nucleons and complex nuclei. Three different methods were used for studying interactions between nuclei and nucleons, especially 675-Mev protons (beginning with Li): the group headed by M. G. Meshcheryakov used a magnetic spectrometer, the group of V. N. Mekhedov used radiochemical methods, and the group headed by B. S. Dzhelepov and A. N. Murin (Leningrad University) used spectroscopy of neutron-deficient nuclei.

Meshcheryakov reported on the work of the magnetic spectrometer group. The direct ejection of deuterons from light nuclei by 657-Mev protons had been observed. As an explanation D. I. Blokhintsev has suggested that a proton collides with a "quasi-deuteron" which can form in the nucleus as the result of density fluctuations of the nuclear matter.

6. Study of the properties of muons and the investigation of weak interactions. Several methods were used (emulsions, electronics and bubble chambers) in various directions. The angular asymmetry of $\mu$-e decay is being studied and an attempt is being made to test the hypothesis of a two-component neutrino. The interactions of fast muons with nucleons and nuclei are being studied.

All of these lines of investigation are included in the program of the Laboratory for Nuclear Problems. In the future even greater attention will be paid to interactions of polarized particles and to polarization effects during inelastic interactions.

The Laboratory for Nuclear Problems is also preparing to participate in work with the proton synchrotron. Many studies are planned using various modern methods of studying interactions of pions and K mesons with nucleons up to 10 Bev. V. P. Dmitrievsky will direct the continued work on a number of problems connected with the acceleration of charged particles to high energies.

Professor G. N. Flerov reported briefly on the production of transuranic elements; for this purpose a cyclotron will be used to accelerate multicharged ions. The cyclotron is now being constructed by the Joint Institute.

The Laboratory of Theoretical Physics, like the Laboratory of Neutron Physics, is among the new laboratories of the Institute. The former has a large staff of young theoreticians under the direction of Professor N. N. Bogolyubov, D. I. Blokhintsev, V. Yu. Votrub, Ya. Zhevussky, M. A. Markov, Y. A. Smorodinsky, S. V. Fomin and Khu Nin. The report of this laboratory was presented by its director, Academician N. N. Bogolyubov. The following are the principal subjects of study of the laboratory:

1. General problems of quantum field theory: studies of relativistic quantum field theory, nonlocal field theory, etc.

2. Dispersion relations: the application of dispersion relations to elementary particle scattering and the derivation of the dispersion relations from general quantum field theory, the analysis of experimental tests of the dispersion relations and application of the method to processes involving K mesons as well as more complex processes.

3. The structure of elementary particles: a theoretical study of the influence of the internal structure of nucleons on interactions with pions, electrons and photons.

4. New particles: an explanation of the existence of new particles (heavy mesons and hyperons), clarification of the place of leptons in the current systematics of elementary particles and the formulation of recommendations for new experiments on the proton synchrotron based on current theories and phenomenological concepts. These problems are occupying a group of theoretical physicists directed by M. A. Markov, V. Yu. Votrub and Khu Nin.

5. The theory of elementary particle interactions: the development of phenomenological methods of calculation which will make it possible to estimate expected particle yields in collisions of high-energy particles. The laboratory is also studying the possibility of using available experimental data on cross sections, polarization etc to establish a scattering matrix for the processes to be studied.

The work of the Laboratory of Nuclear Physics was reported by its director, Professor I. M. Frank, who spoke of the studies connected with the construction of a pulsed reactor by the Institute. He spoke of very promising developments in neutron spectrometry and of the observation of polarization effects in neutron-capturing nuclei. The development of methods for investigations with neutrons from the pulsed reactor is a huge and laborious problem. It is therefore planned to hold a meeting in the autumn of 1957 of representatives from the countries which are members of the Institute to discuss this work.

International Relations of the Institute. The Scientific Council heard a report by the Vice Director of the Institute, Professor M. Ya. Danysh, on the international relations of the Institute. He especially emphasized that the development of international scientific collaboration on the problems studied by the Joint Institute will create very favorable conditions for the progress of science in the member countries of the Institute. This collaboration should exist both between the scientific centers and scientists of the member countries and of countries which do not participate in the work of the Institute, by the broadest exchange of scientific information and participation in scientific conferences.

The Scientific Council adopted resolutions for the creation in the Joint Institute of the most favorable conditions for international scientific collaboration.

The meetings of the Scientific Council were marked by an atomsphere of sincere friendship, and by the desire of the member scientists to create the best possible conditions for the work of the laboratory groups of the Institute, which aims at the exclusive development of nuclear physics for peaceful purposes in the member countries.

# ELEMENT 102

G. Z.

Element 102 (proposed name—nobelium) [1] has been obtained by bombardment of $Cm^{244}$ by ions of $C^{13}$ with an energy of 110-120 Mev in a 225-centimeter cyclotron at the Nobel Institute in Stockholm. For the first time in Europe the combined efforts of Swedish, English, and American scientists have synthesized a new element. It emits $\alpha$-particles with an energy of 8.5 Mev and has a half-life period of 10 minutes [2]. The probable atomic weight is 251-253 [2].

The energy of the bombarding ions had to be strictly controlled, inasmuch as the probability of forming a new element is rigidly dependent on the number of neutrons lost in the reaction [3].

A target of a thin film of curium on aluminum foil was placed in a special sampling device in which the generated atoms were gathered on clean foil and quickly identified. The best results were obtained by gathering on organic foils. The foils were dissolved from a platinum target in a drop of acetone and then, to obtain a thin source for measuring the impulses, the material was evaporated in a flame. For getting the activity into solution, the platinum target was treated with HCl. The solution was passed through an ionic-exchange column and the new element was extracted by $\alpha$-hydroxyisobuteric acid [2].

## LITERATURE CITED

[1] Chem. Eng. News 35, 28, 7 (1957).

[2] Engineering 4768, 124 (1957).

[3] Nature 4577, 120 (1957).

# DETERMINATION OF ABSOLUTE AGE OF ROCKS

V. B.

In Sverdlovsk from May 22 to May 27, 1957, the sixth session of the Committee on the Determination of Absolute Age of Rocks convened, with the Division of Geological-Geographical Sciences of the Academy of Sciences of the USSR meeting jointly with the Uralian Affiliate of the Academy of Sciences of the USSR.

Disintegration of natural radioactive isotopes, occurring at a definite rate, leads to the formation of stable products, the accumulation of which is a measure of time.

The application of radioactive methods to the determination of the age of rocks was first proposed by Rutherford, laying the foundation of a new geological chronology.

At present the methods chiefly used are the uranium–thorium–lead, uranium–thorium–helium, and potassium–argon.

Communications at the session have shown that a scientific nucleus has been created in a series of institutions of the Soviet Union to master the methods and theories of determination of absolute age. In order to solve some of the problems of geochronology the work must be conducted jointly by geologists and radiologists.

At the present time enough reliable information on age calculations has been obtained within the Soviet Union that it may serve as a basis for a national geologic-time scale. Thus, an age of 1900 million years has been established for northern Karelia; several complexes in the Ukraine have been distinguished with ages from 1600 to 2000 million years. Four complexes of different ages have been determined in the Caucasus, ranging from 15 to 400 million years old.

Reports in recent years have shown that large errors may be introduced if post-magmatic changes in the investigated material is not taken into account.

In this connection a number of laboratories have produced very interesting orderly reports on the regularity of migration, redeposition, and replacement of radioactive isotopes and their radiogenic products.

Of substantial interest is a series of mutually related works produced in the laboratory of I. E. Starik, corresponding member of the Academy of Sciences of the USSR (Radium Institute, Academy of Sciences of the USSR), and also the work of A. I. Tugarinov and others (Geochemical Institute).

Many opinions are offered on the perfection of techniques and methods of age determination, particularly on the determination of argon by isotope dilution techniques, of potassium by means of flame photometry, on the isotopic determination of small quantities of lead, on study of the mode of occurrence of lead in radioactive minerals, and so forth.

The results of the very worth-while session indicate that methods of determination of absolute age of rocks are being successfully developed in the Soviet Union and it is hoped that a national scale of geochronology will be established in the near future; absolute age determination in many cases is of decisive importance in clarifying the debatable questions of geology and ore genesis.

# EXPERIMENTAL BOILING WATER REACTOR OF THE ARGONNE NATIONAL LABORATORY

Yu. K.

At the Geneva Conference on Peacful Uses of Atomic Energy (1955), the American delegation presented a report on the experimental boiling water reactor(EBWR) under construction at the Argonne National Laboratory.

The reactor was officially set into operation in February of 1957. This reactor is the first of five reactors contemplated by the so-called demonstration reactor program in the USA.

The reactor has a heat output of 20 Mw, and an electrical output of 5 Mw. The relatively small reactor output was selected for experimental verification of the possibility of direct utilization of steam, which is generated directly in the reactor core.

Ordinary water is used in the loop at the present time; the use of heavy water is proposed for this purpose in the future.

The EBWR reactor is located on the grounds of the Argonne National Laboraotry, approximately 25 miles south of Chicago. Since this is an experimental reactor, much attention has been given to questions of operational safety. The reactor, turbine, condenser and auxiliary equipment are housed in a steel enclosure 24 m in diameter and 36 m in height. Since the enclosure, which has a volume ~ 11,000 $m^3$, is designed for an internal pressure of 1 atmosphere, radioactive steam will not travel beyond the reactor enclosure in the event the reactor explodes. The reactor is controlled from a room located outside the reactor enclosure.

The reactor fuel loading is of the combined type – both natural and low enrichment uranium are used. Natural water convection is employed in the reactor core, but forced water circulation can be adopted easily, for study of the effect of forced circulation on the operational stability of the reactor, for example.

A unique characteristic of the EBWR is the possibility of employing cores of various sizes. For example, a core 1.2 m in diameter can be easily increased to 1.5 m in diameter if necessary. Provision has been made for the use of fuel elements of various sizes in the reactor; varying of the uranium to water volume ratio in the core will enable studying the effect of the steam reactivity coefficient on the operational stability of the reactor.

The core is located in a steel vessel 2 m in diameter and 7 m in height with a wall thickness of 6 cm. Since the walls of the vessel attain a temperature of 260° as a result of radiation heating during reactor operation, they are protected from thermal neutrons by a shield of boron stainless steel.

The reactor vessel was manufactured by the firm "Babcock and Wilcox," and consists of SA-212 Grade B steel. The quality of the reactor vessel weldments was checked radiographically; a hydraulic check with water under 84 atmospheres and a gas tightness check with helium were performed. Helium leakage was determined by means of a mass spectrometer with a sensitivity of $8 \cdot 10^{-6}$ $cm^3$/sec.

At the present time, the EBWR core contains 114 fuel element assemblies, of which 106 contain enriched uranium (1.44% $U^{235}$) and 8 contain natural uranium. Thus, the average fuel enrichment is 1.4%. One reactor fuel loading requires 550 kg of uranium. The size of the reactor vessel is such that the number of fuel element assemblies can be increased to 148. The space between the core and vessel wall is filled with circulating water of the first loop which cools the vessel walls. The reactor core is provided with a grid plate which fulfills three main functions: to it are attached the upper ends of the fuel element assemblies, it provides an additional space above the assemblies for natural water circulation, and, finally, it holds the nine control rods (Fig. 1).

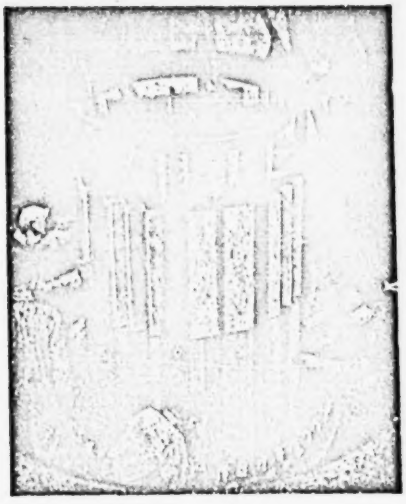

Fig. 1. Reactor core, assembled.

Fig. 2. Mechanisms of the nine control rods (under the reactor core).

The fuel elements in the assemblies are of the plate type with aluminum-nickel cladding 1.6 mm thick. This alloy, which was tested on a fuel element assembly model under laboratory conditions, gave indications of good corrosion resistance. Its use in place of zirconium is also explained by economic considerations.

The control rods (of which there are nine) are of two types of construction, both of which are used at the same time. Five of the rods employ hafnium as the absorbing material; these rods are placed in the locations with the greatest neutron density. The remaining rods are made of stainless steel containing 2% boron. A hafnium rod weighs 24 kg, and a boron steel rod, 56 kg.

Although the control rods are inserted and withdrawn from the reactor through the removable upper cover of the reactor, their motion in operation takes place through labyrinth packing at the bottom of the core tank (Fig. 2). The rod drop time is less than one second. In emergencies the rods are actuated by a spring. During normal operation the control rods are actuated by an electric motor. All the moving mechanisms of the control system are located outside the reactor vessel, and can easily be inspected, serviced and replaced.

The reactor shield was designed for a power capacity on the order of 40 Mw, which it will have in the event heavy water is employed. On the sides the reactor is shielded by a layer of stainless steel and heavy concrete with a total thickness of 2.5 m. From below the reactor is also shielded by heavy concrete, and from above, by water and steel.

Supplementary emergency shielding is effected by injection under pressure into the core of a solution of boric acid.

The basic characteristic of the EBWR is the generation of steam in the core and its direct use in the turbine. This steam differs from ordinary steam in that it is radioactive and possesses greater corrosive activity due to the presence of a relatively large amount of oxygen and hydrogen, which are liberated by decomposition of water under the influence of radiation. During normal operation, when the steam leaves the reactor it has a moisture of up to 1%, which then decreases to 0.1%; the salt content comprises less than 0.001 parts per million. The condensate formed in the turbine condensers is continually cleaned in ion exchange filters.

The system employs a 5 Mw turbogenerator operated by steam under a pressure of 40 atmospheres and temperature of 250°C. Due to the radioactivity of the steam, special attention is paid to sealing the turbine, in which connection labyrinth packing is used on the turbine shaft to reduce steam and water leakage to a minimum.

Operation of the reactor will clarify very important and as yet little understood problems of direct use of steam, generated in the core.

## LITERATURE CITED

[1] Engineer, 203, 5282, 623 (1957).

[2] Engineer, 203, 5283, 661 (1957).

[3] Engineer, 203, 5284, 699 (1957).

## REACTOR FOR EDUCATIONAL PURPOSES•

Yu. K.

At the beginning of February, 1957, the low-power reactor "Argonaut" was set in operation at the Argonne National Laboratory (USA). This reactor is somewhat unusual in construction and is intended for educational institutions. The first reactor was installed in the School of Nuclear Physics and Technology at the Argonne Laboratory. Two American firms will soon start producing the reactor.

The "Argonaut" is a heterogeneous thermal reactor with a graphite moderator and cooling by ordinary water, which also performs the function of a moderator. The reactor has a hollow cylindrical core (Fig. 1) with an outside diameter of 90 cm, and inside diameter and height of 60 cm. The space inside the core is filled with graphite, which forms the second (inner) reflector.

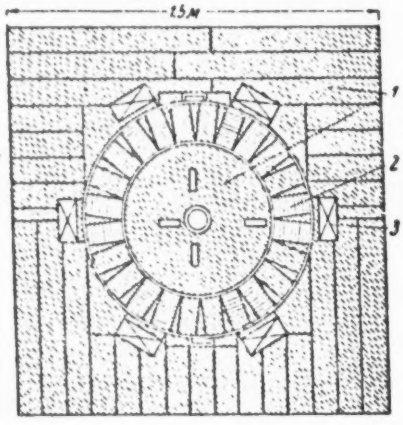


Fig. 1. Horizontal cross-sectional view of the "Argonaut" reactor.
1) graphite; 2) fuel assemblies; 3) cavities for control rods.

The graphite in the reactor has a total weight of about 190 kg, and the total volume of the water is about 0.4 $m^3$.

The core contains 204 fuel plates (12 assemblies with 17 plates to each assembly). The dimensions of each plate are 60 × 7.5 × 0.25 cm. The fuel used is the oxide $U_3O_8$ dispersed within an aluminum matrix. The critical mass of the reactor is 3.7 kg of uranium with an enrichment of 20%. Cooling water flows between the plates in the assemblies.

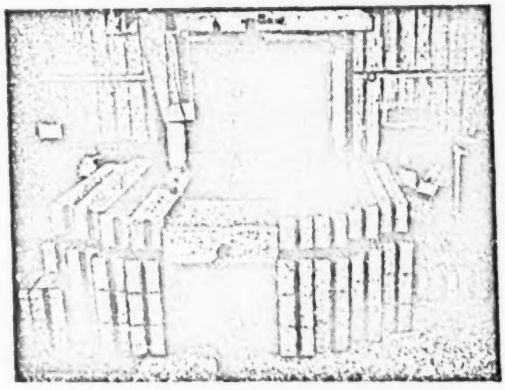

Fig. 2. General view of reactor "Argonaut."

The maximum power capacity of the reactor is 10 kw, and the thermal neutron flux is $10^{11}$ neutrons/$cm^2$ sec. In low-power operation the reactor is cooled by natural water circulation; at high power, forced circulation (with a consumption of 30 liter/min) is employed. The total reactor diameter, including the shield, is 5 m, and the height is 2 m (Fig. 2).

In this reactor, which is designed for educational purposes, special attention was given to the problem of safety. Two independent systems are provided for emergency shut down of the reactor: the water is drawn from the reactor into a tank through a dumping tube, and nitrogen is piped into the core at the same time.

The large amount of gas bubbles formed greatly decreases the moderator density, and the chain reaction ceases. The artificial bubbles can also be used to simulate boiling of the water. The cadmium control and emergency rods are used both in normal operation of the reactor and in emergencies.

The experimental reactor equipment is conventional. For conducting exponential experiments, the inner cylindrical graphite reflector can be removed completely or partially, and the cavity thus formed can be filled with fuel assemblies.

The "Argonaut" and building cost approximately $100,000.

## INTEGRATION OF THE $U^{235}$ FISSION NEUTRON SPECTRUM [1]

Iu. K.

The energy distribution of the $U^{235}$ fission neutron spectrum, as is well known, is described by the equation

$$N(E)\,dE = Ae^{-E}\,\mathrm{sh}\sqrt{2E}\,dE,$$

where N(E)dE is the number of neutrons produced in the energy interval from E to E+dE, and A is a normalizing factor [2].

It is, however, often useful to know the integral

$$N(a \to b) = \int_a^b N(E)\,dE,$$

which gives the number of fission neutrons having an initial energy between a and b.

The integral of the distribution function can be written as the sum of a hyperbolic function and an error function. Since the tables of these functions are widely available, the relations given below can be easily used to calculate the integral.

Let us write the first expression in the exponential form

$$N(E)\,dE = \frac{A}{2}\left[e^{-(E-\sqrt{2E})} - e^{-(E+\sqrt{2E})}\right]dE. \qquad (1)$$

Multiplying Equation (1) by $e^{1/2}\cdot e^{-1/2} = 1$, we obtain

$$N(E)\,dE = \frac{Ae^{1/2}}{2}\left[e^{-\left(\sqrt{E}-\frac{1}{\sqrt{2}}\right)^2} - e^{-\left(\sqrt{E}+\frac{1}{\sqrt{2}}\right)^2}\right]dE. \qquad (2)$$

Writing $\sqrt{E} - \frac{1}{\sqrt{2}} \equiv \xi$ and $\sqrt{E} + \frac{1}{\sqrt{2}} \equiv \zeta$, let us insert these into (2); integrating from E = 0 to E = x, we obtain

$$\int_0^x N(E)\,dE = \frac{Ae^{1/2}}{2}\left[\int_{-\frac{1}{\sqrt{2}}}^{\sqrt{x}-\frac{1}{\sqrt{2}}} e^{-\xi^2}(2\xi+\sqrt{2})\,d\xi - \int_{\frac{1}{\sqrt{2}}}^{\sqrt{x}+\frac{1}{\sqrt{2}}} e^{-\zeta^2}(2\zeta-\sqrt{2})\,d\zeta\right]. \qquad (3)$$

Equation (3) can be written in the form

$$\int_0^x N(E)\,dE = \frac{Ae^{1/2}}{2}\left[\int_{\left(\sqrt{x}-\frac{1}{\sqrt{2}}\right)^2}^{\left(\sqrt{x}+\frac{1}{\sqrt{2}}\right)^2} e^{-\tau}\,d\tau + \sqrt{2}\int_{-\frac{1}{\sqrt{2}}}^{\sqrt{x}-\frac{1}{\sqrt{2}}} e^{-\xi^2}\,d\xi + \sqrt{2}\int_{\frac{1}{\sqrt{2}}}^{\sqrt{x}+\frac{1}{\sqrt{2}}} e^{-\zeta^2}\,d\zeta\right]. \tag{4}$$

In this expression terms containing $2\xi e^{-\xi^2}d\xi$ and $2\zeta e^{-\zeta^2}d\zeta$ are inserted into the first integral on the right side with the substitution $\tau \equiv \xi^2 \equiv \zeta^2$. This first integral can be calculated with no difficulty. The second two integrals on the right side of (4) are in the form of the error integral

$$\operatorname{erf}(x) \equiv \frac{2}{\sqrt{\pi}}\int_0^x e^{-\lambda^2}\,d\lambda.$$

The error integral has the following properties which can be used here:

$$\operatorname{erf}(b) - \operatorname{erf}(a) = \frac{2}{\sqrt{\pi}}\int_a^b e^{-\lambda^2}\,d\lambda,$$

$$\operatorname{erf}(x) = \operatorname{erf}(-x).$$

Integrating the first term and using the last three relations we obtain

$$N(0 \to x) = \int_0^x N(E)\,dE =$$
$$= \frac{Ae^{1/2}}{2}\sqrt{\frac{\pi}{2}}\left[\operatorname{erf}\left(\sqrt{x}+\frac{1}{\sqrt{2}}\right) + \operatorname{erf}\left(\sqrt{x}-\frac{1}{\sqrt{2}}\right)\right] - Ae^{-x}\operatorname{sh}\sqrt{2x}. \tag{5}$$

For normalization, we must set

$$\lim_{x\to\infty}\int_0^x N(E)\,dE = 1. \tag{6}$$

Now $\lim_{x\to\infty}\operatorname{erf}(x) = 1$ and $\lim_{x\to\infty} e^{-x}\operatorname{sh}\sqrt{2x} = 0$. Thus inserting Equation (5) into (6), we obtain

$$A = \sqrt{\frac{2}{\pi}}\,e^{-1/2} \simeq 0{,}48394.$$

We thus obtain

$$N(E)\,dE = \sqrt{\frac{2}{\pi}}\,e^{-1/2}e^{-E}\operatorname{sh}\sqrt{2E}\,dE.$$

*[Here and elsewhere "sh" = sinh – Ed.]

Equation (5) becomes

$$N(0 \to x) = \frac{1}{2}\left[\operatorname{erf}\left(\sqrt{x} + \frac{1}{\sqrt{2}}\right) + \operatorname{erf}\left(\sqrt{x} - \frac{1}{\sqrt{2}}\right)\right] - \sqrt{\frac{2}{\pi}}\, e^{-1/2} e^{-x} \operatorname{sh} \sqrt{2x}. \tag{7}$$

We note that the first term in Equation (7) is exactly equal to the mean value of the error integral for $\sqrt{x} + \frac{1}{\sqrt{2}}$ and $\sqrt{x} - \frac{1}{\sqrt{2}}$. For large values of $y$, it is known that erf $y \approx 1$ (for instance, erf (3) = 0.999978). Therefore if $x$ is large, we can write

$$N(0 \to x) \approx 1 - \sqrt{\frac{2}{\pi}}\, e^{-1/2} e^{-x} \operatorname{sh} \sqrt{2x}.$$

Thus $N(0 \to \infty) = 1$. For large $x$,

$$N(x \to \infty) \simeq \sqrt{\frac{2}{\pi}}\, e^{-1/2} e^{-x} \operatorname{sh} \sqrt{2x}.$$

In order to determine the fraction of neutrons having energy between $E = x_1$ and $E = x_2$, where $x_2 > x_1$, we need only calculate $N(0 \to x_1)$ and $N(0 \to x_2)$, and then

$$N(x_1 \to x_2) = N(0 \to x_2) - N(0 \to x_1).$$

## LITERATURE CITED


[1] F. T. Binford, Nucleonics 15, 2, 94 (1957).

[2] B. E. Watt, Spectrum of neutrons from fission induced by thermal neutrons, AECD- 3073, USA, 1951.

# PREPARATION OF HIGH PURITY $U^{233}$ AND $U^{235}$ POWDERS

G. Z.

Small parts of fissionable isotopes $U^{233}$ and $U^{235}$ are required for measurement and study of nuclear properties in the development of fuel elements. Since these metals are exceedingly expensive and dangerous to workers due to their high $\alpha$-activity (that of $U^{235}$ is 150 times more active than natural uranium, and that of $U^{233}$ is 15,000 times more active) [1], it is necessary to obtain maximum yield with dispersion and losses kept to a minimum. These conditions are fulfilled by applying the method of powder metallurgy, one of the most economical methods of producing small parts.

Powders of these isotopes are obtained [1] by reducing uranium dioxide by means of calcium in a reaction vessel (Fig. 1). The operations and conditions of this technique for producing 200 to 350-gram lots of metal are given below.

Technique for Preparing the Powder

| | |
|---|---|
| 1. Preparation of the batch | A mixture of 400 g of $UO_2$ and 255 g calcium, (50% excess), which has been processed twice, with a coarseness of 12 to 20 mesh is pressed into a briquette. |
| 2. Reduction | The briquette is placed into the reaction vessel on a base of fired lime covered with calcium with a coarseness of 20 to 60 mesh. The vessel is sealed, flushed with argon, heated to 1,200°C, held at this temperature for 30 minutes, and then rapidly cooled. |
| 3. Crushing of the batch | The hard and pasty, dark colored compact, (not the usual green), is crushed in a small jaw crusher. |
| 4. Leaching of the powder | The crushed compact is treated with water acidified by 1.5N $HNO_3$, calculated so that after neutralization the pH of the solution does not exceed 5.5. A spiral tube carrying cooling water is inserted into the rotating leaching tank so that the temperature of the solution does not exceed 21°C during leaching. |
| 5. Drying of the powder | The light round particles of powder 10-15 $\mu$ in diameter are washed first with 1.5N $HNO_3$, then with distilled water, dried in a vacuum (the particles are evacuated through the drying system), and then sifted. |

The following points were noted during development of the technique.

Careful mixing and sufficient time for high-temperature treatment are required for complete reduction. A criterion of completeness of reduction is the formation of round globules of uranium 10-15 $\mu$ in diameter, in the amount of not less than 95%, which is the most suitable shape for subsequent pressing of the part (angular particles are harmful). The excess of calcium serves as a kind of flux. If it comprises about 30% or less of the theoretical amount, 70% spherical particles are obtained. The percentage of spherical particles is also reduced by slow cooling of the melt. With an excess greater than 50%, the compact becomes very pasty and is difficult to crush.

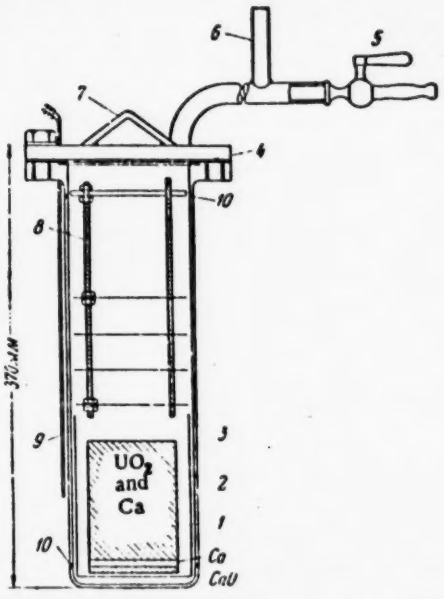


Fig. 1. Reaction vessel.
1) briquette charge; 2) thin metal crucible; 3) stainless steel container 3.2 mm thick, outside diameter – 100 mm; 4) asbestos gasket; 5) pressure tap; 6) tube to rubber cylinder – receiver for excess pressure; 7) hanging bracket; 8) shields, mounted on stainless steel rods; 9) Pt-PtRh thermocouple; 10) welded seam.

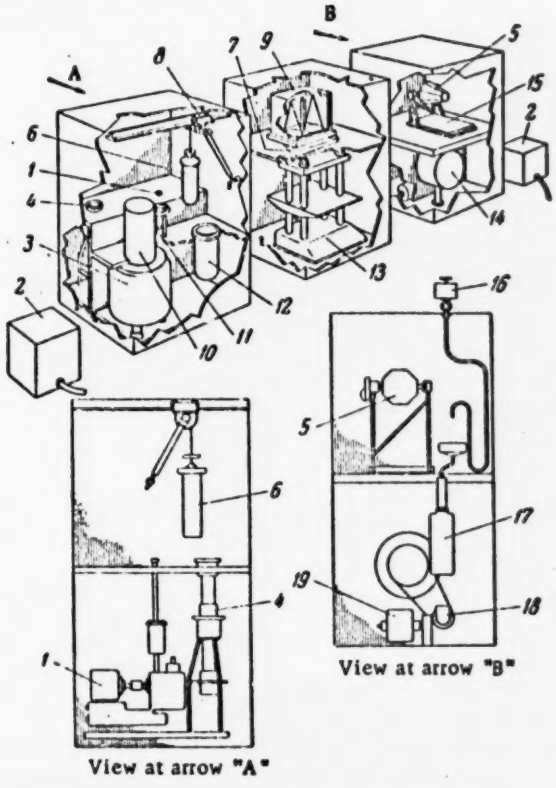


Fig. 2. Schematic diagram and arrangement of dry chambers for preparing metallic $U^{233}$ and $U^{235}$ in 200 to 350-gram lots. 1) mechanical vacuum pump; 2) cooling apparatus; 3) oven; 4) oil diffusion pump; 5) leaching apparatus; 6) reaction vessel, assembled; 7) shock mounting; 8) lifting mechanism; 9) scales; 10) radiation shield; 11) mounting base for reaction vessel; 12) cooler for reaction vessel; 13) 35 ton press; 14) crusher; 15) drip pan; 16) liquid inlet; 17) liquid outlet; 18) speed reducer; 19) crusher motor.

Careful control of the pH is required in leaching the $HNO_3$, to avoid uranium losses. If the temperature of the solution exceeds 30°C, the uranium becomes acidified and pyrophoric.

The entire process takes place in three connected hermetically sealed changers [2] (Fig. 2), which are filled (at the time the active substance is used) with argon under a pressure of 2 cm of water column, below atmospheric pressure. In the left chamber there is a vertical oven with a Pt-Rh winding, which is provided with water cooling, and a lifting mechanism for the reaction vessel. In the center chamber are scales and a press. The raw materials enter and are taken from this chamber. In the right chamber is a crusher and leaching device. The equipment is arranged to permit the operator to work with the least physical exertion.

By means of this technique, metallic $U^{233}$ and $U^{235}$ powders are obtained with a yield of 97-98% from the dioxide. The yield obtained by hot pressing of parts consisting of these powders is greater than 99%.

## LITERATURE CITED

[1] R. G. Bellamy and J. H. Buddery, Nucl. Power 2, 13, 175-179 (1957).

[2] Problems of Modern Metallurgy 2, 67 (1957).

# DILATOMETRIC DETERMINATION OF THE COEFFICIENT OF EXPANSION OF α-URANIUM

G. Z.

In a dilatometric study of α-uranium it has been observed [1] that there is considerable variation of the expansion coefficient, which is attributed to the presence of a preferred orientation. Reference [2] contains a recent study of the expansion of statistically pure isotropic α-uranium (that is, uranium without any preferred orientation and sufficiently fine-grained to compensate for the anisotropy of individual grains) and of monocrystalline uranium.

In order to produce an isotropic structure, 4 × 4 × 50 mm specimens of uranium of various origins and different orientations were heated for a few minutes in a saline bath above the temperature of the α-β transformation and were then quenched in water. A metallographic study showed that the quenched specimens were uneven, possessing jagged grains of various sizes and nonparallel twinning inside of the grains. After annealing for a few hours at 600°C recrystallization occurred and the structure became stable, with more uniformly sized round grains and strictly parallel twinning.

| | Expansion coefficient from 20°C to | | | | | |
|---|---|---|---|---|---|---|
| | 250° C | 325° C | 400° C | 475° C | 550° C | 625° C |
| $\alpha_a \cdot 10^6$ | 23.1 | 24.2 | 25.5 | 27.1 | 29.0 | 31.3 |
| $\alpha_b \cdot 10^6$ | −0.3 | −1.3 | −2.5 | −3.9 | −5.5 | −7.5 |
| $\alpha_c \cdot 10^6$ | 22.6 | 24.3 | 26.2 | 28.2 | 30.4 | 33.3 |
| $v=(\alpha_a+\alpha_b+\alpha_c)\cdot 10^6$ | 45.4 | 47.2 | 49.2 | 51.4 | 53.9 | 56.8 |
| Isotropic specimen | 45.5 | 47.2 | 48.9 | 50.8 | 53.1 | 55.8 |

Note: The error of measurement of the expansion coefficient is $1 \cdot 10^{-6}$ for an α single crystal and $\alpha_{av} = 0.75 \cdot 10^{-6}$ for an isotropic specimen.

Single crystals of the same specimens were obtained by Cahn's method [3] but the temperature gradient in the α-β zone was reduced as much as possible. The specimens were drawn at the rate of 3 mm per hour. Electrolytic etching of the macrostructure showed that the specimens consisted of many thin crystals elongated in the direction of growth. An x-ray study showed that although the orientation of these crystals perpendicular to the direction of growth differed considerably, in the growth direction this difference did not exceed ±2°. Therefore the specimens possessed a fibrous "pseudomonocrystalline" structure.

The dilatometric studies were conducted with a differential dilatometer in a vacuum and a pyrox standard. The heating and cooling rate for cycles up to 630°C was 150°C/hour. It appeared from the results that isotropic specimens exhibit the same behavior independently of their origin, with very small variation of the expansion coefficient. The dilatometric curves showed good reproducibility, which was not the case for uranium with preferred orientation because of "thermal coupling."

The dilatometric curves of monocrystalline uranium were ideally reversible. From measurements of

the expansion coefficient of differently oriented single crystals it was possible to calculate the expansion coefficients along the a, b and c axes. All measurements are given in the table. These results show little difference from x-ray data [4].

## LITERATURE CITED


[1] J. Bernard, Rev. Metall. 51, 737 (1954).

[2] P. Lehr and J. P. Langerson, Rev. Metall. 54, 257 (1957).

[3] R. W. Cahn, Acta Met. 1, 176 (1953).

[4] J. Bridge, C. M. Schwartz and D. A. Vaughan, J. Metals 8, Sec. 2, 1282 (1956).


## NITRO-OXALATE COMPOUNDS OF RUTHENIUM


O. Zvyagintsev


Radioruthenium is one of the fragments of uranium fission and the study of its chemical behavior in the reprocessing products from uranium slugs is of great interest. At the N. S. Kurnakov Institute of General and Inorganic Chemistry of the Academy of Sciences USSR, O. E. Zvyagintsev and S. M. Starostin have worked on the synthesis and study of complex nitroso compounds of ruthenium: $RuNOX_3 \cdot nH_2O$, $M[RuNOX_3]$, $M_2[RuNOY_2]$ etc., where X is a monobasic acid radical, Y is a dibasic acid radical and M is a cation. Of great interest are the ruthenium nitroso-oxalates of ammonium, magnesium and calcium $(NH_4)_2[RuNO(C_2O_4)_2]$, $Mg[RuNO(C_2O_4)_2]$, $Ca[RuNO(C_2O_4)_2(OH)_2] \cdot 6H_2O$ and the complex acid $H_2[RuNO(C_2O_4)_2]$.

The complex acid is produced by prolonged heating of a solution of ruthenium nitrosonitrate $RuNO(NO_3)_3 \cdot nH_2O$ with oxalic acid followed by evaporation of the solution and removal of the excess oxalic acid through heating at 150°. The molecular weight and electrical conductivity of the complex acid were determined, confirming the given formula. It was established that in crystalline form the compound is diamagnetic. An aqueous solution of the acid reacts with metallic magnesium, liberating hydrogen and forming a magnesium salt. With calcium oxide the acid gives a calcium salt of somewhat different composition than with magnesium, and with ammonia it gives an ammonium salt.

The ammonium salt is soluble in hot water but is almost insoluble in cold water. The magnesium and calcium salts are insoluble in water. The last two salts possess very high thermal and chemical stability. Thus the magnesium salt begins to decompose only above 200° and is completely decomposed at 800°. Ordinary reagents with ruthenium (thiourea, thionalide, mercaptobenzothiazole) do not react with all of the above oxalates. All of the compounds show a deep dark brown color.

Ruthenium nitroso-oxalates are of interest because the ruthenium here possesses the unusual coordination number 5. The ruthenium valence here is 2 if the nitroso group is considered neutral. However the valence of ruthenium in such compounds cannot be regarded as definitely decided.

# THE TOTAL RADIATION DOSE DURING ACCIDENTS INVOLVING NUCLEAR REACTORS*

S. L.

The paper discussed here concerns the calculation of the dosages of various forms of radiation from nuclear reactors in a supercritical state. When accidents occur in a nuclear reactor the personnel near the reactor is subjected to the danger of intense radiation damage. The calculation of the dosage is difficult because it is necessary to take int · account both external gamma and neutron radiation. A fast and reliable method of calculation is required for medical prognosis and suitable therapy.

For the purpose of estimating the total dosage the authors have used data obtained during two accidents involving experimental reactors at Los Alamos in 1945 and 1946.* *

The total doses received by the affected laboratory workers is composed of the following (in order of decreasing importance):

a) Fast neutrons which produce recoil protons in the tissues;

b) 2.2-Mev gamma radiation resulting from the capture of slow neutrons by hydrogen atoms in the tissues;

c) Protons of about 0.6 Mev resulting from the capture of slow neutrons by nitrogen atoms (the $N^{14}(n,p)C^{14}$ reaction);

d) An "instantaneous" dose of external gamma radiation resulting from the nuclear reaction;

e) Induced radioactivity of sodium, chlorine, phosphorus and manganese atoms in the organism.

One of the important factors causing sickness was the soft gamma radiation of high intensity connected with the "blue glow" of a chain reaction.

The calculations for each of the components are given below. The induced radioactivity of $Na^{24}$ and $P^{32}$ was determined by measuring the specific activity of these substances in the urine. The highest value for $P^{32}$ was 357 disintegrations per second ($9.4 \cdot 10^{-3}$ microcuries) and the lowest value was 1.4 disintegrations per second ($3.7 \cdot 10^{-5}$ microcuries). For $Na^{24}$ the corresponding values were 248 disintegrations per second ($6.5 \cdot 10^{-3}$ microcuries) and 1.27 disintegrations per second ($3.3 \cdot 10^{-5}$ microcuries).

Knowledge of the radioactivity of $Na^{24}$ in the serum and of the amount of the stable isotope (3.25 mg/cm$^3$) permitted a calculation of the slow neutron flux that passed through the bodies of the affected persons. In the worst case the neutron flux was $477 \cdot 10^9$ neutrons per cm, and in the mildest case $7.1 \cdot 10^9$ neutrons per cm. This data on the neutron flux also made it possible to calculate the neutron captures by hydrogen and nitrogen nuclei and the resulting doses of gamma rays (from hydrogen) and of protons (from nitrogen).

---

* J. G. Hoffman and L. H. Hempelman, Amer. J. Roentg., Rad. Therapy and Nucl. Medicine 77, 1, 144 (1957)

** A detailed clinical description of these cases and a provisional calculation of the dosages is given in the book by Hempelman, Lisco and Hoffman entitled "The Acute Radiation Syndrome" (Russian translation, Moscow, IL, 1953).

To determine the gamma dosage from the reaction H(n,γ) experiments were made on a model of the human body made of thin copper sheet (0.75 mm) and filled with an aqueous solution of $Na^{24}Cl$ with the radioactivity 80,978 dis/min/cm³ ($3.54 \cdot 10^{-2}$ microcuries/cm³). Since the energy of the gamma radiation from $Na^{24}$ (1.38 Mev and 2.76 Mev) is close to that of the gamma radiation of hydrogen from neutron capture (2.2 Mev), from knowledge of the radioactivity of $Na^{24}$ and the dosage in different parts of the model and close to it the dose of hydrogen gamma radiation could be determined when the neutron flux was known. From such measurements it was established that the H(n,γ) reaction had given the victims doses of from 1.4 r to 87.0 r.

| No. of case | Dose | | | | Gamma equivalent | |
|---|---|---|---|---|---|---|
| | reaction H(n,γ)x | fast neutrons, rep | reaction $N^{14}(n,p)C^{14}$, rep | external gamma radiation, r | average dose, r | total dose (including soft radiation), r |
| 1 | 33.0 | 27.0 | 3.23 | 220.0 | 404 | 587 |
| 2 | 1.9 | 1.7 | 0.20 | | 11 | 16 |
| 3 | 87.0 | 109.0 | 13.20 | 11.4 | 709 | 1125 |
| 4 | 21.0 | 19.6 | 2.38 | 4.5 | 136 | 219 |
| 6 | 9.5 | 10.5 | 1.26 | 2.4 | 71 | 110 |
| 7 | 5.9 | 5.7 | 0.87 | 1.3 | 39 | 56 |
| 8 | 3.0 | 3.0 | 0.37 | 1.3 | 21 | 30 |
| 9 | 2.3 | 2.2 | 0.28 | 0.5 | 15 | 22 |
| 10 | 1.4 | 1.8 | 0.21 | 0.5 | 12 | 17 |

The fast-neutron dose produced by recoil protons was computed on the assumption that each neutron during the process of slowing down to thermal speeds liberates 0.5 Mev. Since 1 rep represents $5.8 \cdot 10^{13}$ ev/g, each fast neutron before capture yields $8.62 \cdot 10^{-8}$ rep. This quantity multiplied by the number of neutron captures by hydrogen nuclei is the dosage of each victim depending on the neutron flux to which he was subjected. The computations show that this dose lies between 1.4 and 83.6 rep.

A similar calculation gave the dosage from neutron capture by nitrogen atoms, based on the fact that the protons emitted in the reaction $N^{14}(n,p)C^{14}$ possess 0.6 Mev. This dose ranged from 0.18 to 11.15 rep.

The surface dose of external gamma radiation during the explosion was determined from the fact that at a distance of 1 meter the instantaneous dose was 7.2 r and that the dosage varied with distance according to $1/r^{1.6}$. This dosage varied from 0.7 to 18.1 r. The entire dose received by the body of a victim was computed for 1 Mev gamma radiation from Mainord's tables; the resulting figure varied from 0.5 to 11.4 r.

From knowledge of the $Na^{24}$ radioactivity in the serum the beta and gamma radiation doses from this element were calculated. The amounts were negligibly small; the gamma radiation from $Na^{24}$ is less than 1% of the gamma radiation resulting from neutron capture by hydrogen atoms. Therefore in computing the total dosages these amounts were omitted. The same holds for $Cl^{38}$, $K^{42}$, $Mn^{56}$ and $Mg^{27}$. The table shows the total doses received by each of the ten victims.

The gamma equivalent was computed from the relative biological effectiveness of heavy particles, which was taken as 5.

Persons near the reactor when the supercritical state was reached received severe arm burns. At that time the reactor was surrounded by a blue glow, which was visible in the well-lighted room. The glow was accompanied by the emission of soft gamma rays which produced the burns. In case No. 1 the right arm received 20,000 to 40,000 r and the left arm received 5000-15000 r. In case No. 3 the respective doses were 3000-1000 r and 15000-30000 r, while in case No. 4 the left arm received only 400-600 r.

# $Sr^{90}$ IN THE HUMAN ORGANISM*

S. L.

The amount of $Sr^{90}$ in the human organism was investigated using more than 1500 bone specimens obtained from 17 geographical locations and from individuals ranging from childhood to 60 years of age. More than 600 analyses were made using the most precise methods for determining the $Sr^{90}$ content. Specimens were received from the USA, Canada, Brazil, Chile, Columbia, Venezuela, Denmark, England, Germany, Italy, Switzerland, Liberia, Taiwan and Puerto Rico. The investigators endeavored to obtain specimens from the most varied geographical and dietetic regions, although for technical reasons this was not always possible.

The investigation showed that at the present time a sufficiently large specimen will reveal $Sr^{90}$ in the human organism independently of age or geographical location. The following results were obtained. The average world concentration of $Sr^{90}$ in human bones in the autumn of 1955 was about 0.12 micromicrocuries per gram of calcium, which is about 0.0001 of the maximum permissible concentration. This agrees with the amount predicted from measurements of radioactive fallouts and the subsequent fractionating of the radioactive substance in the soil-plant-(milk)** cycle of humans.

The average values computed for the different continents are remarkably alike. This shows that following explosions of nuclear weapons (equivalent to the explosions of a few million tons of TNT) the $Sr^{90}$ deposited from the stratosphere combines the local concentrations produced by test explosions in the USA and the Soviet Union. However, in the Southern Hemisphere, in Chile and Brazil, the concentrations are lower than at points in the Northern Hemisphere, because of the location of the regions in which the Soviet Union and the United States conduct their experimental nuclear explosions.

The bones of children one year old show 3 to 4 times more $Sr^{90}$ per gram of calcium than for adults. This results from the more rapid growth of bones in children.

As was to be expected, the average concentration of $Sr^{90}$ in human bones in different places does not differ more than the average concentrations of combined fission products. Individuals in the same place show considerable deviations of $Sr^{90}$ content from the average. For the majority of 10-year children the deviation is 50%. Specimens from North America show that individuals can contain 10 times more $Sr^{90}$ than the average. This must evidently be attributed to diet. An attempt was made to determine the change of $Sr^{90}$ content in human bones with time. Specimens from Germany permitted a comparison of the periods March to September 1955 and October 1955 to January 1956 in the age group from 0 to 9 years. The results were, respectively, 0.21 and 0.34 micromicrocuries of $Sr^{90}$ per gram of calcium. It is expected that the bones from the winter of 1956 to 1957 will show an increase of $Sr^{90}$.

The authors of the article calculate the average probable $Sr^{90}$ concentration in human bones for the United States in 1970 (from the power of explosions to date, which are estimated at 50 megatons) at about 2 micromicrocuries per gram of calcium, compared with a world average of 1.3 micromicrocuries. On this basis it is predicted that the average concentration of $Sr^{90}$ in all populated parts of the world will reach its maximum permissible level when the total pwer of nuclear explosions reaches 35000 megatons.

---

* Science 125, 3241, 219 (1957).

** The parentheses denote that $Sr^{90}$ can enter the human organism directly in plant food.

## THE ABSORPTION OF RADIOACTIVE MATTER BY CLAMS•

S. L.

After the explosion of an atom bomb in the Pacific Ocean in March 1954 some of the northern Marshall Islands were contaminated with radioactive fallout. Since that time the Radiological Defense Laboratory of the US Navy has conducted periodic surveys of this region to determine the residual contamination of plants, sea and land animals, soil and water. Among the specimens collected for study during the two postdetonation years were two "killer" clams of the genus Tridacna gigas from the Rongelap atoll.

The soft tissue of these clams was analyzed. They showed beta and gamma radiation with the energies 1.17 and 1.33 Mev which are characteristic of $Co^{60}$. The results are given in the table; for comparison the total gamma ray intensities are given. The figures show that the gamma activity was caused by the presence of $Co^{60}$.

$Co^{60}$ and the Total Gamma Radiation from the Molluscs

| Specimens | Weight of clams g | Gamma ray intensity | | $Co^{60}$, disintegration per min• |
|---|---|---|---|---|
| | | Gross count per min. | $Co^{60}$ count, per min. | |
| A | 1800 | 142,700 | 90,300 | 210,000 |
| B | 882 | 356,700 | 303,000 | 705,000 |

• Disintegrations per minute determined by comparison with data for $Co^{60}$ obtained from the National Bureau of Standards.

The presence of easily measured amounts of $Co^{60}$ in the molluscs is of interest for two reasons. First, $Co^{60}$ is not a fission product. It can therefore be assumed that these atoms were produced by the action of neutrons from the bomb explosion on some element in the environment. This may be natural $Co^{59}$, which is transformed by neutrons to $Co^{60}$. Secondly and more important, this radioactive element was not detected in many materials subjected to radioactive deposits, which were analyzed during the year following the explosion. This artificial radioactivity was evidently of extremely low intensity. The accumulation of $Co^{60}$ from an extremely dilute source shows the huge absorptive capacity of this mollusc.

The great ability of molluscs to absorb radioactive matter was also reported at a meeting of the Federation of American Societies for Experimental Biology by another worker at the same laboratory who stated that edible marine molluscs can be used to determine small concentrations of radioactive substances in the ocean.

The investigations of various forms of animal and plant life which were subjected to fallout in the Marshall Islands showed that a mollusc concentrates a larger amount of radioactive material than any other animal or plant.

The laboratory also tested the effect of water waste from atomic installations on molluscs taken from San Francisco Bay. It was found that the radioactivity of a mollusc is 2000 times greater than that of an equal weight of water. In a year one such mollusc passes through itself about 23000 liters of water and concentrates radioactive material in its soft tissues. This important characteristic of molluscs makes it unnecessary to study large water samples. Molluscs can also be used to detect the radioactive contamination due to water waste from atomic energy plants.

The laboratory is continuing to investigate the effects of radioactive fallout on marine fauna and flora.

• Science 125,3250,695,(1957).

S. L.

# BRIEF COMMUNICATIONS

USSR. The experimental heavy water reactor which was described at the Geneva conference in 1955 has been redesigned for improvement. The new reactor parameters are: maximum thermal neutron flux $2 \cdot 10^{13}$ neutrons/cm$^2$-sec, power 2500 kw, lattice spacing 13 cm, volume of heavy water 4.5 m$^3$ and $U^{235}$ enrichment 7%. This reactor will be used for studies in neutron physics, radiation chemistry, biology and physics of metals, as well as for the production of radioactive isotopes. (P. K.).

USSR. In Georgia construction of an experimental reactor has begun to serve the scientific institutions of Georgia, Armenia and Azerbaydzhan. About 30 research institutions in Georgia are now doing work on the peaceful uses of atomic energy. During the past year more than 200 investigators worked on 80 problems concerning the use of isotopes and radiation in various branches of science and technology. (Zarya Vostoka, July 24, 1957).

USSR. In Tashkent construction of the Institute of Nuclear Physics of the Uzbek Academy of Sciences has begun. For this purpose a large tract has been set aside for production facilities, laboratories and shops. (Industrial Economy Gazette (USSR), August 14, 1957).

USSR. On June 19 the Presidium of the Academy of Medical Sciences discussed the contamination of the earth's surface by strontium 90. Reports were heard from Associate Academician A. V. Lebedinsky, N. A. Kraevsky and A. N. Marei and specific plans were made to extend the study of this problem. (S.L.)

USSR. The Tallin measuring instrument plant has begun production of radioactive counters for the food industry. The instrument was designed by the Latvian Academy of Sciences. The counter uses artifically radioactive strontium, and will differ from currently produced mechanical and photoelectric counters by its greater universality and reliability. (Industrial Economy Gazette (USSR), August 2, 1957).

Rumania. Construction has begun on a reactor for research purposes, which is rated at 2000 kw and was designed by Rumanian and Soviet specialists. (Industrial Economy Gazette, August 2, 1957).

France. In January 1957 at the plant of the Compagnie Francaise de l'Eau Lourde in Toulouse a new method was instituted for the production of heavy water, requiring less power than other methods. The Toulouse plant is the first industrial facility in the world where the process takes place at only 20°C above absolute zero [1].

The Societe pour l'Obtention du Deuterium is now producing heavy water from $H_2S$ in natural gas. This method of production, which was developed by the German physicist Hart..., is based on isotope exchange. When $H_2S$ containing deuterium comes into contact with ordinary steam the following exchange reaction takes place: $D_2S + H_2O = D_2O + H_2S$. Such exchange reactions are used by other firms producing heavy water such as the Canadian "Consolidated Mining and Smelting Company" and the Norwegian "Norsk Hydro" [2]. (1. Appl. Atomics 67, 13, 1957; 2. Atomics and Nucl. Energy 8, 5, 193, 1957).

West Germany. In May 1957 there occurred the official unveiling of the first synchrocyclotron constructed after the war, at the Institute of Radiation and Nuclear Physics in Bonn. Operation of the accelerator will begin this year. Deuterons will be accelerated to 35 Mev and alpha particles to 70 Mev. The accelerator was designed by the Institute; the first plans were prepared in 1952. The magnet weight is 200 tons, copper coils 20 tons, high-frequency voltage 10 kv, frequency 10 megacycles. Frequency modulation is accomplished by ferro-induction. It is planned to increase the frequency to 20 megacycles in order to accelerate protons to 70 Mev and to generate a magnetic field for increasing proton energies to 100-120 Mev. The cost of the synchrocyclotron was 1.5 million marks. (Atomwirtschaft 5, 176, 1957).

West Germany. Following the example of England it is planned to build reactors using natural uranium. It is proposed to purchase 500 tons of natural uranium in Canada, which will supply the uranium needs of the country for a few years. (Atomic Energy Newsletter 17, 7, 3, 1957).

West Germany. The Physical Institute of the University of Bonn is building a synchrotron for the acceleration of electrons to 600 Mev. (Atomwirtschaft 5, 176, 1957).

England. Plans have been formulated to begin construction of two new atomic power plants to produce 500 megawatts, in North Wales and at Dungeness in Kent. The power of the first station during periods of partial load will be used to pump water into a mountain reservoir. During peak periods the water will turn generator turbines.

The number of planned atomic power plants will be reduced from 19 to 12-15 because of considerable increase in the power of some plants. (Financial Times, June 13, 1957, p. 1).

England. During the period 1960-1975 capital expenditures for the construction of atomic power plants in England will be reduced by 30-40%, and the service life of the plants now under construction will be not less than 20 years. The cost of fuel for the first atomic power plants in England is about 30 pounds Sterling per kilowatt. (Appl. Atomics 79, 3, 1957).

Canada. Construction of the NPD power reactor has been suspended for about a year in order to introduce improvements into the design. It has been decided to replace a pressure vessel with pressure channels. These changes will not affect the basic design, which uses heavy water as the moderator and natural uranium as fuel. (Appl. Atomics 87, 7, 1957).

USA. The University of California this year began operation of a linear accelerator for heavy ions (Hilac) which will accelerate ions of all elements up to argon. At present nitrogen ions are being accelerated to 140 Mev. It is planned to synthesize and study transuranic elements, particularly elements heavier than element 101. (Engineer, 5293, 33, 1957).

USA. It is reported that a linear accelerator can be used to produce isotopes which cannot be obtained from a nuclear reactor (such as $F^{18}$ and $Fe^{53}$). Using a 20-Mev accelerator (of 60 kw power) costing five hundred thousand dollars it is possible to obtain thermal neutron fluxes of $10^{12}$ neutrons/cm$^2$-sec, which is of the same order as in a 25 kw homogeneous reactor. Such an accelerator can also produce a gamma ray flux equivalent to the flux from a $Co^{60}$ source with a strength of 2 million curies. The cost of producing neutrons and gamma rays will be 10 and 4 times less, respectively, than for other types of accelerators (Appl. Atomics 87, 17, 1957).

USA. A reactor has been developed to use molten fuel in the form of fluorides containing enriched uranium. During experimental operation the reactor worked continuously at full capacity for four days at a maximum reactor temperature of ~ 540°C. (Appl. Atomics 86, 9, 1957).

USA. For the air transportation of units of the portable APPR power reactor recently started at Fort Belvoir, from 60 to 120 large transport planes are required. American specialists believe that this is the only shortcoming of the reactor except for the fact that not less than 6 months will be required for assembly at the point of arrival. Work is therefore being done in the USA on other designs for portable power reactors. At Arco, Idaho, a low-power boiling water reactor is being constructed at a cost of 1.2 million dollars. Construction of an experimental reactor with gas coolant is being planned, and a reactor with liquid metal fuel is being designed. (Appl. Atomics 86, 10, 1957).

USA. The US War Department has ordered the planning of an atomic-powered trailer train for use in Alaska. The train will consist of from 4 to 5 trailers each 8 meters long. The train will be operated from the front but the power plant and shielding will be located in the last unit. (Appl. Atomics 86, 1, 1957).

USA. The Walter Kidde Laboratory has produced a miniature atomic battery which will furnish electric power without reloading for at least 5 years. The battery is of the size of a thumb tack and is rated at 20 microwatts. The source of light is a mixture of ground phosphorus and beta-active oxide (4.5 curies) and promethium 147. (Electr. Engineering 76, 4, 361, 1957).

USA. An International Conference on Neutron Physics took place at Columbia University from September 9 to 13, 1957. The Soviet delegation at the conference consisted of N. A. Vlasov, V. V. Vladimirsky, L. V. Groshev, V. I. Mostovoy and M. I. Pevzner.

BLANK
PAGE

# BIBLIOGRAPHY

## RECENT LITERATURE

### Books and Collections

Bresler, S. E., Radioactive Elements. Third revised edition, Gostekhizdat, 1957, 550 pp, 16 rubles 30 kopecks. The first edition appeared in 1949. The book has been thoroughly revised, some chapters have been rewritten, and the chapter on nuclear reactions has been replaced with a chapter on the radiochemistry of fission. Additions have been made to the section on the "Chemistry of the Radioelements" and also to the sections on the most promising separation methods, extraction and chromatography. The book contains an introduction and chapters on the most important methods of studying radioactive elements, the enrichment and separation of radioactive substances, electrochemistry and the adsorption of radioactive substances, chemistry of the radioelements, the production of artificially radioactive materials by the use of nuclear reactions, fission of heavy nuclei, some important artificially radioactive substances and investigations with tagged atoms.

Problems of Nuclear Power, Collection No. 2 of translations and reviews of foreign periodical literature, 1957, IL, 1044 pp, 7 rubles.

The section on Economics contains a condensed translation of an article by Mueller in "Atompraxis" (May-June, 1956) entitled "Prospects for Economical Atomic Power." The section on Power Plants contains translations of a number of articles concerning the Calder Hall plant, the translation of an article from Engineering 181, No. 4695 (1956) entitled "Water-cooled Reactors," the translation of a supplementary report by Milne and Moore at the 5th World Power Conference: "The New York Atomic Power Plant."

The section on Construction Materials contains the translation of an article from Nucleonics No. 7 (1956) by Colichman and Gercke entitled "The Radiation Stability of the Polyphenyls."

The section on References contains a continuation of the list of reactors by countries (under construction or planned), taken from Die Atomwirtschaft No. 9 (1956); the beginning of the list was published in the preceding collection.

The section on News of Nuclear Power contains the translation of a review from Nucleonics No. 8 (1956) on "Experimental Power Reactors."

Korablev, I. N., New Applications of Pulsed Cold-Cathode Lamps. Gostekhizdat, Academy of Sciences USSR, VINITI branch, 1956, 200 pp, illustrated, 56 rubles.

This book examines in detail the methods of using cold-cathode gas discharge lamps, elements of pulse circuits and instruments constructed of these elements which were developed by the author at the P. N. Lebedev Physical Institute of the Academy of Sciences USSR.

Joliot-Curie, F., Selected Works, Frederick and Irene Joliot-Curie, Complete Works, Acad. Sci. USSR Press, 1957, 562 pp, 32 rubles. The book contains papers on the electrochemistry of radioelements and on the electrical properties of thin metal layers. A large number of papers are devoted to ionization by alpha rays. There is an article on the properties of nuclear particles and the world-famous work on artificial radioactivity. There is a series of papers on nuclear fission and the theoretical basis for nuclear power. The book contains the last papers on the use of tagged atoms ($I^{131}$) in biology and a number of popular works and reviews. The book will be of interest to a wide audience of scientists and engineers working in the field of the application of atomic power.

International Conference on the Peaceful Uses of Atomic Energy (Geneva, August 8-20, 1955) Vol 4. Cross sections needed for reactor design, Acad. Sci. USSR Press, 1957, 420 pp, 30 rubles. This volume contains

special reports and discussions of atomic technology. It contains the cross sections of fissioning materials and of fuels, which are needed for designing reactors.

Methods of Recording Atomic Particles. Problems of Modern Physics No. 4 (1957). This issue contains articles which describe apparatus used in nuclear physics to record radiation. There are several sections: ionization methods of recording radiation, scintillation counters, Cherenkov counters, Wilson cloud chambers, bubble chambers and photographic plate methods.

Four Lectures on Nuclear Power. Translation from English. Ill. This collection contains 4 lecures by English specialists at the All-British Conference on Nuclear Power in March, 1956. It is intended for electrical engineers and other specialists in atomic energy.

## JOURNALS

Baz, A. I., Charge Invariance in Nuclear Reactions, J. Expt. Theoret. Phys. (U.S.S.R.) 32, No. 3 (1957).

Belenky, S. Z. and Gerasimova, N. M., On the Absorption of High-Energy Nuclear-Active Particles, J. Exptl. Theoret. Phys. (U.S.S.R.) 32, No. 3 (1957).

Brodsky, A. M., On the Derivation of Low's Equations in the Theory of Meson Scattering, J. Exptl. Theoret. Phys. (U.S.S.R.) 32, No. 3 (Letter to the Editor) (1957).

Vdovin, Yu. A., The Production of Proton-Antiproton Pairs by High-Energy Quanta, J. Exptl. Theoret. Phys. (U.S.S.R.) 32, No. 3 (1957).

Volkova, N. I., Some Problems of Hygiene in the Use of Radioactive Isotopes in Ferrous Metallurgy, Industrial Hygiene and Occupational Diseases (U.S.S.R.) No. 2 (1957).

Galanin, A. D., On the Possibility of Formulating a Meson Theory with Several Fields, J. Exptl. Theoret. Phys. (U.S.S.R.) 32, No. 3 (1957).

Gracheva, N. D., An Autoradiographic Study of the Distribution of Radioactive $P^{32}$ in Some Parts of the Nervous System, Dokl. Akad. Nauk SSSR 113, No. 2 (1957).

Gershman, B. N. et al., Electromagnetic Wave Propagation in a Plasma (the Ionosphere), Usp. Fiz. Nauk, 61, No. 4 (1957).

Grinyuk, N. A., Experience of the Industrial Hygiene Physicians of Moscow in Controlling the Conditions of Working with Radioactive Materials, Industrial Hygiene and Occupational Diseases (U.S.S.R.) No. 2 (1957).

Dmitriev, I. S., On the Probability of Electron Losses by Multiply-Charged Ions, J. Exptl. Theoret. Phys. (U.S.S.R.) 32, No. 3 (1957).

Dovzhenko, O. I., et al., The Muon Energy Spectrum in Extensive Air Showers, J. Exptl. Theoret. Phys. (U.S.S.R.) 32, No. 3 (1957).

Dolginov, A. Z., On the Nature of the Forces between Nucleons, J. Exptl. Theoret. Phys. (U.S.S.R.) 32, No. 3 (Letter to the Editor) (1957).

Drukarev, G. F., Dependence of Inelastic Cross Sections on Energy near the Threshold, J. Exptl. Theoret. Phys. (U.S.S.R.) 32, No. 3 (Letter to the Editor) (1957).

Eleonsky, V. M. and Zyryanov, P. S., On the Theory of Collective Particle Motion in Quantum-Mechanical Systems, J. Exptl. Theoret. Phys. (U.S.S.R.) 32, No. 3 (1957).

Zvereva, N. P., On Lanthanum Sulfides, Dokl. Akad. Nauk SSSR 113, No. (1957).

Ivanenko, I. P., Energy Spectrum of Cascade Electrons in Lead, J. Exptl. Theoret. Phys. (U.S.S.R.) 32, No. 3 (1957).

Kogan, A. V. and Rusinov, L. I., Neutron Emission by Excited Nuclei of RaD, J. Exptl. Theoret. Phys. (U.S.S.R.) 32, No. 3 (1957).

Komar, A. P. and Yavor, I. P., Photodisintegration of Neon Nuclei, J. Exptl. Theoret. Phys. (U.S.S.R.) 32, No. 3 (Letter to the Editor) (1957).

Konyukov, M. V., Low-Frequency Vibrations in Plasmas of Electro-Negative Gases, J. Exptl. Theoret. Phys. (U.S.S.R.) 32, No. 3 (1957).

Kulakov, Yu. I., On Inelastic Proton-Proton Scattering, J. Exptl. Theoret. Phys. (U.S.S.R.) 32, No. 3 (1957).

Kunin, P. E. and Talsar, I. M., Some Relativistic Properties of Spin 1/2 Particles, J. Exptl. Theoret. Phys. (U.S.S.R.) 32, No. 3 (1957).

Leksin, G. A., Elastic and Quasi-Elastic Scattering of 600-Mev Protons by Deuterons, J. Exptl. Theoret. Phys. (U.S.S.R.) 32, No. 3 (1957).

Logunov, V. I. et al., Dependence of Betatron Bremsstrahlung on Injection Parameters, J. Tech. Phys. (U.S.S.R.) 27, No. 5 (1957).

Logunov, V. N. et al., Nonstationary Circulating Current with Electron Injection in a Betatron, J. Tech. Phys. (U.S.S.R.) 27, No. 5 (1957).

Mitin, N. A. and Grigorev, E. L., Elastic Proton Scattering by Positive Pions at 360 Mev, J. Exptl. Theoret. Phys. (U.S.S.R.) 32, No. 3 (1957).

Peker, I. K. and Sliv, L. A., Electric Monopole Transitions in Nuclei of Odd Mass Number, J. Exptl. Theoret. Phys. (U.S.S.R.) 32, No. 3 (1957).

Peredelsky, A. A. et al., On the Use of Ionizing Radiation Against Insect Enemies of Grain Stocks, Biophysics (U.S.S.R.) 11, No. 2 (1957).

Perel, V. I., Calculation of Ion Drift Velocity in a Gas in an Electric Field, J. Exptl. Theoret. Phys. (U.S.S.R.) 32, No. 3 (1957).

Post, R., The Application of High Temperature Plasma Physics to Produce Controlled Fusion, Usp. Fiz. Nauk 61, No. 4 (1957).

Puzikov, L. et al., Reconstruction of the Scattering Matrix of a Two-Nucleon System, J. Exptl. Theoret. Phys. (U.S.S.R.) 32, No. 3 (1957).

Rezanov, A. I., Electron Energy in an Almost Periodic Field, Physics of Metals and Metallurgy (U.S.S.R.) 4, No. 1 (1957).

Romankevich, A. V., On the Lifetime of the Two Forms of the Neutral Pion (Letter to the Editor), J. Exptl. Theoret. Phys. (U.S.S.R.) 32, No. 3 (1957).

Sautin, A. I., On the Dosimetry of Wounds and Burns Infected with Radioactive Matter, Mil. Med. Journal (U.S.S.R.) No. 4 (1957).

Sysoev, M. I., Alpha, Beta and Gamma Rays and the Electrical Strength of Compressed Air, Elektrichestvo No. 5 (1957).

Uchitel, I. Ya., The Use of Radioactive Tracers in Immunology, Usp. Sovremennoi Biologii 63, No. 2 (1957).

Frish, S. E., The Role of Atomic Cross Sections in the Excitation of Spectra, Usp. Fiz. Nauk 61, No. 4 (1957).

Khaletsky, M. M., Measurement of Total Cross Sections for 14.8-Mev Neutrons from the Count of (n,$\alpha$) Coincidences, Dokl. Akad. Nauk SSSR 113, No. 2 (1957).

Chudars, Ya., Calculations of the Attenuation of Monoenergetic Electron Beams in Layers of Matter, Izv. Akad. Nauk (Latvian SSR) No. 3 (1957).

Shpetny, A. I., Energy and Angular Distributions of Neutrons Emitted in the $Be^9$ (d,n)$B^{10}$ Reaction, J. Exptl. Theoret. Phys. (U.S.S.R.) 32, No. 3 (1957).

BLANK
PAGE